

Some pages of this thesis may have been removed for copyright restrictions.

If you have discovered material in AURA which is unlawful e.g. breaches copyright, (either yours or that of a third party) or any other law, including but not limited to those relating to patent, trademark, confidentiality, data protection, obscenity, defamation, libel, then please read our [Takedown Policy](#) and [contact the service](#) immediately

**THE REACTIONS OF DIRECTLY RELATED TELLURIUM AND
SELENIUM HETEROCYCLIC COMPOUNDS WITH TRIIRON
DODECACARBONYL**

By

ZULFIQAR MAJEED

A thesis submitted for the degree of
Doctor of Philosophy

Aston University

July 1999

This copy of the thesis has been supplied on condition that anyone who consults it is understood to recognise that its copyright rests with its author and that no quotation from the thesis and no information derived from it may be published without proper acknowledgement.

THE REACTIONS OF DIRECTLY RELATED TELLURIUM AND SELENIUM HETEROCYCLIC
COMPOUNDS WITH TRIIRON DODECACARBONYL

By Zulfiqar Majeed

A thesis submitted for the degree of Doctor of Philosophy at Aston University

April 1999

SUMMARY

The reactions of directly related tellurium and selenium heterocyclic compounds with triiron dodecacarbonyl are described. The reaction of 2-telluraphthalide, C_8H_8OTe with $[Fe_3(CO)_{12}]$ gave $[Fe\{C_6H_4(CH_2)Te\}(CO)_3]_2$, (1). An iron atom has inserted into the telluracyclic ring, and it is probable that one co-ordinated CO ligand arises from the initially organic carbonyl group. X-ray analysis of compound (1) showed that the compound has a Fe_2Te_2 core, which is achieved by dimerisation. The reaction of telluraphthalic anhydride, $C_8H_4O_2Te$ with $[Fe_3(CO)_{12}]$ gave a known, but unexpected, organic phthalide product, $C_8H_6O_2$, which was confirmed by X-ray crystallography. Selenaphthalic anhydride, $C_8H_4O_2Se$ gave intractable products on reaction with $[Fe_3(CO)_{12}]$. 2-selenaphthalide, C_8H_6OSe , on reaction with $[Fe_3(CO)_{12}]$ gave a major product $[Fe_2\{C_6H_4(CH_2)Se\}(CO)_6]$, (2) and a minor product $[Fe_3\{C_6H_4(CH_2)Se\}(CO)_8]$, (3) which is an intermediate in the formation of (2). X-ray analysis of (2) shows that compound (2) is very similar to (1) except that the 18 electron rule is satisfied by co-ordination of a $Fe(CO)_3$ moiety, rather than dimerisation. Compound (3), also studied by X-ray crystallography, differs from (2) mainly in the addition of an $Fe(CO)_2$ moiety.

Telluraphthalic anhydride, $C_8H_4O_2Te$, and selenaphthalic anhydride, $C_8H_4O_2Se$, are both monoclinic and crystallise in space group $P2_1/n$. 2-Selenaphthalide, C_8H_6OSe , is also monoclinic, space group $P2_1/c$.

The reactions of the following compounds (1,3-dihydrobenzo[c]selenophene, 1,3,7,9-tetrahydrobenzo[1,2c;4,5c']ditellurophene, dibenzoselenophene, phenoxselenine, 3,5-naphtho-1-telluracyclohexane and 3,5-naphtho-1-selenacyclohexane) with $[Fe_3(CO)_{12}]$ are reported. It is unfortunate that the above compounds do not react under the conditions employed; this may be due to differing degrees of ring strain.

1,8-bis(bromomethyl)naphthalene, $C_{12}H_{10}Br_2$ is monoclinic and crystallises in space group $C2/c$. 1,1-diiido-3,5-naphthotelluracyclohexane, $C_{12}H_{10}TeI_2$ and 3,5-naphtho-1-telluracyclohexane, $C_{12}H_{10}Te$ are monoclinic and crystallise in space group $P2_1/c$. 3,5-naphtho-1-selenacyclohexane, $C_{12}H_{10}Se$ and 2,2,8,8-tetraiodo-1,3,7,9-tetrahydrobenzo[1,2c;4,5c']ditellurophene are also monoclinic, space group $P2_1/a$.

The syntheses of intramolecular stabilised organo-tellurium and selenium compounds are reported, having a general formula of REX (where R = phenylazophenyl; E = Se, Te; X = electronegative group, for example Cl, Br or I).

The crystal structures of $RTeBr$, $RTeI$, $RSeCl$, $RSeCl/I$ and $RSeI$ (where R = phenylazophenyl) are reported. The tellurium containing X-ray structures are triclinic and have a space group $P-1$. The selenium containing X-ray structures are monoclinic with space group $P2_1/n$.

The inclusion of nitrogen in selenium heterocycles provides access to an entirely new area of organometallic chemistry. The reaction of 2-methylbenzoselenazole with $[Fe_3(CO)_{12}]$ gave $[Fe_2\{C_6H_4(NCH_2CH_3)Se\}(CO)_6]$. The reactions of 2-(methyltelluro)benzanilide or 2-(methylseleno)benzanilide with $[Fe_3(CO)_{12}]$ gave reaction products $[Fe_2(\mu-TeMe)_2(CO)_6]$ and $[Fe_2(\mu-SeMe)_2(CO)_6]$ respectively, which were confirmed by X-ray crystallography.

The use of Mössbauer spectroscopy on the products obtained from the reactions of heterocyclic compounds with $[Fe_3(CO)_{12}]$ can give useful information, for example the number of iron sites and the environments of these iron sites within the products.

To my little sister.

These are the voyages of the starship Enterprise.

Its five year mission.....

to boldly go where no man has gone before.

Gene Roddenberry 1921 – 91 : Star Trek (Television series from 1966)

These are the voyages of my PhD.

Its three year mission.....

to boldly go where no man has gone before.

Zulfiqar Majeed 1972 – ? : (Adapted from above)

ACKNOWLEDGMENTS

I would like to express my sincere gratitude to Professor W.R. McWhinnie for his supervision, encouragement and unfailing interest throughout the course of this work and his helpful remarks during the writing of this thesis.

I am grateful to Dr T.A. Hamor (University of Birmingham) and Dr. P. Lowe (Aston University) for their assistance in obtaining X-ray crystallographic data. I also acknowledge with thanks, Dr M. Perry (Aston University) for recording NMR spectra, Dr. D.J. Evans (John Innes Centre, Norwich) for recording Mössbauer spectra and members of the technical staff for the services rendered to me.

My thanks also extend thanks to members of Lab. 304 for letting me experiment with chemicals (bang!).

I would also like to express my gratitude to Dr. M.S. Beevers, Mrs. R. Wright, Dr. S. Ghose and Dr. S.C. Generails for their friendship.

Specials thanks to Dr. A. Wiggett for his friendship.

Thanks to Paul (soon to be Dr.) Douglas for desk space and listening.

A special thank-you goes out to Samantha for not letting me give up, helping me throughout my final year and being there for me.

I would like to thank Steve and Lesley for their friendship and assistance in helping me prepare this thesis.

I would like to take time out to say thank you to Maz and Q.

Finally I would like to thank my family for their support.

CONTENTS

THE REACTIONS OF DIRECTLY RELATED TELLURIUM AND SELENIUM HETEROCYCLIC COMPOUNDS WITH TRIIRON DODECACARBONYL	1
SUMMARY	2
ACKNOWLEDGMENTS.....	4
CONTENTS	5
LIST OF TABLES	11
LIST OF FIGURES	15
LIST OF SCHEMES.....	17
CHAPTER ONE.....	18
INTRODUCTION	18
Introduction	19
1.1 Heterocyclic compounds	19
1.1.1 Aromaticity in group 16	20
1.1.2 The carbon-chalcogen bond strength	20
1.2 The co-ordination chemistry of heterocyclic selenium and tellurium compounds	21
1.2.1 The co-ordination chemistry of heterocyclic compounds with trinuclear carbonyls, of Fe or Ru or Os	21
1.2.2 The co-ordination chemistry of heterocyclic compounds containing a tellurium or selenium heteroatom with transition metals.....	33
1.3 Kinetic stabilisation of organotellurium(II) derivatives (R ₂ TeX; X = electronegative group) by intramolecular co-ordination.....	35
1.3.1 Order of Lewis acidity in organotellurium compounds	35
1.3.1.2 Short-range intermolecular co-ordination	35
1.3.1.3 Long-range intermolecular co-ordination.....	36
1.3.1.4 Intra-molecular co-ordination	36
CHAPTER TWO.....	38
GENERAL EXPERIMENTAL AND PHYSICAL TECHNIQUES.....	38
2.1 General experimental and physical techniques.....	39
2.1.1 Reactions in an inert atmosphere	39
2.1.2 Chemicals and solvents	39
2.1.3 Elemental analysis.....	39

2.1.4 Melting points	39
2.1.5 Infra-red spectroscopy	39
2.1.6 Nuclear magnetic resonance spectroscopy	40
2.1.7 Mass spectroscopy	40
2.1.8 Mössbauer spectroscopy	40
2.1.9 X-ray crystallography	40
CHAPTER THREE	42
THE REACTIONS OF FIVE MEMBERED HETEROCYCLIC SYSTEMS CONTAINING EITHER TELLURIUM OR SELENIUM AS THE HETEROATOM WITH TRIIRON DODECACARBONYL	42
3.1 Introduction	43
3.2 Experimental	44
3.2.1 Reactions of tellurium heterocycles	44
3.2.1.1 Preparation of heterocyclic tellurium compounds	44
3.2.1.2 Reaction of triiron dodecacarbonyl with 2-telluraphthalide	44
3.2.1.3 Reaction of triiron dodecacarbonyl with telluraphthalic anhydride	45
3.2.2.1 Preparation of heterocyclic selenium compounds	46
3.2.2.2 Reaction of triiron dodecacarbonyl with 2-selenaphthalide	46
3.2.2.3 Reaction of triiron dodecacarbonyl with selenaphthalic anhydride	47
3.3 Results and discussion	48
3.3.1 Reaction of triiron dodecacarbonyl with 2-telluraphthalide	48
3.3.2 Reaction of triiron dodecacarbonyl with telluraphthalic anhydride	53
3.3.3 Reaction of triiron dodecacarbonyl with 2-selenaphthalide	56
3.3.4 Reaction of triiron dodecacarbonyl with selenaphthalic anhydride	62
3.3.5 Time dependent ^1H and ^{13}C NMR spectroscopy for compound (35)	63
3.4 X-ray crystallography	68
3.4.1 X-ray crystallography of products (33), (34), (35) and (36)	68
3.4.1.1 Crystallographic analysis for products (33), (34), (35) and (36)	68
3.4.1.2 Discussion of the structures of (33), (34), (35) and (36)	76
3.4.2 X-ray crystallography of telluraphthalic anhydride (37), 2-selenaphthalic anhydride (38) and 2-selenaphthalide (39)	83
3.4.2.1 Crystallographic analysis for telluraphthalic anhydride (37), 2- selenaphthalic anhydride (38) and 2-selenaphthalide (39)	83

3.4.2.2 Discussion of the structures of telluraphthalic anhydride, (37), selenaphthalic anhydride, (38) and 2-selenaphthalide, (39).....	88
3.5 Conclusion.....	94
CHAPTER FOUR	96
THE REACTIONS OF SIX MEMBERED HETEROCYCLIC SYSTEMS CONTAINING EITHER TELLURIUM OR SELENIUM AS THE HETEROATOM WITH TRIIRON DODECACARBONYL	96
4.1 Introduction	97
4.2 Experimental.....	99
4.2.1 Reactions of tellurium and selenium heterocycles.....	99
4.2.2 Preparation of heterocyclic tellurium and selenium compounds.....	99
4.2.3 Standard procedure for reaction of triiron dodecacarbonyl with heterocyclic compounds	100
4.2.3.1 1,3-Dihydrobenzo[c]selenophene	100
4.2.3.2 1,3,7,9-Tetrahydrobenzo[1,2c;4,5c']ditellurophene	101
4.2.3.3 Dibenzoselenophene.....	101
4.2.3.4 Phenoxselenine.....	101
4.2.3.5 3,5-Naphtho-1-telluracyclohexane.....	101
4.2.3.6 3,5-Naphtho-1-selenacyclohexane.....	102
4.3 Results and discussion.....	103
4.4 X-ray crystallography.....	105
4.4.1 Crystallographic analysis for 1,8-bis(bromomethyl)naphthalene, (42), 1,1- diiodo-3,5-naphthotelluracyclohexane, (43), 3,5-naphtho-1-telluracyclohexane, (44) and 3,5-naphtho-1-selenacyclohexane, (45).....	105
4.4.1.1 Discussion of the structures of 1,8-bis(bromomethyl)naphthalene, (42), 1,1- diiodo-3,5-naphthotelluracyclohexane, (43), 3,5-naphtho-1-telluracyclohexane, (44) and 3,5-naphtho-1-selenacyclohexane, (45).....	113
4.4.2 Crystallographic analysis for 2,2,8,8-tetraiodo-1,3,7,9-tetrahydrobenzo[1,2- c;4,5-c']ditellurophene, (46).....	119
4.4.2.1 Discussion of the structure of 2,2,8,8-tetraiodo-1,3,7,9-tetrahydrobenzo[1,2- c;4,5-c']ditellurophene, (46).....	123
4.5 Conclusion	126
CHAPTER FIVE	127

INTRAMOLECULAR STABILISATION OF ORGANOSELENIUM(II) AND – TELLURIUM(II) DERIVATIVES (REX; E = Se, Te; X = ELECTRONEGATIVE GROUP) BY <i>INTRA</i> -MOLECULAR CO-ORDINATION	127
5.1 Introduction	128
5.2 Experimental	130
5.2.1 Formation of intramolecular stabilised organotellurium compounds	130
5.2.1.1 Preparation of intramolecular stabilised organotellurium compounds.....	130
5.2.1.2 Attempted synthesis of (2-phenylazophenyl-C,N')tellurium(IV) tribromide	130
5.2.1.3 Synthesis of (2-phenylazophenyl-C,N')tellurium(II) bromide.....	131
5.2.1.4 Synthesis of (2-phenylazophenyl-C,N')tellurium(II) iodide	131
5.2.2 Formation of intramolecular stabilized organoselenium compounds	132
5.2.2.1 Preparation of intramolecular stabilized organoselenium compounds	132
5.2.2.2 Attempted synthesis of (2-phenylazophenyl-C,N')selenium(IV) trichloride	132
5.2.2.3 Synthesis of (2-phenylazophenyl-C,N')selenium(II) chloride	133
5.2.2.4 Synthesis of (2-phenylazophenyl-C,N')selenium(II) chloride	133
5.2.2.5 Synthesis of (2-phenylazophenyl-C,N')selenium(II) chloride : (2- phenylazophenyl-C,N')selenium(II) iodide (1:1).....	133
5.2.2.6 Synthesis of (2-phenylazophenyl-C,N')selenium(II) iodide	134
5.3 Results and discussion.....	135
5.3.1 (2-Phenylazophenyl-C,N')tellurium(IV) tribromide, (RTeBr ₃), (2- phenylazophenyl-C,N')tellurium(II) bromide, (RTeBr) and iodide, (RTeI).....	135
5.3.2 (2-Phenylazophenyl-C,N')selenium(IV) trichloride, (RSeCl ₃), (2- phenylazophenyl-C,N')selenium(II) chloride, (RSeCl), chloride : iodide (1:1), (RSeCl/I) and iodide, (RSeI)	139
5.4 X-ray crystallography.....	147
5.4.1 X-ray crystallography for intramolecular stabilized organotellurium compounds.....	147
5.4.1.1 Crystallographic analysis for (2-phenylazophenyl-C,N')tellurium(II) bromide and iodide.	147
5.4.1.2 Discussion of the structures of (2-phenylazophenyl-C,N')tellurium(II) bromide and iodide.	152

5.4.2 X-ray crystallography for intramolecular stabilized organoselenium compounds.....	155
5.4.2.1 Crystallographic analysis for (2-phenylazophenyl-C,N')selenium(II) chloride, chloroiodide and iodide	155
5.4.2.2 Discussion of the structures of (2-phenylazophenyl-C,N')selenium(II) chloride, chloride : iodide (1:1) and iodide.	162
5.5 Conclusion	167
CHAPTER SIX.....	168
THE REACTIONS OF NITROGEN-CONTAINING SELENIUM OR TELLURIUM HETEROCYCLES WITH TRIIRON DODECACARBONYL	168
6.1 Introduction	169
6.2 Experimental.....	170
6.2.1 Reactions of nitrogen-containing heterocycles.....	170
6.2.1.1 Preparation of nitrogen-containing compounds.....	170
6.2.1.2 Reaction of triiron dodecacarbonyl with 2,1,3-benzoselenadiazole	170
6.2.1.3 Reaction of triiron dodecacarbonyl with 1,2,5-selenadiazolo[3,4-b]pyridine	171
6.2.1.4 Reaction of triiron dodecacarbonyl with 2-phenyl-1,2-benzisoselenazol-3(2H)-one.....	171
6.2.1.5 Reaction of triiron dodecacarbonyl with 2-methylbenzoselenazole	171
6.2.1.6 Reaction of triiron dodecacarbonyl with (2-phenylazophenyl-C,N')tellurium(II) bromide	172
6.2.1.7 Reaction of triiron dodecacarbonyl with (2-phenylazophenyl-C,N')selenium(II) chloride.....	172
6.2.1.8 Reaction of triiron dodecacarbonyl with 2-(methyltelluro)benzanilide	173
6.2.1.9 Reaction of triiron dodecacarbonyl with 2-(methylseleno)benzanilide	173
6.3 Results and discussion.....	174
6.3.1 Reaction of triiron dodecacarbonyl with 2-methylbenzoselenazole	174
6.3.2 Reactions of triiron dodecacarbonyl with 2-(methyltelluro)benzanilide or 2-(methylseleno)benzanilide	178
6.4 X-ray crystallography.....	180
6.4.1 X-ray crystallography for product (48).	180
6.4.1.1 Crystallographic analysis for product (48).	180
6.4.2 Discussion of the structure (48)	186

6.4.2.1 Crystallographic analysis for $[\text{Fe}_2(\mu\text{-TeMe})_2(\text{CO})_6]$, (49), and $[\text{Fe}_2(\mu\text{-SeMe})_2(\text{CO})_6]$, (50).....	186
6.4.3.2 Crystallographic discussion for $[\text{Fe}_2(\mu\text{-TeMe})_2(\text{CO})_6]$, (49), and $[\text{Fe}_2(\mu\text{-SeMe})_2(\text{CO})_6]$, (50).....	194
6.5 ^{57}Fe Mössbauer spectroscopy of iron containing compounds.....	197
6.5.1 Results and discussion.....	199
6.5 Conclusion.....	206
REFERENCES.....	207
APPENDIX.....	218
PAPER 1 : THE REACTIONS OF HETEROCYCLIC ORGANOTELLURIUM AND SELENIUM COMPOUNDS WITH TRIIRON DODECACARBONYL.....	219
PAPER 2 : THE STRUCTURAL CHARACTERISATION OF TELLURAPHTHALIC ANHYDRIDE, SELENAPHTHALIC ANHYDRIDE AND OF 2-SELENAPHTHALIDE.....	225
PAPER 3 : OBSERVATIONS ON THE SYNTHESIS AND CHEMISTRY OF A COMPLETE SERIES OF PHENYLAZOPHENYL(C,N')TELLURIUM(II) HALIDES (FLUORIDE, CHLORIDE, BROMIDE AND IODIDE).....	230

LIST OF TABLES

Table 1.1 Bond strengths of the gaseous diatomic species C-X.....	21
Table 3.1 FTIR bands in the carbonyl region for product from reaction of 2-telluraphthalide and $[\text{Fe}_3(\text{CO})_{12}]$	48
Table 3.2 ^1H , ^{13}C and ^{125}Te NMR data collected for (33).....	49
Table 3.3 FTIR band in the carbonyl region for product from reaction of telluraphthalic anhydride and $[\text{Fe}_3(\text{CO})_{12}]$	53
Table 3.4 ^{13}C NMR data for (34).....	54
Table 3.5 FTIR bands in the carbonyl region for products from reaction of 2-selenaphthalide and $[\text{Fe}_3(\text{CO})_{12}]$	56
Table 3.6 EI mass spectra peaks for products from reaction of 2-selenaphthalide and $[\text{Fe}_3(\text{CO})_{12}]$ (^1H , ^{12}C , ^{56}Fe and ^{80}Se).....	57
Table 3.7 ^1H and ^{13}C NMR data for (35).....	58
Table 3.8 ^1H and ^{13}C NMR data collected for (36).....	61
Table 3.9 FTIR bands in the carbonyl region for product from reaction of selenaphthalic anhydride and $[\text{Fe}_3(\text{CO})_{12}]$	63
Table 3.10 Crystallographic data for products (33), (34), (35) and (36).....	69
Table 3.11 Atomic coordinates ($\times 10^4$) and equivalent isotropic displacement parameters ($\text{\AA}^2 \times 10^3$) for (33). $U(\text{eq})$ is defined as one third of the trace of the orthogonalized U_{ij} tensor.	70
Table 3.12 Atomic coordinates ($\times 10^4$) and equivalent isotropic displacement parameters ($\text{\AA}^2 \times 10^3$) for (34). $U(\text{eq})$ is defined as one third of the trace of the orthogonalized U_{ij} tensor.	71
Table 3.13 Atomic coordinates ($\times 10^4$) and equivalent isotropic displacement parameters ($\text{\AA}^2 \times 10^3$) for (35). $U(\text{eq})$ is defined as one third of the trace of the orthogonalized U_{ij} tensor.	72
Table 3.14 Atomic coordinates ($\times 10^4$) and equivalent isotropic displacement parameters ($\text{\AA}^2 \times 10^3$) for (36). $U(\text{eq})$ is defined as one third of the trace of the orthogonalized U_{ij} tensor.	73
Table 3.15 Selected bond lengths (\AA) and angles ($^\circ$) for compounds 33 - 36.....	74
Table 3.15 Cont Selected bond lengths (\AA) and angles ($^\circ$) for compounds 33 – 36.....	75

Table 3.16 Crystallographic data for telluraphthalic anhydride, selenaphthalic anhydride and 2-selenaphthalide.	84
Table 3.17 Atomic coordinates ($\times 10^4$) and equivalent isotropic displacement parameters ($\text{\AA}^2 \times 10^3$) for telluraphthalic anhydride (37). U(eq) is defined as one third of the trace of the orthogonalized Uij tensor.	85
Table 3.18 Atomic coordinates ($\times 10^4$) and equivalent isotropic displacement parameters ($\text{\AA}^2 \times 10^3$) for selenaphthalic anhydride (38). U(eq) is defined as one third of the trace of the orthogonalized Uij tensor.	86
Table 3.19 Atomic coordinates ($\times 10^4$) and equivalent isotropic displacement parameters ($\text{\AA}^2 \times 10^3$) for 2-selenaphthalide (39). U(eq) is defined as one third of the trace of the orthogonalized Uij tensor.	87
Table 3.20 Selected bond lengths (\AA) and angles ($^\circ$) with e.s.d's in parentheses for compounds (37), (38) and (39).	90
Table 4.1 Crystallographic data for products (42), (43), (44) and (45).	106
Table 4.2 Atomic coordinates ($\times 10^4$) and equivalent isotropic displacement parameters ($\text{\AA}^2 \times 10^3$) for 1,8-bis(bromomethyl)naphthalene, (42). U(eq) is defined as one third of the trace of the orthogonalized Uij tensor.	107
Table 4.3 Atomic coordinates ($\times 10^4$) and equivalent isotropic displacement parameters ($\text{\AA}^2 \times 10^3$) for , 1,1-diiodo-3,5-naphthotelluracyclohexane, (43). U(eq) is defined as one third of the trace of the orthogonalized Uij tensor.	108
Table 4.4 Atomic coordinates ($\times 10^4$) and equivalent isotropic displacement parameters ($\text{\AA}^2 \times 10^3$) for, 3,5-naphtho-1-telluracyclohexane, (44). U(eq) is defined as one third of the trace of the orthogonalized Uij tensor.	109
Table 4.5 Atomic coordinates ($\times 10^4$) and equivalent isotropic displacement parameters ($\text{\AA}^2 \times 10^3$) for 3,5-naphtho-1-selenacyclohexane, (45). U(eq) is defined as one third of the trace of the orthogonalized Uij tensor.	110
Table 4.6 Selected bond lengths (\AA) and angles ($^\circ$) for 1,8-bis(bromomethyl)naphthalene, (42).	111
Table 4.7 Selected bond lengths (\AA) and angles ($^\circ$) for 1,1-diiodo-3,5-naphthotelluracyclohexane, (43).	111
Table 4.8 Selected bond lengths (\AA) and angles ($^\circ$) for 3,5-naphtho-1-telluracyclohexane, (44).	112

Table 4.9 Selected bond lengths (Å) and angles (°) for 3,5-naphtho-1-selenacyclohexane, (45).	112
Table 4.10 Atomic coordinates ($\times 10^4$) and equivalent isotropic displacement parameters ($\text{\AA}^2 \times 10^3$) for, $\text{C}_{10}\text{H}_{10}\text{Te}_2\text{I}_4 \cdot 2\text{DMF}$, (46). U(eq) is defined as one third of the trace of the orthogonalized Uij tensor.	121
Table 4.11 Selected bond lengths (Å) and angles (°) for $\text{C}_{10}\text{H}_{10}\text{Te}_2\text{I}_4 \cdot 2\text{DMF}$, (46).	122
Table 5.1 Analytical data for RTeBr₃ , RTeBr and RTeI .	135
Table 5.2 Mass spectral data for RTeBr₃ and RTeBr (¹ H, ¹² C and ¹³⁰ Te).	136
Table 5.3 ¹³ C and ¹²⁵ Te NMR data collected for RTeBr and RTeI .	137
Table 5.4 Analytical data for RSeCl , RSeCl/I and RSeI .	140
Table 5.5 Mass spectral data for RSeCl , RSeCl/I and RSeI (¹ H, ¹² C and ⁸⁰ Se).	140
Table 5.6 ¹³ C and ⁷⁷ Se NMR data collected for RSeCl , RSeCl/I and RSeI .	141
Table 5.7 Crystal and experimental data for RTeBr and RTeI .	148
Table 5.8 Atomic coordinates ($\times 10^4$) and equivalent isotropic displacement parameters ($\text{\AA}^2 \times 10^3$) for RTeBr . U(eq) is defined as one third of the trace of the orthogonalized Uij tensor.	149
Table 5.9 Atomic coordinates ($\times 10^4$) and equivalent isotropic displacement parameters ($\text{\AA}^2 \times 10^3$) for RTeI . U(eq) is defined as one third of the trace of the orthogonalized Uij tensor.	150
Table 5.10 Selected bond lengths (Å) and angles (°) with e.s.d's in parentheses for RTeBr and RTeI .	151
Table 5.11 Crystal and experimental data for RSeCl , RSeCl/I and RSeI .	157
Table 5.12 Atomic coordinates ($\times 10^4$) and equivalent isotropic displacement parameters ($\text{\AA}^2 \times 10^3$) for RSeCl . U(eq) is defined as one third of the trace of the orthogonalized Uij tensor.	158
Table 5.13 Atomic coordinates ($\times 10^4$) and equivalent isotropic displacement parameters ($\text{\AA}^2 \times 10^3$) for RSeCl/I . U(eq) is defined as one third of the trace of the orthogonalized Uij tensor.	159
Table 5.14 Atomic coordinates ($\times 10^4$) and equivalent isotropic displacement parameters ($\text{\AA}^2 \times 10^3$) for RSeI . U(eq) is defined as one third of the trace of the orthogonalized Uij tensor.	160

Table 5.15 Selected bond lengths (Å) and angles (°) with e.s.d's in parentheses for RSeCl, RSeCl/I and RSeI.	161
Table 6.1 FTIR bands in the carbonyl region for product from reaction of 2-methylbenzselenazole and [Fe ₃ (CO) ₁₂].	175
Table 6.2 EI mass spectrum registered peaks for product from reaction of 2-methylbenzselenazole and [Fe ₃ (CO) ₁₂] (¹ H, ¹² C, ⁵⁶ Fe and ⁸⁰ Se).	175
Table 6.3 Crystal and experimental data for (48).	181
Table 6.4 Atomic coordinates (x 10 ⁴) and equivalent isotropic displacement parameters (Å ² x 10 ³) for (48). U(eq) is defined as one third of the trace of the orthogonalized Uij tensor.	182
Table 6.5 Selected bond lengths (Å) and angles (°) for compound (48).	183
Table 6.5 Cont. Selected bond lengths (Å) and angles (°) for compound (48).	184
Table 6.6 Crystal and experimental data for (49) and (50).	188
Table 6.7 Atomic coordinates (x 10 ⁴) and equivalent isotropic displacement parameters (Å ² x 10 ³) for C ₈ H ₆ O ₆ Fe ₂ Te ₂ , (49). U(eq) is defined as one third of the trace of the orthogonalized Uij tensor.	189
Table 6.8 Atomic coordinates (x 10 ⁴) and equivalent isotropic displacement parameters (Å ² x 10 ³) for C ₈ H ₆ O ₆ Fe ₂ Se ₂ , (50). U(eq) is defined as one third of the trace of the orthogonalized Uij tensor.	190
Table 6.9 Selected bond lengths (Å) and angles (°) with e.s.d's in parentheses for (48).	191
Table 6.10 Selected bond lengths (Å) and angles (°) with e.s.d's in parentheses for (49).	192
Table 6.10 Cont. Selected bond lengths (Å) and angles (°) with e.s.d's in parentheses for (49).	193
Table 6.11 Mössbauer spectra results for compounds (33), (35), (36), (49) and (50).	199
Table 6.12 Assignment of the Mössbauer peaks.	202
Table 6.13 ¹ H NMR region of CH ₂ group in the heterocyclic ring for products (33), (35) and (36); ¹ H NMR region of CH ₃ group in products (49) and (50).	203
Table 6.14 ¹³ C NMR region of CH ₂ and CO groups in the heterocyclic ring for products (33), (35) and (36); ¹³ C NMR region of CH ₃ and CO groups in products (49) and (50).	204

LIST OF FIGURES

Figure 3.1 ^1H NMR spectrum of $[\text{Fe}(\text{C}_7\text{H}_6\text{Te})(\text{CO})_3]_2$, (33).....	50
Figure 3.2 ^{13}C NMR spectrum of $[\text{Fe}(\text{C}_7\text{H}_6\text{Te})(\text{CO})_3]_2$, (33).....	50
Figure 3.3 ^{125}Te NMR (decoupled) spectrum of $[\text{Fe}(\text{C}_7\text{H}_6\text{Te})(\text{CO})_3]_2$, (33).....	51
Figure 3.4 ^{125}Te NMR (coupled) spectrum of $[\text{Fe}(\text{C}_7\text{H}_6\text{Te})(\text{CO})_3]_2$, (33)	51
Figure 3.5 ^1H NMR spectrum of selenoferrole, $[\text{Fe}_2(\text{C}_7\text{H}_6\text{Se})(\text{CO})_6]$ (35)	
Figure 3.6 ^{13}C NMR spectrum of selenoferrole, $[\text{Fe}_2(\text{C}_7\text{H}_6\text{Se})(\text{CO})_6]$ (35)	59
Figure 3.7 ^1H NMR spectrum of selenoferrole, $[\text{Fe}_3(\text{C}_7\text{H}_6\text{Se})(\text{CO})_8]$ (36)	59
Figure 3.8 ^{13}C NMR spectrum of selenoferrole, $[\text{Fe}_3(\text{C}_7\text{H}_6\text{Se})(\text{CO})_8]$ (36)	60
Figure 3.9 Time dependent ^1H NMR spectrum of selenoferrole, $[\text{Fe}_2(\text{C}_7\text{H}_6\text{Se})(\text{CO})_6]$ (35).....	64
Figure 3.10 Time dependent ^{13}C NMR spectrum of selenoferrole, $[\text{Fe}_2(\text{C}_7\text{H}_6\text{Se})(\text{CO})_6]$ (35).....	64
Figure 3.11 The molecular structure of $[\text{Fe}(\text{C}_7\text{H}_6\text{Te})(\text{CO})_3]_2$ (33)	79
Figure 3.12 The molecular structure of $\text{C}_8\text{H}_6\text{O}_2$ (34)	80
Figure 3.13 The molecular structure of $[\text{Fe}_2(\text{C}_7\text{H}_6\text{Se})(\text{CO})_6]$ (35)	81
Figure 3.14 The molecular structure of $[\text{Fe}_3(\text{C}_7\text{H}_6\text{Se})(\text{CO})_8]$ (36)	82
Figure 3.15 The molecular structure of telluraphthalic anhydride (37).....	91
Figure 3.16 The molecular structure of selenaphthalic anhydride (38)	92
Figure 3.17 The molecular structure of 2-selenaphthalide (39)	93
Figure 4.1 The molecular structure of 1,8-bis(bromomethyl)naphthalene, (42) ...	115
Figure 4.2 The molecular structure of 1,1-diiodo-3,5-naphthotelluracyclohexane, (43).....	116
Figure 4.3 The molecular structure of 3,5-naphtho-1-telluracyclohexane, (44). ...	117
Figure 4.4 The molecular structure of 3,5-naphtho-1-selenacyclohexane, (45) ...	118
Figure 4.5 View of the tetraiodide, together with four weakly-bonded oxygen atoms of neighbouring DMF molecules. Primed atoms are related to the corresponding unprimed atoms by the centre of symmetry at (0,0,0). Atoms O1'' and O1* are related to O1 by the symmetry operations $\frac{1}{2}+x$, $\frac{1}{2}-y$, z and $-\frac{1}{2}-x$, $-\frac{1}{2}+y$, $-z$, respectively.	125
Figure 5.1 ^{77}Se NMR spectrum of RSeCl	142
Figure 5.2 ^{77}Se NMR spectrum of RSeCl/I	142
Figure 5.3 ^{77}Se NMR spectrum of RSeI	143

Figure 5.4 The molecular structure of RTeBr	154
Figure 5.5 The molecular structure of RSeCl	164
Figure 5.6 The molecular structure of RSeCl/I	165
Figure 5.7 The molecular structure of RSeI	166
Figure 6.1 The molecular structure of $[\text{Fe}_2\{\text{C}_6\text{H}_4(\text{NCH}_2\text{CH}_3)\text{Se}\}(\text{CO})_6]$, (48)	185
Figure 6.2 The molecular structure of $[\text{Fe}_2(\mu\text{-TeMe})_2(\text{CO})_6]$, (49)	195
Figure 6.3 The molecular structure of $[\text{Fe}_2(\mu\text{-SeMe})_2(\text{CO})_6]$, (50)	196

LIST OF SCHEMES

Scheme 3.1 Suggested reaction pathway for the reaction of 2-telluraphthalide and $[\text{Fe}_3(\text{CO})_{12}]$	53
Scheme 3.2 Suggested reaction pathway for the reaction of telluraphthalic anhydride and $[\text{Fe}_3(\text{CO})_{12}]$	55
Scheme 3.3 Suggested reaction pathway for the reaction of 2-selenaphthalide and $[\text{Fe}_3(\text{CO})_{12}]$	62
Scheme 5.1 Suggested charge transfer reaction pathway for the formation of RTel	139
Scheme 5.2 Reaction pathway suggested for the formation of RSeCl/I and RSeI	145
Scheme 6.1 Formation of (49) by Bachman <i>et al.</i>	178
Scheme 6.2 Formation of (50) by Mathur <i>et al.</i>	179

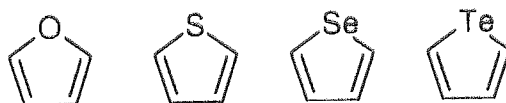
CHAPTER ONE
INTRODUCTION

Introduction

The research described in this thesis relates to the reactions of directly related tellurium and selenium heterocyclic compounds with triiron dodecacarbonyl $[\text{Fe}_3(\text{CO})_{12}]$ and the investigation of the reaction pathway for dechalcogenation reactions. This research originates from the study of desulfurisation of coal. Sulfur heterocyclic compounds were used to model sulfur in coal^{1,2}. These compounds were found to be unreactive with transition metal reagents (see below). Tellurium heterocyclic compounds were used to model the sulfur compounds³. These compounds reacted with transition metal compounds to give novel organometallic compounds (see below). Therefore it was considered to react selenium derivatives of the tellurium compounds, with the transition metal reagent. Selenium derivatives were considered because it may be possible that products corresponding to an earlier stage of the reaction sequence may be isolable.

1.1 Heterocyclic compounds

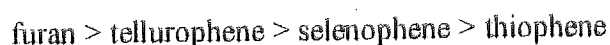
Heterocyclic compounds are cyclic compounds with the ring containing carbon and other elements, the most common being oxygen, nitrogen and sulfur. However, the heteroatom may also be tellurium or selenium (see below). There are a number of heterocyclic rings which are easily opened and do not possess any aromatic properties (for example ethylene oxide).



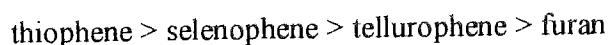
1.1.1 Aromaticity in group 16

The simplest heterocyclic compounds, that exhibit aromatic character in group 16 are furan, thiophene, selenophene, and tellurophene (see above). All of these heterocyclic compounds obey the Hückel rule of aromaticity. The main difference between these heterocyclic systems is the degree of reactivity. But, in general, they follow similar reaction pathways.

It is well known that furan, thiophene and selenophene tend to react with electrophiles by substitution rather than addition. It has also been shown that tellurophene exhibits similar behaviour⁴. The reactivity order observed in all the electrophilic substitutions⁵ examined is (for example the acetylation with acetic anhydride and SnCl_4);



Fringuelli *et al*⁶ have studied the ground state aromaticity of the heterocyclic compounds and have established the order;



To account for the observed order of ground state aromaticities, two properties of the heteroatoms must be taken into consideration; the electronegativity of the heteroatom and the covalent radius. The more electronegative the heteroatom, the more contracted the p orbital is. Hence, conjugation is less efficient. Increasing the covalent radius is unfavorable for good overlap between the p-orbitals of the adjacent carbon atom and the heteroatom.

1.1.2 The carbon-chalcogen bond strength

The strength of a chemical bond M-X is defined as the standard enthalpy change of the reaction in which the bond is broken to form two component atoms, M and X.

Values given in table 1.1 refer to the bond strengths of the gaseous diatomic⁷ species C-X.

Table 1.1 Bond strengths of the gaseous diatomic species C-X

Bond	Enthalpy kJ mol ⁻¹
CO	1076.5 ± 0.4
CS	714.1 ± 1.2
CSe	590.4 ± 5.9

No data can be found regarding the C-Te bond strength. One observation from table 1.1, is that the carbon- chalcogen bond strength in C-X decreases as one goes down group 16. It is reasonable to suppose that the C-Te single bond strengths will follow a similar order.

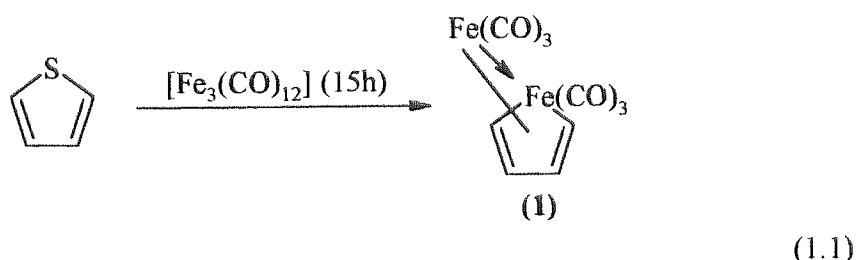
1.2 The co-ordination chemistry of heterocyclic selenium and tellurium compounds

The co-ordination chemistry of selenium and tellurium heterocycles with transition metals has been the subject of relatively little investigation and few examples of their reactivity with transition metals can be found.

1.2.1 The co-ordination chemistry of heterocyclic compounds with trinuclear carbonyls, of Fe or Ru or Os

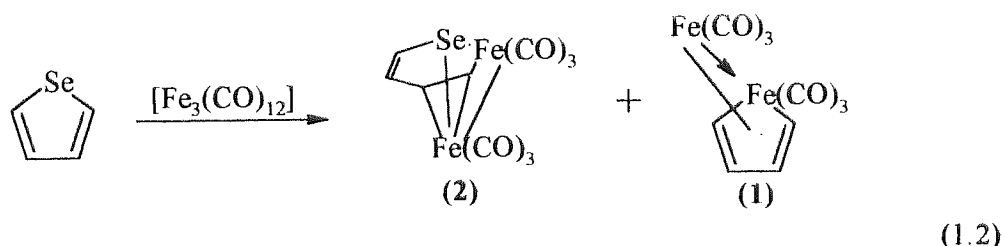
The reactions of thiophene, selenophene and tellurophene with trinuclear carbonyls are outlined below.

In the 1960's, Stone¹ and co-workers discovered that thiophene reacts with [Fe₃(CO)₁₂] giving a low yield (5%) of the first reported ferrole compound [Fe₂(μ-C₄H₄)(CO)₆], (1) (see equation 1.1).

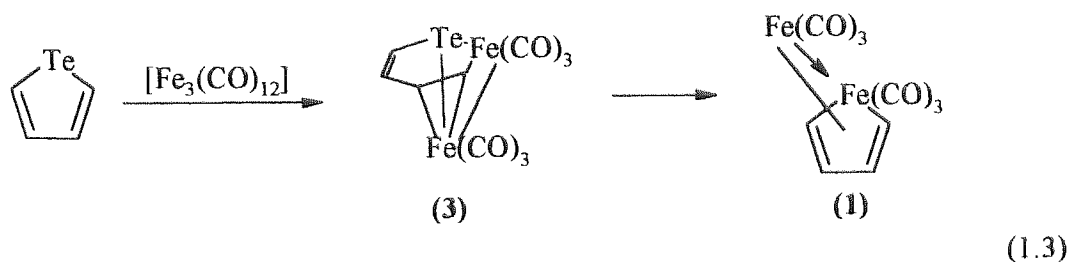


The reaction of thiophene with $[\text{Fe}_3(\text{CO})_{12}]$ was revisited by Ogilvy *et al.*², they reported a similar reaction product to Stone¹. Singh³ and co-workers used microwave heating to accelerate the rate of formation of the ferrole, (1), formed by the reaction of thiophene with $[\text{Fe}_3(\text{CO})_{12}]$. Ogilvy² and co-workers reacted methyl substituted thiophene, which gave improved yields of the corresponding thiaferroles and ferroles, but did not dramatically alter the product ratios.

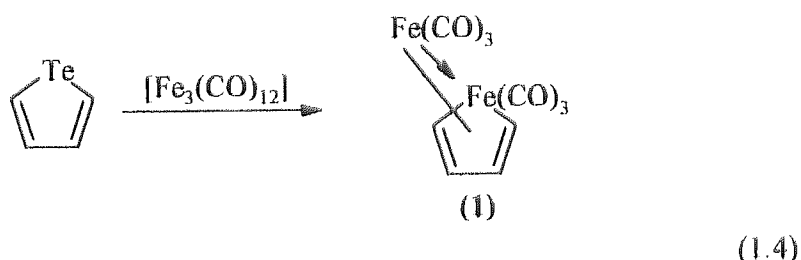
The selenium analogue, selenophene⁸ was reacted under reflux in cyclohexane for 2.5h with $[\text{Fe}_3(\text{CO})_{12}]$ resulting in a 29% yield of the ferrole $[\text{Fe}_2(\mu\text{-C}_4\text{H}_4)(\text{CO})_6]$, (1) and a 34% yield of the selenoferrole $[\text{Fe}_2(\mu\text{-C}_4\text{H}_4\text{Se})(\text{CO})_6]$, (2), (see equation 1.2).



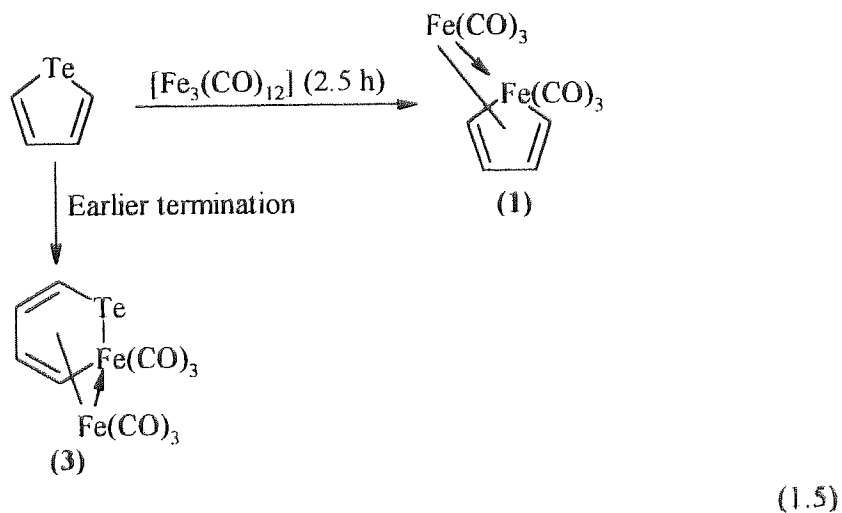
Oefele and Dotzauer⁹ were the first to consider the reaction of tellurophene with triiron dodecacarbonyl. The reactions were carried out in benzene under reflux. This resulted in a black compound $[\text{Fe}_3\text{Te}_2(\text{CO})_9]$ and the ferrole $[\text{Fe}_2(\mu\text{-C}_4\text{H}_4)(\text{CO})_6]$, (1), in an 18% yield. The third compound was believed to be an air sensitive telluraferrole $[\text{Fe}_2(\mu\text{-C}_4\text{H}_4\text{Te})(\text{CO})_6]$, (3), (see equation 1.3).



The reaction of tellurophene⁸ with $[\text{Fe}_3(\text{CO})_{12}]$ in cyclohexane, gave the ferrole $[\text{Fe}_2(\mu\text{-C}_4\text{H}_4)(\text{CO})_6]$, (1), (see equation 1.4). However, no tellurium containing species were isolated.



The reaction of tellurophene³ with $[\text{Fe}_3(\text{CO})_{12}]$ in heptane (2.5 h), gave the ferrole $[\text{Fe}_2(\mu\text{-C}_4\text{H}_4)(\text{CO})_6]$, (1) and a black product, FeTe , which can be considered as a decomposition product of $[\text{Fe}_3\text{Te}_2(\text{CO})_6]$ via the loss of CO and $[\text{Fe}(\text{CO})_5]$ (see equation 1.5). Singh³ and co-workers obtained the telluraferrole, (3), by terminating the reaction earlier (see equation 1.5).

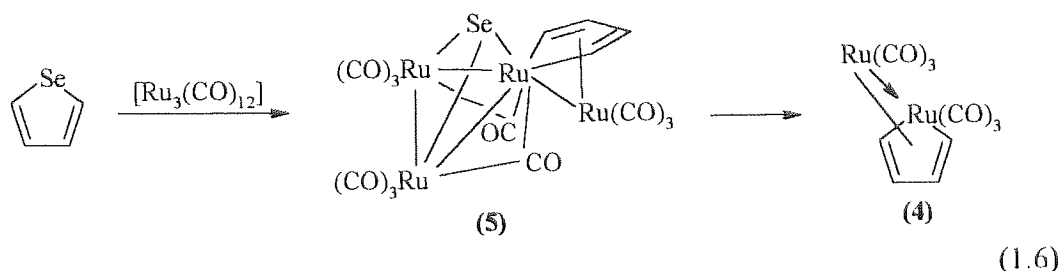


Comparing the reactions of thiophene, selenophene and tellurophene with $[\text{Fe}_3(\text{CO})_{12}]$ it can be seen that tellurophene and thiophene give only the ferrole in 18% and 5% yields respectively. However selenophene gives both the ferrole (29%) and the selenoferrole (34%). If one considers the end point of this reaction to be the formation of the ferrole product and the chalcogenoferroles to be intermediates, then the reaction of tellurophene and $[\text{Fe}_3(\text{CO})_{12}]$ proceeded to completion as the ferrole was formed. However the reaction with selenophene resulted in a selenoferrole which corresponds to a compound that can be considered to be a product from earlier in the reaction pathway. Therefore one could consider that the reaction of selenophene with $[\text{Fe}_3(\text{CO})_{12}]$ gives products originating from early stages of the reaction pathway. On comparing the yields of the ferrole one may suggest that the reactivity of thiophene is less than that of selenophene, therefore giving the reactivity series:

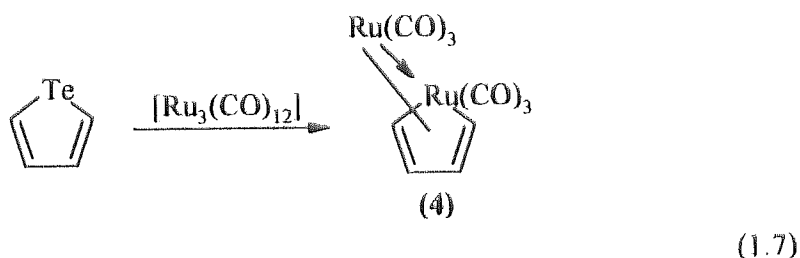


Arce⁸ and co-workers also demonstrated the ability of trinuclear transition metal carbonyls to extrude selenium and tellurium atoms from tellurophene and selenophene. Reactions of $[\text{Fe}_3(\text{CO})_{12}]$ (see above), $[\text{Ru}_3(\text{CO})_{12}]$ and $[\text{Os}_3(\text{CO})_{10}(\text{MeCN})_2]$ with selenophene and tellurophene were studied.

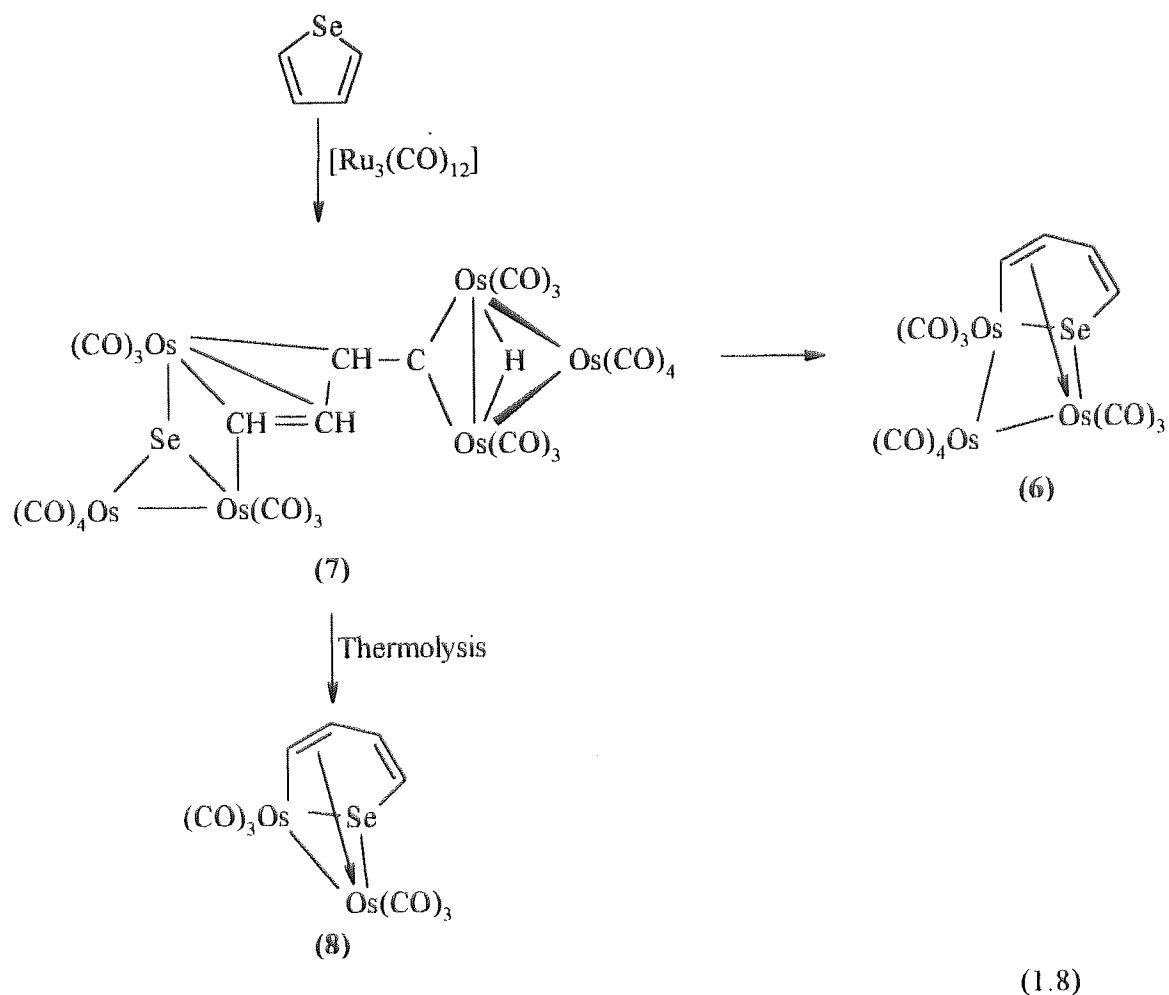
The reaction of selenophene with triruthenium dodecacarbonyl⁸ in dry THF for 3.5h, leads to the extrusion of the heteroatom from the heterocycle, giving rise to $[\text{Ru}_2(\mu\text{-C}_4\text{H}_4)(\text{CO})_6]$, (**4**), which is very similar to the ferrole (**1**). One could suggest that the second product $[\text{Ru}_4(\mu\text{-Se})(\mu\text{-C}_4\text{H}_4)(\text{CO})_{11}]$, (**5**), formed is an intermediate compound in the reaction pathway in the formation of (**4**) (see equation 1.6).



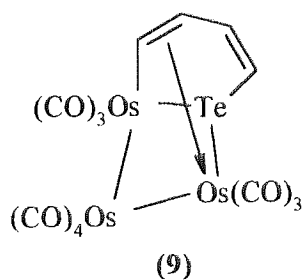
The reaction of tellurophene with triruthenium dodecacarbonyl only afforded the detellurated compound $[\text{Ru}_2(\mu\text{-C}_4\text{H}_4)(\text{CO})_6]$, (4), (see equation 1.7).



In the same work⁸, selenophene was shown to react with triosmium carbonyl in cyclohexane, under reflux to yield an insertion product $[\text{Os}_3(\text{C}_4\text{H}_4\text{Se})(\text{CO})_{10}]$, (6), in a 35% yield. The second product, a bridged hydride complex of $[\text{Os}_6(\mu\text{-H})(\mu_3\text{-Se})(\mu_4\text{-C}_4\text{H}_3)(\text{CO})_{20}]$, (7), could be considered to be an intermediate compound in the reaction pathway (see equation 1.8). Thermolysis of compound (7), in a solution of n-octane under reflux, led to the loss of $\text{Os}(\text{CO})_4$ yielding the product $[\text{Os}_2(\text{C}_4\text{H}_4\text{Se})(\text{CO})_6]$, (8), (see equation 1.8).



The reaction of tellurophene with triosmium carbonyl resulted in the insertion compound $[\text{Os}_3(\text{C}_4\text{H}_4\text{Te})(\text{CO})_{10}]$, (9), in a 38% yield.

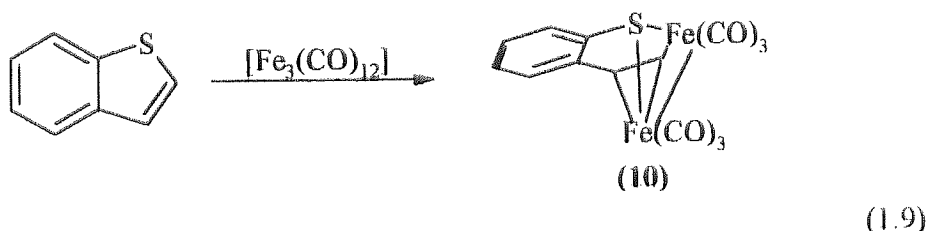


The reactions of trinuclear clusters with selenophene and tellurophene are believed to follow similar reaction pathways. The above reactions of selenophene with trinuclear clusters produced intermediate products. However the reactions of tellurophene with

trinuclear clusters gave no intermediate compounds. Therefore one can assume that all the intermediate compounds formed are converted to the final product.

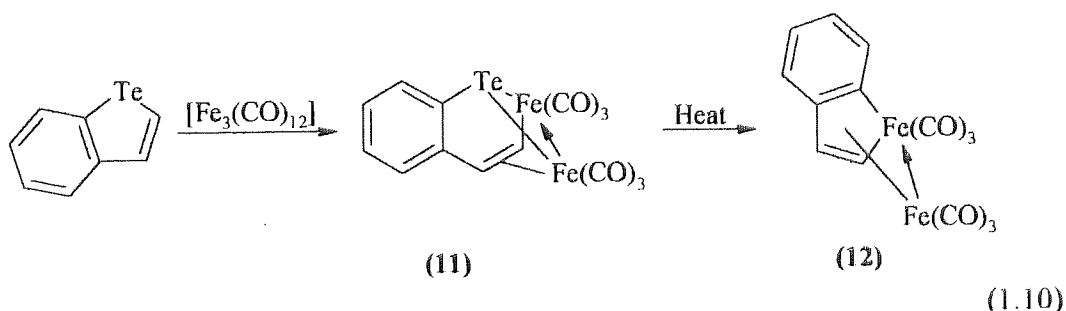
The reactions of benzo[b]thiophene or benzo[b]tellurophene with trinuclear carbonyls are outlined below.

The reaction of benzo[b]thiophene² with $[\text{Fe}_3(\text{CO})_{12}]$ in benzene, under reflux, after 18hrs gave a 49% yield of benzothiaferrole $[\text{Fe}_2(\text{C}_8\text{H}_6\text{S})(\text{CO})_6]$, (10), (see equation 1.9).



Ogilvy *et al.* also showed that thiaferroles are precursors to ferroles, hence establishing plausible reaction intermediate compounds.

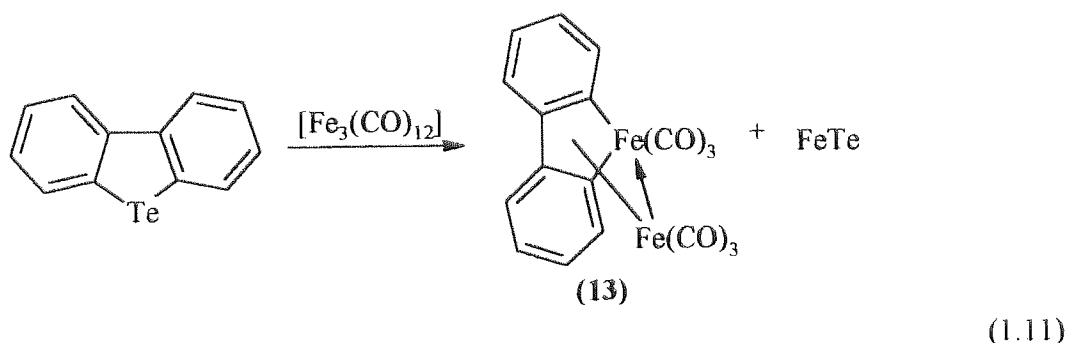
The reaction of benzo[b]tellurophene¹⁰ with $[\text{Fe}_3(\text{CO})_{12}]$ in dry THF, under reflux, after 1.5h, resulted in a 15% yield of the telluraferrole $[\text{Fe}_2(\text{C}_8\text{H}_6\text{Te})(\text{CO})_6]$, (11), and a 7% yield of the ferrole $[\text{Fe}_2(\text{C}_8\text{H}_6)(\text{CO})_6]$, (12), (see equation 1.10).



The reactions of dibenzothiophene and dibenzotellurophene with trinuclear carbonyls are outlined below.

Dibenzothiophene does not react with $[\text{Fe}_3(\text{CO})_{12}]$ ².

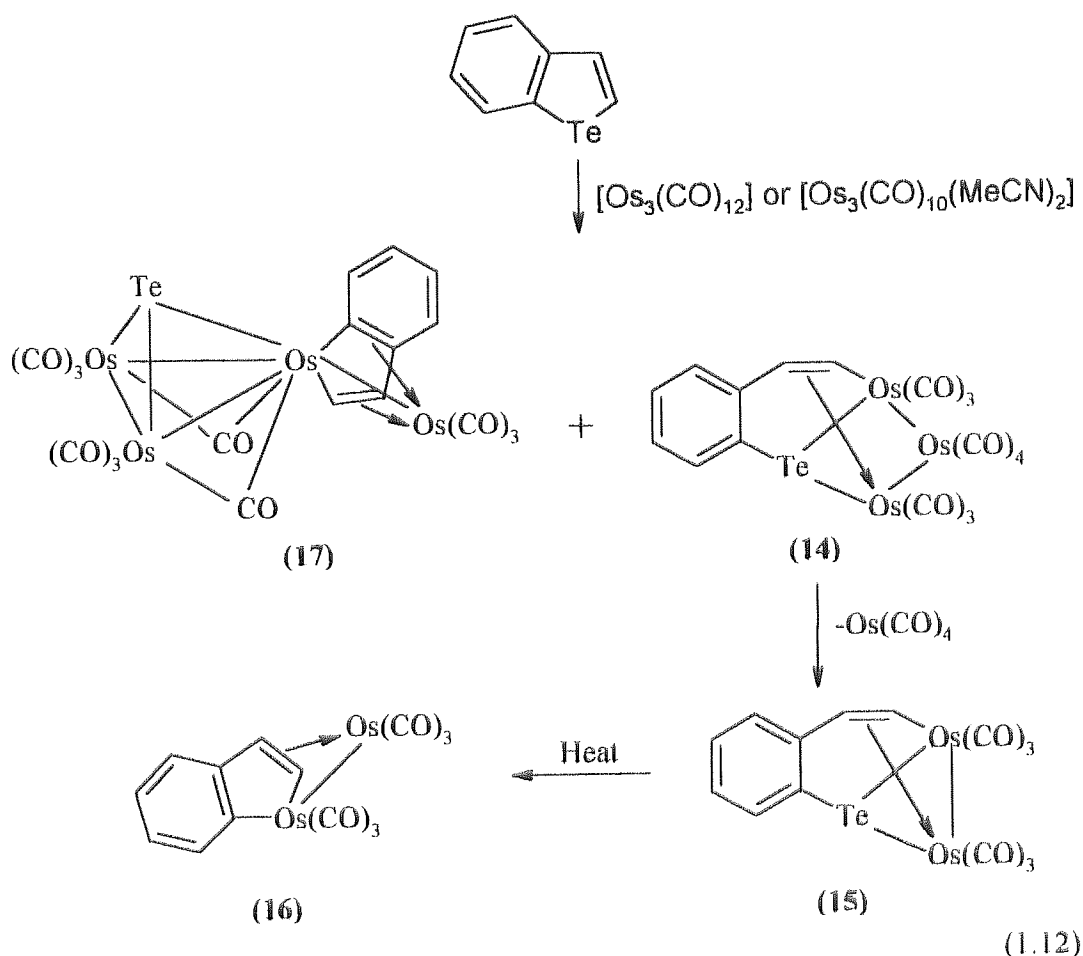
The dibenzotellurophene³ undergoes detelluration, when it is reacted with $[\text{Fe}_3(\text{CO})_{12}]$ to give dibenzoferrole, (13), and FeTe (see equation 1.11).



One could suggest that the reactions are more likely to proceed to completion with the heterocycles containing tellurium. One could also presume that the reactions with the corresponding selenium analogues produce materials that correspond to an earlier stage of the reaction sequence.

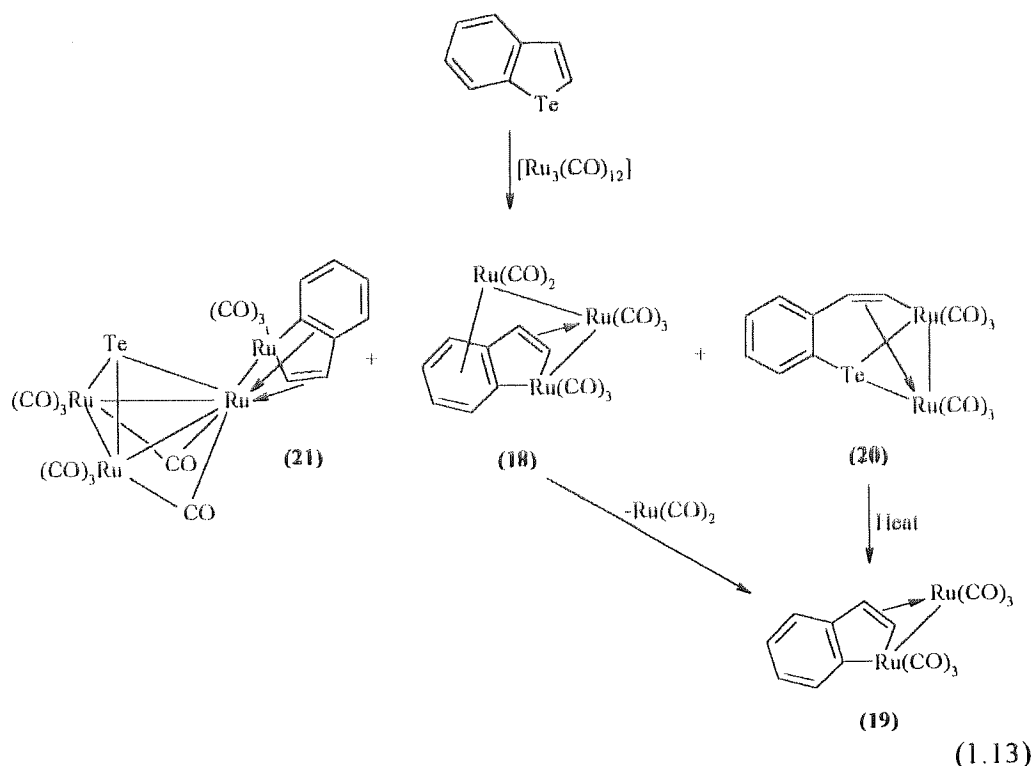
Arce¹⁰ and co-workers reacted benzo[b]tellurophene with trinuclear carbonyls of $[\text{Fe}_3(\text{CO})_{12}]$ (see above), $[\text{Ru}_3(\text{CO})_{12}]$, $[\text{Os}_3(\text{CO})_{12}]$ and $[\text{Os}_3(\text{CO})_{10}(\text{MeCN})_2]$, under similar conditions to give insertion products or to give detellurated products (see below).

Benzo[b]tellurophene reacts with $[\text{Os}_3(\text{CO})_{10}(\text{MeCN})_2]$ in THF, under reflux, for 1h to give the product $[\text{Os}_3(\mu\text{-C}_8\text{H}_6\text{Te})(\text{CO})_{10}]$, (14). $[\text{Os}_3(\text{CO})_{12}]$ reacts with benzo[b]tellurophene in THF, under reflux, for 10h to afford compound (14), a dinuclear compound of $[\text{Os}_2(\mu\text{-C}_8\text{H}_6\text{Te})(\text{CO})_6]$, (15), an osmametallaindene compound $[\text{Os}_2(\mu\text{-C}_8\text{H}_6)(\text{CO})_6]$, (16) and $[\text{Os}_4(\mu\text{-C}_8\text{H}_6)(\mu_3\text{-Te})(\text{CO})_{11}]$, (17) (see equation 1.12).



Compound (14) contains a doubly-bridging ring-opened benzo[b]tellurophene ligand (see above); the C_8H_6Te ligand is a six-electron donor co-ordinated through a μ -Te (three-electron donor) atom and a μ - η^2 -vinyl (three-electron donor) C_8H_6 group. The thermal treatment of (14) in heptane, under reflux, led to the loss of the $Os(CO)_4$ unit giving (15). Thermolysis of (15) in n-octane, under reflux, resulted in a detellurated compound, (16). Arce¹⁰ and co-workers did not have any clear evidence for the chemical route to cluster (17), but suggested that the cluster is formed by the oxidative addition of a C-Te bond of the benzo[b]tellurophene ring to an osmium atom, followed by subsequent transfer of Te to a μ_3 -position as the other C-Te is broken.

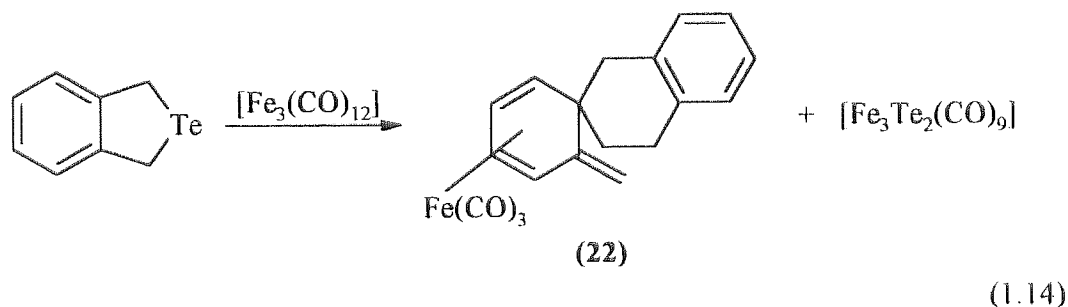
Benzo[b]tellurophene reacts with $[\text{Ru}_3(\text{CO})_{12}]$ to yield four products. The first two compounds are $[\text{Ru}_3(\text{C}_8\text{H}_6)(\text{CO})_8]$, (18) and $[\text{Ru}_2(\mu\text{-C}_8\text{H}_6)(\text{CO})_6]$, (19), which are derived from benzo[b]tellurophene by substitution of a Te atom by a $[\text{Ru}(\text{CO})_3]$ moiety. The third is a insertion product $[\text{Ru}_2(\text{C}_8\text{H}_6\text{Te})(\text{CO})_6]$, (20) and the fourth is $[\text{Ru}_4(\text{C}_8\text{H}_6)(\text{Te})(\text{CO})_{11}]$, (21) (see equation 1.13).



The products obtained by Arce¹⁰ and co-workers for the reaction of benzo[b]tellurophene with $[\text{Ru}_3(\text{CO})_{12}]$ are very similar to the compounds obtained by the reaction of the triosmium carbonyls.

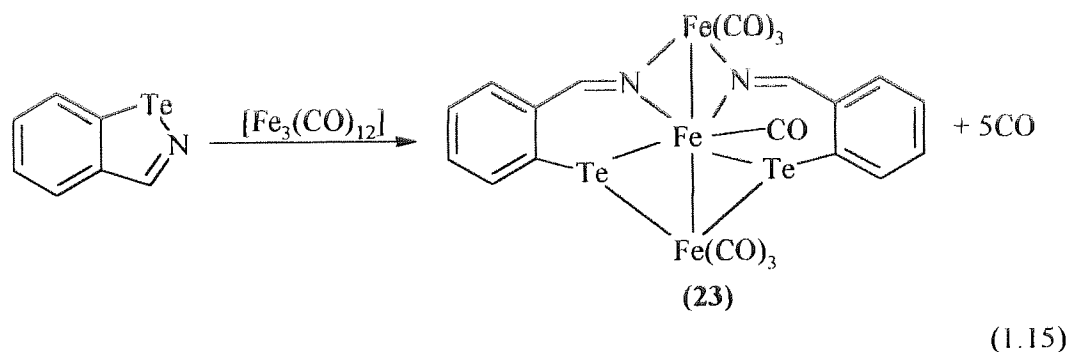
Arce and co-workers have shown that the trinuclear carbonyls react with benzo[b]tellurophene in a similar manner, to give non-hydridic compounds containing the open-chain ligands $\text{C}_6\text{H}_4\text{CHCHTe}$ or the fragments Te and C_8H_6 as bridging ligands, for which a C-Te rather than a C-H bond has been broken.

2-Telluraindane³ was reacted with $[\text{Fe}_3(\text{CO})_{12}]$ to give a novel complex $[\text{Fe}(\text{CO})_3(\text{C}_{16}\text{H}_{16})]$, (22) and a cluster compound, $[\text{Fe}_3\text{Te}_2(\text{CO})_9]$ (see equation 1.14).



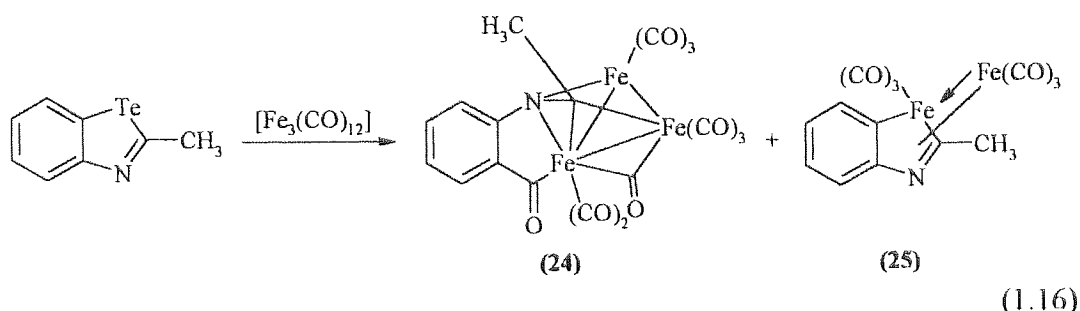
Badyal¹¹ and co-workers demonstrated the potential of heterocyclic compounds containing both tellurium and nitrogen in the heteroring, as precursors for novel organoiron compounds.

The reaction of benzisotellurazole¹¹ with $[\text{Fe}_3(\text{CO})_{12}]$ gave a dark green compound, $[\text{Fe}_3\{\text{C}_6\text{H}_4(\text{CHN})\text{Te}\}_2(\text{CO})_7]$, (23), (see equation 1.15)



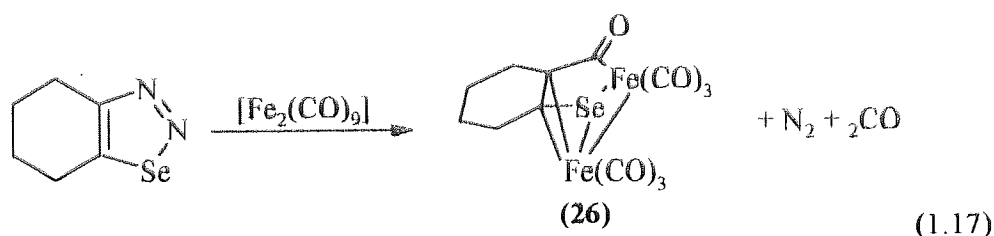
The centre iron in compound (23) is seven co-ordinated whereas the outer two irons are six co-ordinated. This is the first time this type of system involving single or double bridging by nitrogen and tellurium of adjacent iron atoms in a three iron chain has ever arisen within the literature.

The reaction of 2-methylbenzotellurazole¹¹ with $[\text{Fe}_3(\text{CO})_{12}]$ yielded three major products; a cluster compound $[\text{Fe}_3\text{Te}_2(\text{CO})_9]$ and two detellurated compounds $[\text{Fe}_3\{\text{C}_6\text{H}_4(\text{CO})\text{NCCH}_3\}(\text{CO})_9]$, (24) and $[\text{Fe}_2(\text{C}_8\text{H}_7\text{N})(\text{CO})_6]$, (25), (see equation 1.16).



Badyal and co-workers suggested that the three reaction products arose from a complex reaction sequence, involving the detelluration of the heterocycle and the replacement of the tellurium by both an iron atom and an inserted carbonyl group.

Pettersen¹² reacted cyclohexeno-1,2,3-selenadiazole with diiron nonacarbonyl yielding deep red crystals with the formula $[\text{Fe}_2(\text{C}_6\text{H}_8(\text{CO})\text{Se})(\text{CO})_6]$, (26), (see equation 1.17).

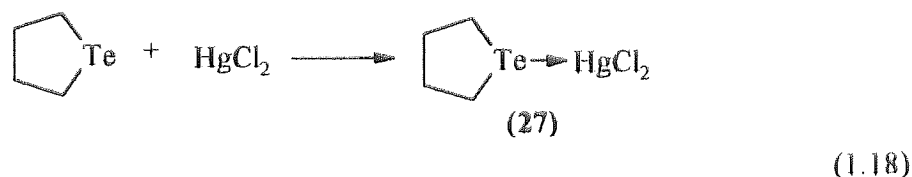


The structure analysis of the selenoferrole (see equation 1.17) indicates retention of one of the bridging carbonyls from $[\text{Fe}_2(\text{CO})_9]$, which is bonded to the iron atom and to a delocalized sp^2 carbon atom of the cyclohexene ring.

Badyal¹¹ and Pettersen¹² have shown that the presence of nitrogen in the heterocyclic ring provides an attractive feature for these reactions. These compounds can be seen as precursors for the formation of novel organometallic compounds. Therefore, it could be suggested that a selenium and nitrogen containing heterocyclic compound would show similar reactivity. It would also be interesting to see whether the $[\text{Fe}_3(\text{CO})_{12}]$ reagent would be reactive towards the nitrogen or the selenium.

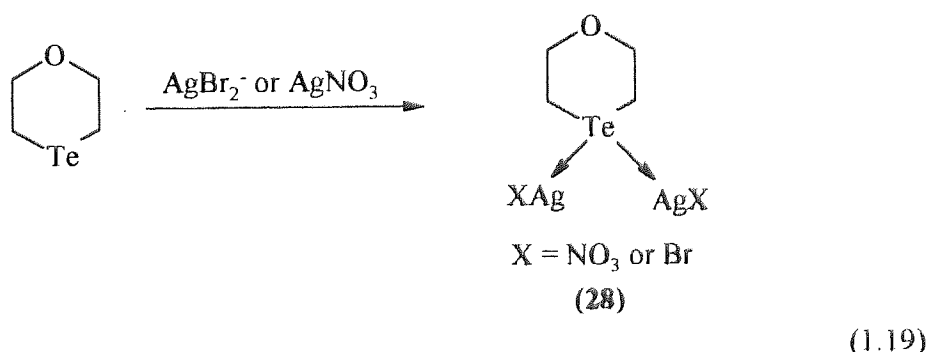
1.2.2 The co-ordination chemistry of heterocyclic compounds containing a tellurium or selenium heteroatom with transition metals

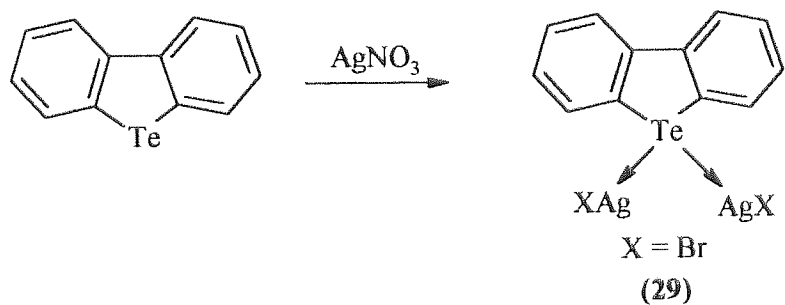
The first example of the co-ordination of a tellurium heterocycle with a transition metal was reported in 1931 by Morgan and Burstall¹³ who reacted telluracyclopentane with mercury(II) chloride to yield the complex $[\text{HgCl}_2(\text{C}_4\text{H}_8\text{Te})]$, (27), (see equation 1.18).



The telluracyclopentane displays strong Lewis basicity compared to tellurophene due to non-delocalisation of the lone pair of electrons on the tellurium atom, enabling it to co-ordinate strongly to the soft Lewis acid HgCl_2 .

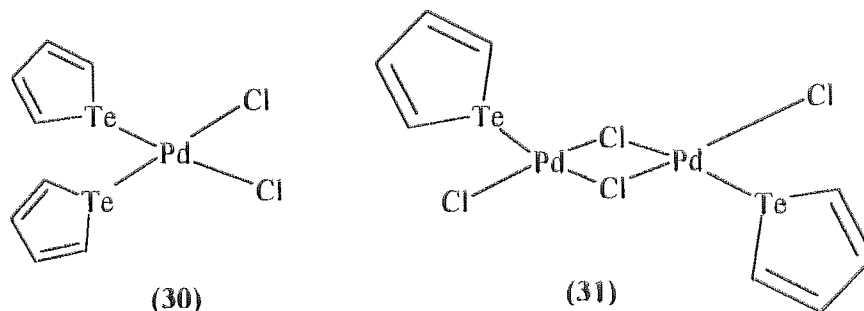
Complexes of the formula $(\text{AgX})_2\text{L}$, where $\text{L} = 1\text{-oxa-4-telluracyclohexane}$, $\text{X} = \text{NO}_3$ or Br^{14} , (28); $\text{L} = \text{dibenzotellurophene}$, $\text{X} = \text{Br}^{15}$, (29), were prepared by the addition of an aqueous solution of AgNO_3 or AgBr_2^- to an acetone solution of the ligand (see equation 1.19 and 1.20).





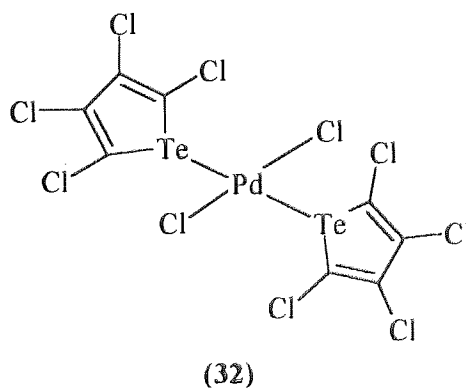
(1.20)

Monomeric⁹ (30) and dimeric⁹ (31) complexes were obtained from the reaction of Na_2PdCl_4 and tellurophene in methanol at 40-50°C.



Reaction of a suspension of the dimeric complex (31) in CH_2Cl_2 with excess tellurophene gave the monomer, (30).

Reaction of Na_2PdCl_4 in methanol with tetrachlorotellurophene gave a monomeric complex, [*trans*- $\text{PdCl}_2(\text{TeC}_4\text{Cl}_4)$], (32).



1.3 Kinetic stabilisation of organotellurium(II) derivatives (RTeX ; X = electronegative group) by intramolecular co-ordination

In general, organoselenium chemistry is much more advanced in many areas than organotellurium chemistry. However the chemistry of intramolecular stabilised organotellurium derivatives, where molecules stabilized by *intra*-molecular co-ordinate bonds^{16,17,18,19} is much more advanced than the corresponding selenium chemistry. Organotellurium(II) derivatives have a general formula of RTeX , where in the context of this thesis X = a electronegative group, e.g. halogen.

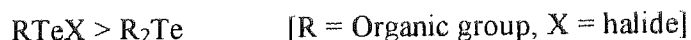
Selenium and tellurium are both in group 16 and one would expect that the elements will have many chemical similarities. It is therefore reasonable to expect that intramolecular stabilized compounds may also be synthesized with selenium.

1.3.1 Order of Lewis acidity in organotellurium compounds

The Lewis acidity of tellurium decreases as the number of organic groups attached to the tellurium atom increases, giving the following order of acidity in tellurium(IV) compounds.



Also the same effect can be seen in tellurium(II) compounds.



1.3.1.2 Short-range intermolecular co-ordination

Short-range intermolecular co-ordination is found in organotellurium(II) monohalides and occurs when a halogen bridges two Lewis acidic centres.



1.3.1.3 Long-range intermolecular co-ordination

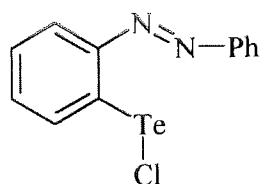
Long-range intermolecular co-ordination can be shown as;



The Te-----X bonds are much longer than the sum of the covalent radii of tellurium and X, but shorter than the van der Waals distance. This type of bonding is known as secondary bonding.

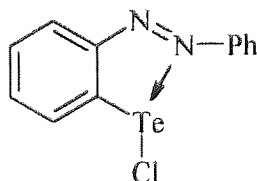
1.3.1.4 Intra-molecular co-ordination

Intra-molecular co-ordination occurs when it is sterically feasible for the acidic and basic centres to interact within the molecule. The co-ordination may only occur when the organic group attached to the tellurium atom has a donor group in it, for example phenylazophenyl(C,N')tellurium(II) chloride¹⁷.



Te	=	Centre of Lewis acidity
N	=	Centre of Lewis basicity

The molecule shown above may undergo *intra*-molecular co-ordination because the aryl- group has a basic functional group in the *ortho*- position to the tellurium. Therefore, co-ordination will occur between the tellurium and the nitrogen atom, as shown below.



Intramolecular co-ordination occurs through a dative bond. If one considers a dative bond to be similar to a covalent bond then one may consider *intra*-molecular compounds to be *pseudo*-heterocyclic compounds. Reaction of these *pseudo*-

heterocyclic compounds with $[\text{Fe}_3(\text{CO})_{12}]$ might produce new areas of chemistry and novel compounds.

CHAPTER TWO
GENERAL EXPERIMENTAL AND PHYSICAL TECHNIQUES

2.1 General experimental and physical techniques

2.1.1 Reactions in an inert atmosphere

Experiments involving moisture sensitive or air sensitive reagents were performed under an atmosphere of pure argon using standard Schlenk line techniques.

2.1.2 Chemicals and solvents

Most chemicals used were obtained from either Aldrich Chemical Company or Lancaster Synthesis Ltd. Tellurium / selenium powder, tellurium / selenium tetrachloride and tellurium / selenium tetrabromide were used as sources of tellurium and selenium. Rhodium trichloride was supplied by Johnson and Matthey Ltd. Common solvents were supplied by the Department of Chemical Engineering and Applied Chemistry and were dried using standard methods, where necessary, prior to use. Analytically pure solvents were used without further purification.

2.1.3 Elemental analysis

Micro-elemental analyses for carbon, hydrogen and nitrogen were carried out by Medac Ltd., Department of Chemistry, Brunel University.

2.1.4 Melting points

A Gallenkamp and Griffin electrically heated melting point apparatus with a mercury thermometer was used to determine all melting points.

2.1.5 Infra-red spectroscopy

Infra-red spectra were recorded on a Bio-rad FTS-40A spectrometer incorporating a 600 microwatt 632.8 nm CW class II laser. The spectra were obtained using a resolution of 8 cm⁻¹ and 16 scans. KBr discs were used for solid samples and liquids

were analysed between NaCl cells. The range investigated was from 4000 – 400 cm^{-1} (with a KBr beam splitter).

2.1.6 Nuclear magnetic resonance spectroscopy

Nuclear magnetic resonance (NMR) spectra (^1H , ^{13}C , ^{77}Se and ^{125}Te) were recorded within the Department of Chemical Engineering and Applied Chemistry using a Bruker AC-300 instrument at 300.13, 75.47, 57.3 and 94.71 MHz respectively. Tetramethylsilane was used as the internal reference for ^1H and ^{13}C . ^{77}Se solution data was collected using phenylselenium chloride as a reference. ^{125}Te solution data was collected using dimethyltelluride as the reference.

2.1.7 Mass spectroscopy

The electron impact (EI), chemical ionisation (CI) and fast atom bombardment (FAB) mass spectra of some compounds were obtained *via* the EPSRC mass spectrometry service, University College, Swansea. Where appropriate, mass spectral peaks were assigned by considering ^{56}Fe , ^{80}Se and ^{130}Te as the most abundant isotopes.

2.1.8 Mössbauer spectroscopy

^{57}Fe Mössbauer spectra were determined on an ES-Technology MS105 constant acceleration spectrometer with a 925 MBq ^{57}Co source in a rhodium matrix. Spectra were recorded at 77 K and referenced against an iron foil (25 μm) at 298 K. Samples were prepared by grinding with boron nitride before transfer to the sample holder.

2.1.9 X-ray crystallography

Suitable crystals for X-ray crystallography technique were obtained by recrystallisation or slow evaporation from high purity solvents. Preliminary

examinations of single crystals were performed using an optical microscope under crossed polarisers in order to check the quality of the crystals.

Cell dimensions and intensity data for some crystals were measured with an Enraf-Nonius CAD4 diffractometer operating in the ω - 2θ scan mode using MoK_α radiation. The angular range for the data collected was 2 - 25° and three standard reflections were measured every one / two hours to check the stability of the system. The structures were determined by direct methods with SHELXS 86 and refined by least squares using anisotropic thermal parameters for the heavier atoms. Hydrogen atoms were placed in calculated positions, riding on their respective bonding atoms.

Data for some crystals was collected on a Rigaku R-axis II area detector diffractometer using graphite monochromated MoK_α radiation.

CHAPTER THREE

THE REACTIONS OF FIVE MEMBERED HETEROCYCLIC SYSTEMS CONTAINING EITHER TELLURIUM OR SELENIUM AS THE HETEROATOM WITH TRIIRON DODECACARBONYL

3.1 Introduction

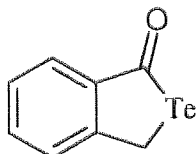
In three recent papers^{3,11,20} it has been shown that heterocyclic compounds containing only tellurium^{3,20}, or containing both tellurium and nitrogen¹¹, may act as precursors for some novel and interesting new organometallic derivatives of iron^{3,11} or rhodium²⁰. Several, although not all, of the products obtained involved detelluration of the heterocyclic molecule. This probably reflects the relatively low carbon-chalcogen bond strengths in the compounds, compared with the sulfur analogues which were generally less reactive under similar conditions^{3,21,22}.

Reactions are more likely to proceed to completion with the heterocycles containing tellurium. If, however the corresponding selenium analogues were to be considered, it is possible that products corresponding to an earlier stage of the reaction sequence may be isolable. This is because the carbon – selenium bond strength is stronger than the carbon – tellurium bond strength. In this chapter we consider reactions of $[\text{Fe}_3(\text{CO})_{12}]$ with selenium and tellurium heterocyclic analogues.

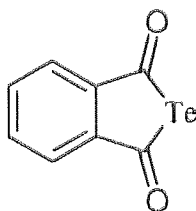
3.2 Experimental

3.2.1 Reactions of tellurium heterocycles

3.2.1.1 Preparation of heterocyclic tellurium compounds



2-Oxo-2,5-dihydrobenzotellurophene (2-telluraphthalide)²³



Telluraphthalic anhydride²⁴

The above heterocycles were prepared using literature methods^{23,24}. The analyses of the above materials were in good agreement with the literature values^{23,24}. Also the X-ray structure of telluraphthalic anhydride has been determined (see section 3.4.2).

3.2.1.2 Reaction of triiron dodecacarbonyl with 2-telluraphthalide

2-Telluraphthalide (1 g, 4 mmol) and $[\text{Fe}_3(\text{CO})_{12}]$ (2.05 g, 4 mmol) were refluxed, with stirring, in the dark in toluene (25 cm³) for 4.5 h. The reaction mixture was cooled to room temperature and filtered to give a dark red filtrate, and a residual black solid which adhered to the sides of the flask. The solvent was removed from the filtrate *in vacuo* leaving a red solid. The red solid was recrystallised from hexane to give bright red needles, (33), which were dried under vacuum. The red crystals decomposed at temperatures greater than 220°C. {0.39 g, 24% based on $\text{Fe}_3(\text{CO})_{12}$ }.

Crystals suitable for X-ray diffraction measurements were grown by cooling a concentrated hexane solution (See section 3.4.1).

3.2.1.3 Reaction of triiron dodecacarbonyl with telluraphthalic anhydride

Telluraphthalic anhydride (0.52g, 2.0 mmol) and $[\text{Fe}_3(\text{CO})_{12}]$ (1g, 2.0 mmol) were refluxed, with stirring, in the dark in toluene (25 cm³) over 4.5 h. On cooling to room temperature, the reaction mixture was filtered to give an orange/red filtrate and a residual black solid which adhered to the side of the flask. The solvent was removed from the filtrate in *vacuo* to give an orange solid. Hot hexane was used to extract a light orange solution, leaving a very small amount of a dirty white residue. The dirty white residue was discarded and the hexane removed from the light orange solution giving a light brown (tan) coloured product. The light brown solid was recrystallised from hexane to give light brown (tan) needle like crystals of phthalide (**34**) which were dried under vacuum. M.p. of (**34**) 70-71°C (Lit²⁵ m.p. 72-74°C). {0.11g, 41% based on $[\text{Fe}_3(\text{CO})_{12}]$ }.

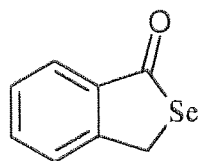
Crystals suitable for X-ray diffraction measurements of (**34**) were grown by cooling a concentrated acetone solution (see section 3.4.1).

Telluraphthalic anhydride (0.52g, 2.0 mmol) in toluene (25 cm³) was refluxed in the dark for 4.5 h. The work up of the reaction mixture was carried out as above. Only the starting materials were recovered.

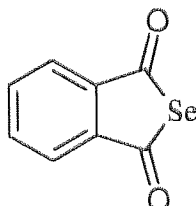
$[\text{Fe}_3(\text{CO})_{12}]$ (1g, 2.0 mmol) in toluene (25 cm³) was refluxed in the dark for 4.5 h. The work up of the reaction mixture was carried out as above. Only the starting materials were recovered.

3.2.2 Reactions of selenium heterocycles

3.2.2.1 Preparation of heterocyclic selenium compounds



2-Selenaphthalide²⁶



Selenaphthalic anhydride²⁴

The above heterocycles were prepared using literature methods^{24,26}. The analyses of the above materials were in good agreement with the literature values^{24,26}. The X-ray structures of 2-selenaphthalide and selenaphthalic anhydride have been determined (see section 3.4.2).

3.2.2.2 Reaction of triiron dodecacarbonyl with 2-selenaphthalide

2-Selenaphthalide (0.79g, 4 mmol) and $[\text{Fe}_3(\text{CO})_{12}]$ (2.05g, 4 mmol) were refluxed, with stirring, in the dark with toluene (25 cm³) over 4.5 h. On cooling to room temperature the reaction mixture was filtered to give a deep red filtrate and a residual black solid which adhered to the sides of the flask. The solvent was removed from the filtrate *in vacuo* to give a deep red oil. The deep red oil was chromatographed on a column of silica gel (pore diameter *ca.* 6 nm) giving a red band followed by another smaller red band, and finally a pale yellow band. Elution with chloroform/hexane (1:1) and removal of the solvent gave a deep red solid, (**35**), from the first eluate, a

black solid, (**36**), from the second eluate, and pale orange crystals from the third eluate (unreacted 2-selenaphthalide).

The deep red solid, (**35**), was recrystallised from boiling hexane yielding red crystals: m.p. 190-192°C (dec.). {0.90g, 50 % based on $\text{Fe}_3(\text{CO})_{12}$ }

The black solid, (**36**), was recrystallised from boiling hexane yielding black crystals: m.p. 159-160°C (dec.). (0.048g, 2 % based on $\text{Fe}_3(\text{CO})_{12}$)

Crystals suitable for X-ray diffraction measurements were grown by cooling a concentrated chloroform/hexane (1:1) solution for (**35**) and a solution in chloroform for (**36**) (see section 3.4.1).

3.2.2.3 Reaction of triiron dodecacarbonyl with selenaphthalic anhydride

Selenaphthalic anhydride (0.49g, 2.3 mmol) and $[\text{Fe}_3(\text{CO})_{12}]$ (1.15g, 2.3 mmol) were refluxed, with stirring, in the dark in toluene (25 cm³) over 4.5 h. On cooling to room temperature, the reaction mixture was filtered to give a deep red filtrate and a residual black solid which adhered to the sides of the flask. The solvent was removed from the filtrate *in vacuo* to give a red solid. The red solid was chromatographed on a column of silica gel (pore diameter ca. 6nm) giving a red band followed by a colourless band (observed by TLC on UV-active silica gel TLC plates). Elution with chloroform/hexane (2:1) and removal of the solvent gave a red solid from the first eluate and pale yellow crystals from the second eluate which were shown to be unreacted selenaphthalic anhydride. The first component has, to date, defied attempts to characterise it: found: C, 27.73; H, 2.40. FTIR (KBr) $\nu(\text{CO})$: 2072 and 1958 cm⁻¹.

3.3 Results and discussion

3.3.1 Reaction of triiron dodecacarbonyl with 2-telluraphthalide

The products obtained from this reaction (4.5 hours) were bright red needles, (**33**) (decom. > 220°C) and a black solid residue. The yield of the product was 0.39g or 24% based on $\text{Fe}_3(\text{CO})_{12}$. Data from the FTIR spectrum in the carbonyl region for the bright red crystals are recorded in table 3.1. The EI mass spectrum registered peaks at $m/z = 277$, $[\text{C}_7\text{H}_4\text{FeTe}]^+$; 91, $[\text{C}_7\text{H}_7]^+$; 77, $[\text{C}_6\text{H}_5]^+$.

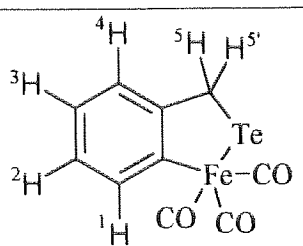
Table 3.1 FTIR bands in the carbonyl region for product from reaction of 2-telluraphthalide and $[\text{Fe}_3(\text{CO})_{12}]$.

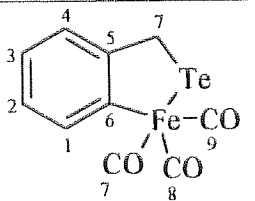
Bright red crystals KBr, $\nu(\text{CO}) \text{ cm}^{-1}$
2049
1980
1953

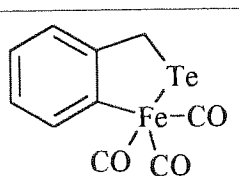
The FTIR band pattern for the bright red crystals in the carbonyl region together with the mass spectrum implies heterocyclic product, $[\text{Fe}(\text{C}_7\text{H}_6\text{Te})(\text{CO})_3]_2$ (**33**). This was further confirmed by elemental analysis:

Calculated (%)	C, 33.5	H, 1.67	$\text{C}_{10}\text{H}_6\text{O}_3\text{FeTe}$
Found (%)	C, 33.7	H, 1.97	

Table 3.2 ^1H , ^{13}C and ^{125}Te NMR data collected for (33)

Compound		^1H (CDCl_3) δ , ppm		^1H (CDCl_3) δ , ppm
	H1 -	range	H5 &	4.32(d)
	H4	7.0 - 7.8 (multiplet)	H5'	3.98(d)

Compound		^{13}C (CDCl_3) δ , ppm		^{13}C (CDCl_3) δ , ppm
	C1 -	124.1 127.3	C7	15.6
	C6	129.5 147.4	CO	202.3 205.3
		153.0 154.4		209.4

Compound		^{125}Te (^1H Decoupled) (CDCl_3) δ , ppm : J, Hz		^{125}Te (CDCl_3) δ , ppm : J, Hz
		-729.7		-728.3(dd)
		$J_{(\text{TeC})}$ 17.95		$J_{(\text{TeH})}$ 50.27 21.55

Data from the ^1H , ^{13}C and ^{125}Te NMR spectra for (33) are shown in table 3.2.

The ^1H NMR spectrum of heterocyclic (33), shown in figure 3.1, displays 4 proton environments. Protons H(5) and H(5') give two resonances, which if examined closely can be resolved into two of doublets.

The ^{13}C NMR spectrum of (33) is shown in figure 3.2. The spectrum is consistent with compound (33) and also shows three carbonyl environments.

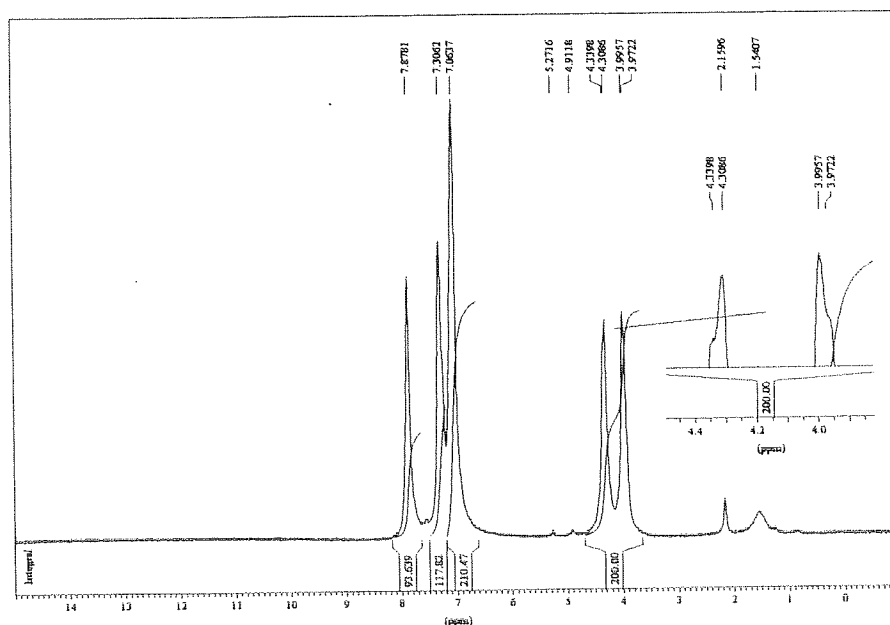


Figure 3.1 ^1H NMR spectrum of $[\text{Fe}(\text{C}_7\text{H}_6\text{Te})(\text{CO})_3]_2$, (33)

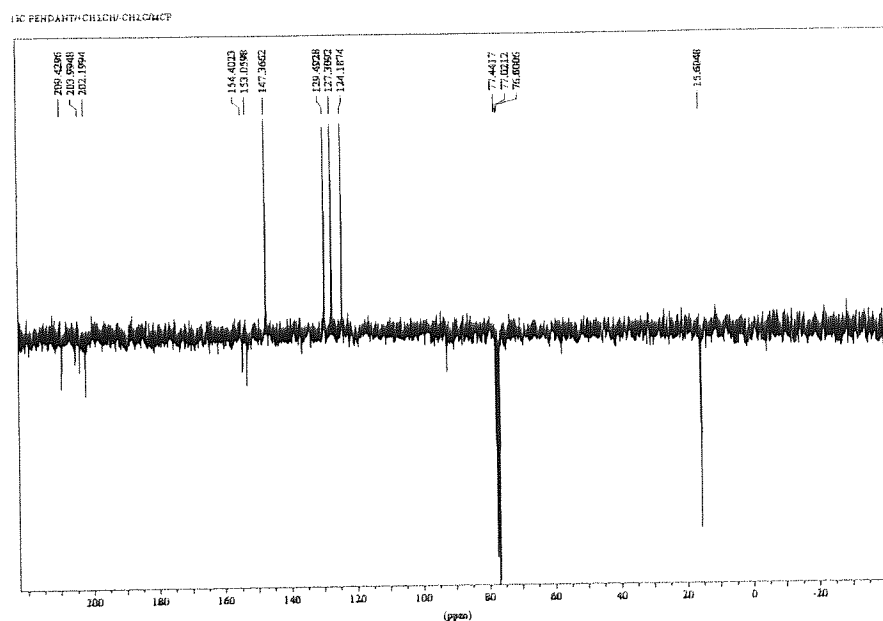


Figure 3.2 ^{13}C NMR spectrum of $[\text{Fe}(\text{C}_7\text{H}_6\text{Te})(\text{CO})_3]_2$, (33)

The ^{125}Te NMR spectrum of (**33**) is shown in figure 3.3 (decoupled) and 3.4 (coupled).

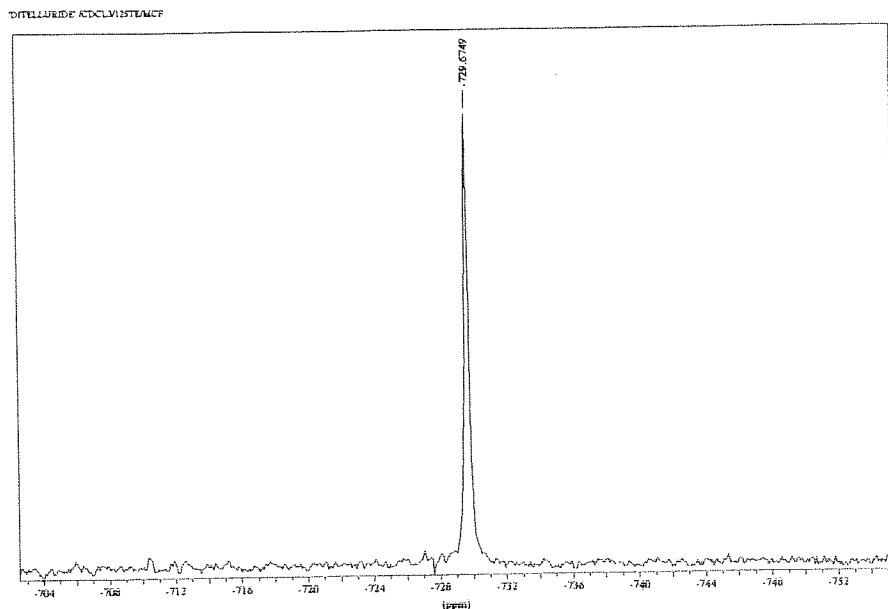


Figure 3.3 ^{125}Te NMR (decoupled) spectrum of $[\text{Fe}(\text{C}_7\text{H}_6\text{Te})(\text{CO})_3]_2$ (**33**)

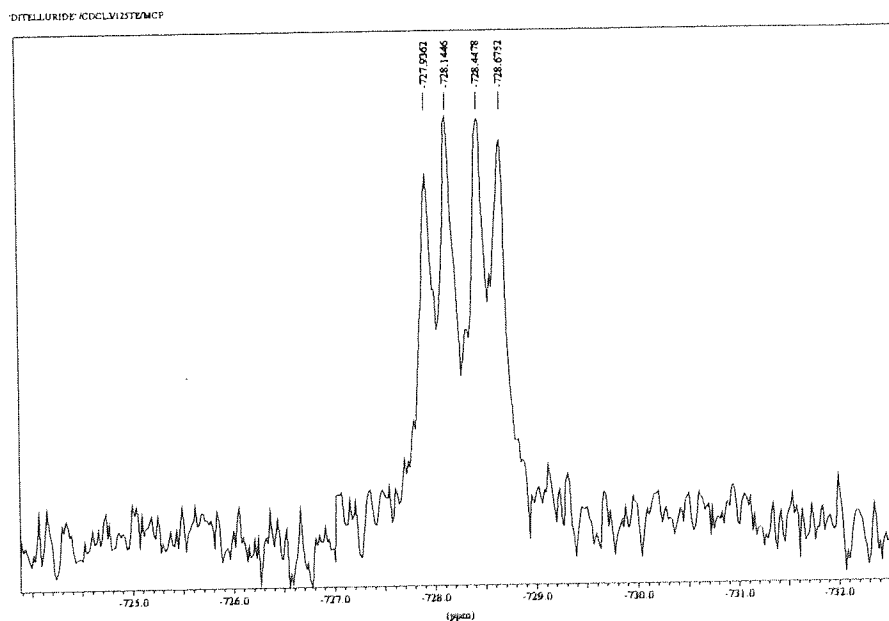
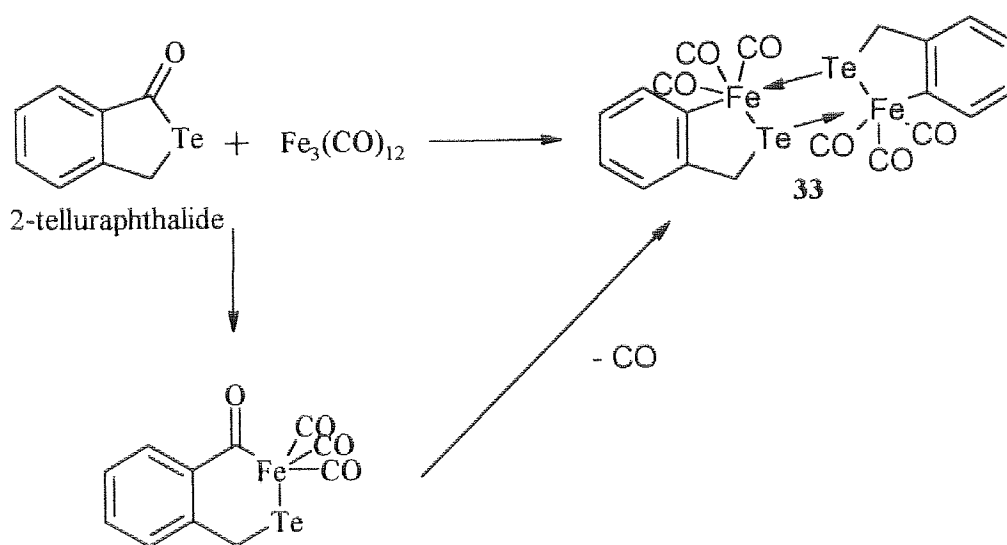


Figure 3.4 ^{125}Te NMR (coupled) spectrum of $[\text{Fe}(\text{C}_7\text{H}_6\text{Te})(\text{CO})_3]_2$ (**33**)

The ^1H decoupled ^{125}Te NMR spectrum gives a single chemical shift of -729.7 ppm and also shows satellites arising from the spin – spin coupling with the ^{13}C . The ^1H coupled ^{125}Te NMR spectrum shows a double doublet (see table 3.2). This is due to the spin – spin coupling with both the hydrogen atoms (H5 and $\text{H5}'$).

The room temperature NMR data (^1H , ^{13}C and ^{125}Te) are entirely consistent with the structure determined by X-ray crystallography (see section 3.4.1).

One could consider that the initial stage of reaction involved insertion of a $\text{Fe}(\text{CO})_3$ unit into the Te-C(O)- bond (see scheme 3.1) and this can be considered as oxidative addition. The next two steps of the reaction occur simultaneously in that the organic carbonyl shifts onto the iron and an iron bonded carbonyl group is released from the $\text{Fe}(\text{CO})_3$ moiety as carbon monoxide. These two steps in the reaction are effectively the reverse of a carbonyl insertion reaction. Thus, one of the carbonyl groups on the iron is probably of “organic” origin. The monomeric unit (with respect to iron and tellurium) only has 16 electrons around the iron atom which does not satisfy the 18-electron rule. The 18-electron rule is satisfied by the dimerisation of two monomeric units where the tellurium atom donates a lone pair of electrons to the iron in the neighbouring *iso* – structural fragment. The tellurium behaves as a Lewis base.



Scheme 3.1 Suggested reaction pathway for the reaction of 2-telluraphthalide and $[\text{Fe}_3(\text{CO})_{12}]$.

3.3.2 Reaction of triiron dodecacarbonyl with telluraphthalic anhydride

The products obtained from this reaction (4.5 hours) were a light brown (tan) crystalline product, phthalide (**34**), (m.p $70 - 72^\circ\text{C}$, lit²⁵ m.p. $72 - 74^\circ\text{C}$) and a black solid residue. The yield of the product was 0.11g or 41% based on $\text{Fe}_3(\text{CO})_{12}$. Data from the FTIR spectrum in the carbonyl region for (**34**) are recorded in table 3.3. The EI mass spectrum registered peaks at $m/z = 134$, $[\text{C}_8\text{H}_6\text{O}_2]^+$; 106, $[\text{C}_7\text{H}_6\text{O}]^+$.

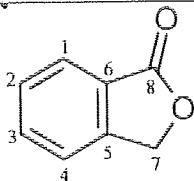
Table 3.3 FTIR band in the carbonyl region for product from reaction of telluraphthalic anhydride and $[\text{Fe}_3(\text{CO})_{12}]$.

Light brown crystals KBr, $\nu(\text{CO}) \text{ cm}^{-1}$
1753

The FTIR band pattern for (34) in the carbonyl region together with the mass spectrum implies that the product is phthalide, $C_8H_6O_2$. This is further confirmed by elemental analysis:

Calculated (%)	C, 71.6	H, 4.47	$C_8H_6O_2$ (phthalide)
Found (%)	C, 71.4	H, 4.55	

Table 3.4 ^{13}C NMR data for (34)

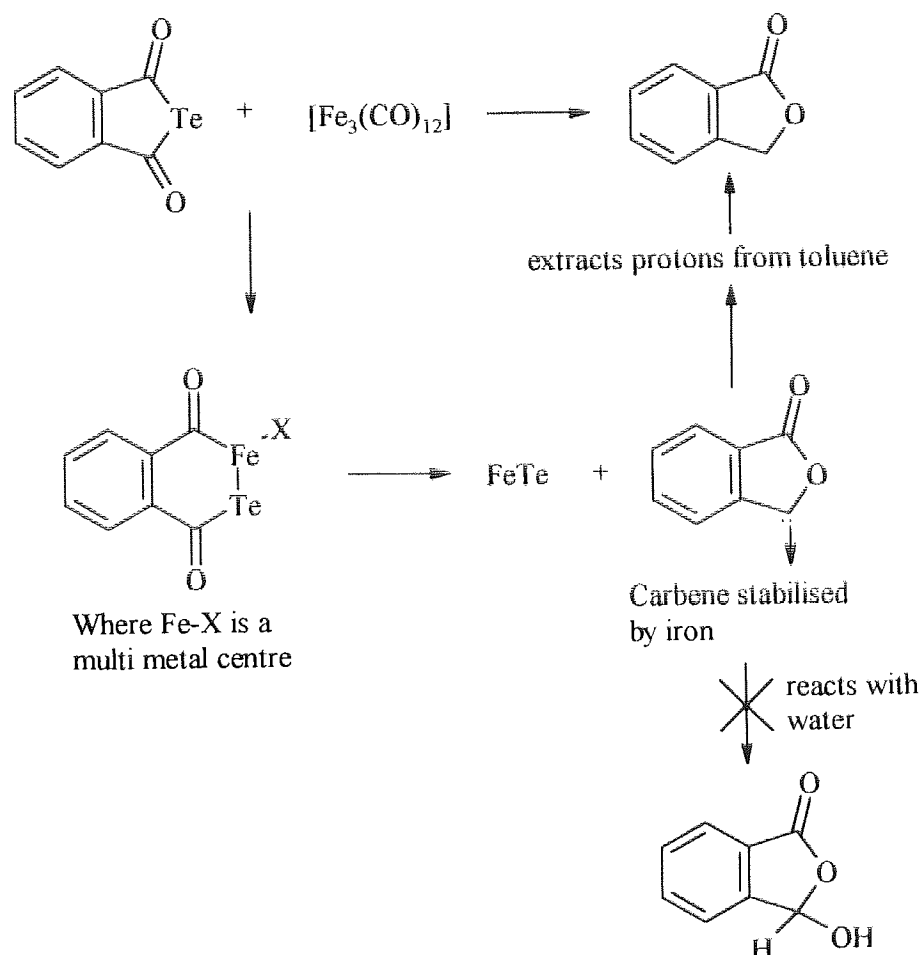
Compound		^{13}C ($CDCl_3$) δ , ppm		^{13}C ($CDCl_3$) δ , ppm
	C1	121.4	C5	145.8
	-	125.0	C6	---
	C4	128.3	C7	68.9
		133.3	C8	170.5

^{13}C NMR data are recorded in table 3.4. and are consistent with those previously reported for phthalide²⁷.

The room temperature NMR data (1H and ^{13}C) are entirely consistent with the structure determined by X-ray crystallography (see section 3.4.1).

In this reaction the synthesis of the product is of more interest than the actual product. The telluraphthalic anhydride used was pure and fully characterised [m.p., FTIR, NMR, CHN analysis²⁴ and X-ray crystallographic analysis [Lit. m.p. 127°C, m.p. found 126 - 127°C : Lit. FTIR (KBr cm^{-1}) 1770, 1660, 1575, 1465, 1440, 1200, 1190, 880, 870, 830, 780, 690, and 640; FTIR (KBr cm^{-1}) found 1775, 1662, 1573, 1441, 1198, 878, 864, 830, 774, 688, and 642 : Lit. mass spectrum (m/z) 262, 130, 105 and 77; mass spectrum (m/z) found 262, 132, 105 and 77]. Thus the origin of the product cannot be attributed to impurities in the starting materials - the yield [0.11g, 41% based on $Fe_3(CO)_{12}$] would also suggest that this explanation is precluded. In additional experiments the telluraphthalic anhydride was recovered unchanged from

refluxing toluene. Also, $[\text{Fe}_3(\text{CO})_{12}]$ did not react with toluene under similar reaction conditions. This indicates that the carbon-skeleton does not originate from toluene. One could consider that the initial stage of the reaction involved the insertion of a iron moiety into the Te-C(O)- bond (see Scheme 3.2) and this can also be considered as oxidative addition.



Scheme 3.2 Suggested reaction pathway for the reaction of telluraphthalic anhydride and $[\text{Fe}_3(\text{CO})_{12}]$.

It is apparent in the detelluration of tellurium heterocycles that a multi – metal centre is needed. Therefore this suggests that at least a second iron is expected to be present at this stage of the reaction. The next two possible steps of the reaction occur

simultaneously. In step one there is an elimination of FeTe and the second step is attack of one of the carbonyl groups on the back-side of the other carbonyl group resulting in a carbene. The carbene may possibly be stabilised by co-ordination to iron. A recent example of an iron stabilised carbene has been reported²⁸. The resulting carbene may undergo two possible reactions; one is the decomposition by adventitious moisture. If this is the case the carbene should give a secondary alcohol. The second route is that the carbene extracts protons from the solvent (toluene). Further speculation is not merited at this juncture (see also chapter 6.3).

3.3.3 Reaction of triiron dodecacarbonyl with 2-selenaphthalide

The products obtained from this reaction (4.5 hours) were three components: a deep red solid (**35**) (m.p. 190 – 192°C), a black solid (**36**) (m.p. 159 – 160°C) and a black solid residue. The yields of the products (**35**) and (**36**) were 0.9g and 0.048g or 50% and 2% based on Fe₃(CO)₁₂ respectively. Data from the FTIR spectra in the carbonyl region for (**35**) and (**36**) are recorded in table 3.5. The EI mass spectra peaks are recorded in table 3.6. ¹H and ¹³C NMR data can be seen in tables 3.7 for (**35**) and 3.8 for (**36**).

Table 3.5 FTIR bands in the carbonyl region for products from reaction of 2-selenaphthalide and [Fe₃(CO)₁₂].

Deep red crystals, (35) KBr, $\nu(\text{CO}) \text{ cm}^{-1}$	Black crystals, (36) KBr, $\nu(\text{CO}) \text{ cm}^{-1}$
2062	2106
2021	2061
1962	2024
	1983
	1956

The FTIR band pattern for (35) in the carbonyl region together with the mass spectrum are consistent with a structure containing a heterocyclic moiety, $[\text{Fe}_2(\text{C}_7\text{H}_6)\text{Se}(\text{CO})_6]$ (35).

This is further confirmed by elemental analysis:

Calculated (%)	C, 34.7	H, 1.34	$\text{C}_{13}\text{H}_6\text{O}_6\text{Fe}_2\text{Se}$
Found (%)	C, 34.6	H, 1.56	

Table 3.6 EI mass spectra peaks for products from reaction of 2-selenaphthalide and $[\text{Fe}_3(\text{CO})_{12}]$ (^1H , ^{12}C , ^{56}Fe and ^{80}Se).

Deep red crystals, (35)		Black crystals, (36)	
m/z	fragment	m/z	fragment
450	$[\text{C}_{13}\text{H}_6\text{O}_6\text{Fe}_2\text{Se}]^+$	562	$[\text{C}_{15}\text{H}_6\text{O}_8\text{Fe}_3\text{Se}]^+$
394	$[\text{C}_{11}\text{H}_6\text{O}_4\text{Fe}_2\text{Se}]^+$	506	$[\text{C}_{13}\text{H}_6\text{O}_6\text{Fe}_3\text{Se}]^+$
		450	$[\text{C}_{13}\text{H}_6\text{O}_6\text{Fe}_2\text{Se}]^+$
		422	$[\text{C}_{12}\text{H}_6\text{O}_5\text{Fe}_2\text{Se}]^+$

The FTIR band pattern for (36) in the carbonyl region together with the mass spectrum are consistent with $[\text{Fe}_3(\text{C}_7\text{H}_6\text{Se})(\text{CO})_8]$ (36), the formulation being further supported by elemental analysis:

Calculated (%)	C, 32.13	H, 1.80	$\text{C}_{15}\text{H}_6\text{O}_8\text{Fe}_3\text{Se}$
Found (%)	C, 33.02	H, 1.80	

Table 3.7 ^1H and ^{13}C NMR data for (35)

Compound		^1H (CDCl_3) δ , ppm		^1H (CDCl_3) δ , ppm
	H1 – H4	6.93 – 8.19 (multiplet)	H5 & H5	3.78(s)

Compound		^{13}C (CDCl_3) δ , ppm		^{13}C (CDCl_3) δ , ppm
	C1 – C6	112.4 123.5 127.8 130.5 139.7 159.2	C7 CO	35.5 209.5

The ^1H and ^{13}C NMR spectra of (35) and (36) are shown in figures 3.5 to 3.8.

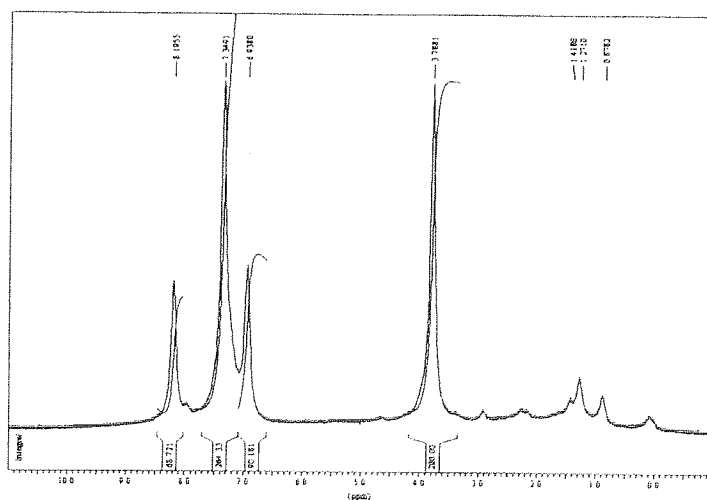


Figure 3.5 ^1H NMR spectrum of selenoferrole, $[\text{Fe}_2(\text{C}_7\text{H}_6\text{Se})(\text{CO})_6]$ (**35**)

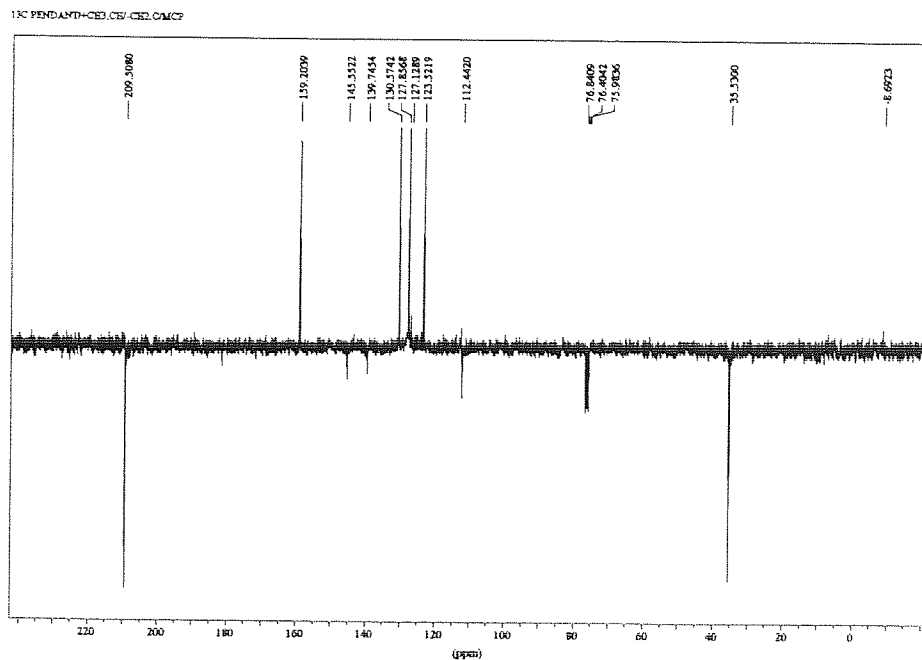


Figure 3.6 ¹³C NMR spectrum of selenoferrole, $[\text{Fe}_2(\text{C}_7\text{H}_6\text{Se})(\text{CO})_6]$ (35)

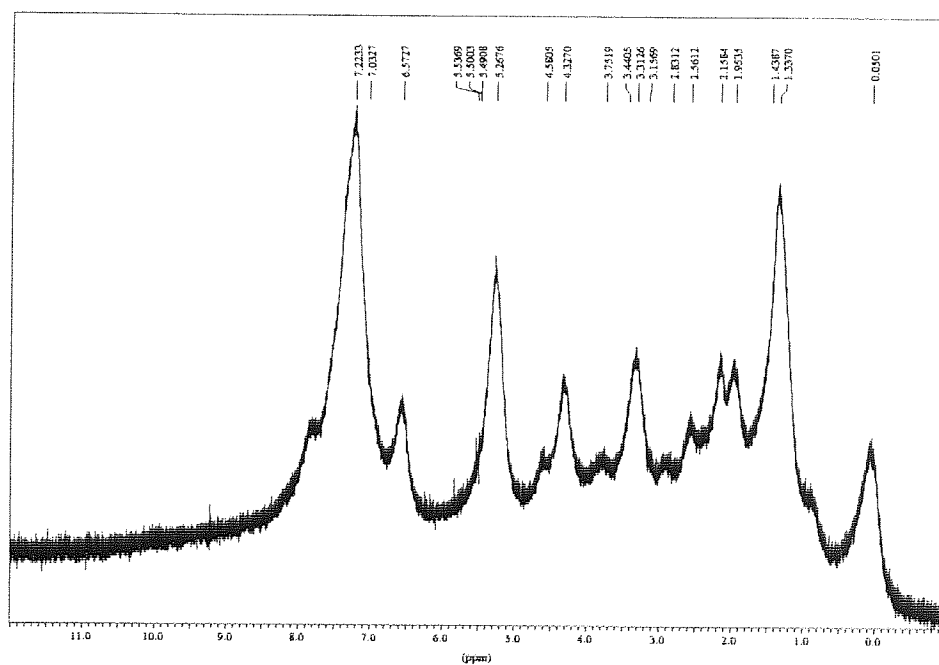


Figure 3.7 ¹H NMR spectrum of selenoferrole, $[\text{Fe}_3(\text{C}_7\text{H}_6\text{Se})(\text{CO})_8]$ (36)

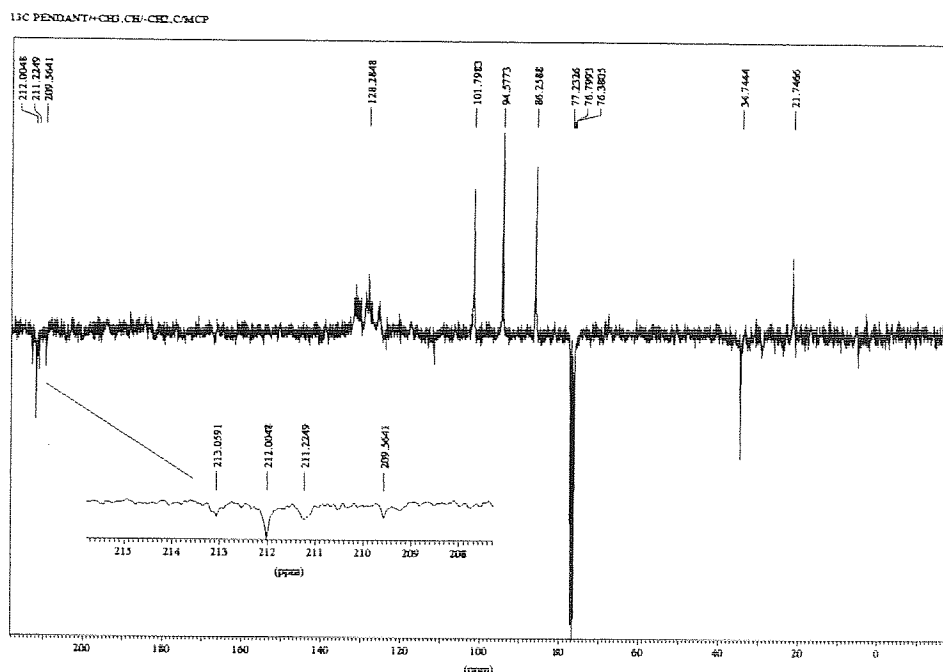
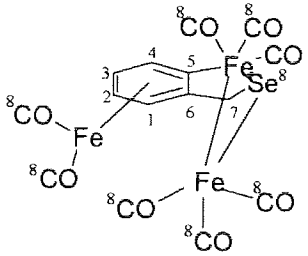
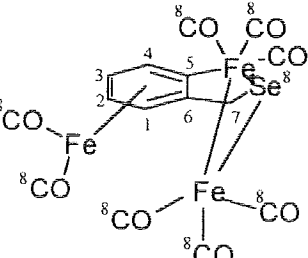


Figure 3.8 ^{13}C NMR spectrum of selenoferrole, $[\text{Fe}_3(\text{C}_7\text{H}_6\text{Se})(\text{CO})_8]$ (**36**)

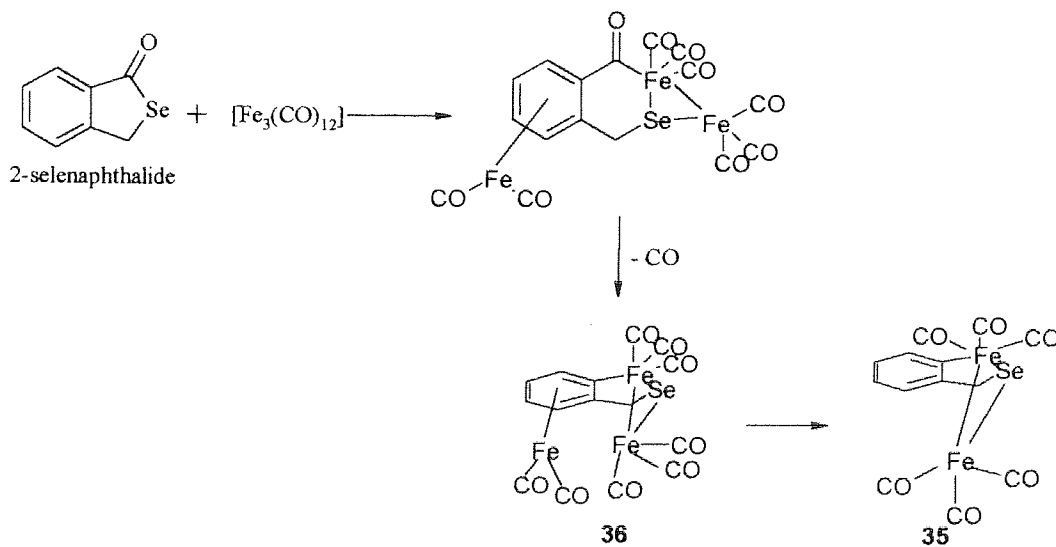
The room temperature NMR data (^1H and ^{13}C) for both (**35**) and (**36**) appear too simple to be consistent with the static structures determined by X-ray methods (see section 3.4.1). As can be seen in the ^1H NMR spectrum of (**35**) the CH_2 protons give a sharp singlet rather than the AB pattern expected from the static structure. Also it can be seen from the ^{13}C NMR spectrum of (**35**), that the six carbonyl ligands are shown to be equivalent which is not the case in the X-ray structure. One suggestion for the simplicity of the NMR spectra is that (**35**) is fluxional in solution at room temperature, where by product (**35**) may undergo rapid interchange of the two iron atoms rendering the methylene protons and the six carbonyl ligands equivalent on the NMR time – scale. Although the methylene resonance broadened on cooling to 218K, the AB pattern did not resolve at this temperature - the lowest available.

Table 3.8 ^1H and ^{13}C NMR data collected for (36)

Compound		^1H (CDCl_3) δ , ppm		^1H (CDCl_3) δ , ppm
	H1 –	7.22 – 5.26	H7	4.58 – 1.95
	H4	(multiplet)		(multiplet)
Compound		^{13}C (CDCl_3) δ , ppm		^{13}C (CDCl_3) δ , ppm
	C1 –	111.7 125.4	CH_2	34.7
	C6	128.2 130.2 132.8	CO	213.0 212.0 211.2 209.5

It is clear from the ^1H and ^{13}C NMR spectra of (36) that this must also be fluxional in solution at room temperature. As can be seen in the ^1H and ^{13}C NMR spectra only four resonances for the carbonyl ligands are observed and a singlet is again seen for the CH_2 protons although in this case the resonance is broad at room temperature and sharpens on heating to 323K. Under these circumstances it is surprising that cooling a sample of (36) in a solution of CDCl_3 to 233K fails to achieve resolution to the expected AB pattern but the signal does broaden further. The fluxional behavior of (36) is complex and must at least involve interchange of the two $\text{Fe}(\text{CO})_3$ groups. The relative yields of these two compounds suggests that (36) (2%) is an intermediate compound in the formation of (35) (50%). The initial insertion of iron into a $-\text{Se}-\text{C}(\text{O})-$ bond (see scheme 3.3) followed by loss of a carbonyl from the iron (as shown

in scheme 3.3) can be postulated, giving product (36). On prolonged heating of compound (36) the loss of the $\text{Fe}(\text{CO})_2$ moiety must occur giving compound (35). It is interesting that the ring iron atom in (35) satisfies the 18 electron rule by retention of a $\text{Fe}(\text{CO})_3$ unit whereas, in the related compound (33) above, loss of this moiety and co-ordination to the tellurium of a neighbouring fragment is preferred. This implies the greater Lewis basicity of tellurium under these conditions.



Scheme 3.3 Suggested reaction pathway for the reaction of 2-selenaphthalide and $[\text{Fe}_3(\text{CO})_{12}]$.

3.3.4 Reaction of triiron dodecacarbonyl with selenaphthalic anhydride

The products obtained from this reaction (4.5 hours) were starting material, a red solid and a black solid residue. The mass of the product was 0.067g. Data from the FTIR spectrum in the carbonyl region for the red solid are recorded in table 3.9.

Table 3.9 FTIR bands in the carbonyl region for product from reaction of selenaphthalic anhydride and $[\text{Fe}_3(\text{CO})_{12}]$.

Red solid KBr, $\nu(\text{CO}) \text{ cm}^{-1}$
2072
1985

Elemental analysis;

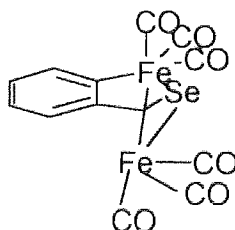
Found (%) C, 27.73 H, 2.40

The red solid failed to give ^1H and ^{13}C NMR spectra.

Unfortunately the red solid has not been characterised to date.

3.3.5 Time dependent ^1H and ^{13}C NMR spectroscopy for compound (35)

Selenaferrole, $[\text{Fe}_2(\text{C}_7\text{H}_6\text{Se})(\text{CO})_6]$, (35) (see below), decomposed over a period of time.



Therefore, one could follow the decomposition of (35) with ^1H and ^{13}C NMR spectroscopy. The ^1H and ^{13}C NMR spectroscopy was carried out in chloroform and the spectra were measured every two weeks. The sample was stored at room temperature.

Time dependent ^1H and ^{13}C NMR spectra of selenaferrole, $[\text{Fe}_2(\text{C}_7\text{H}_6\text{Se})(\text{CO})_6]$, (35), are shown in figures 3.9 and 3.10 respectively.

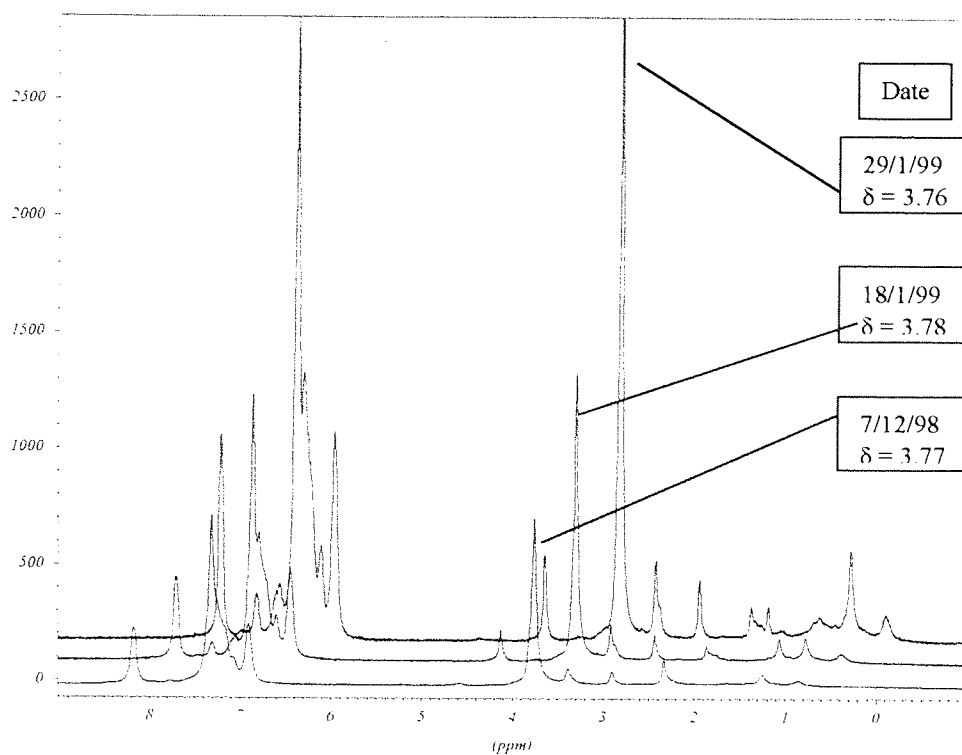


Figure 3.9 Time dependent ^1H NMR spectrum of selenoferrole, $[\text{Fe}_2(\text{C}_7\text{H}_6\text{Se})(\text{CO})_6]$
(35)

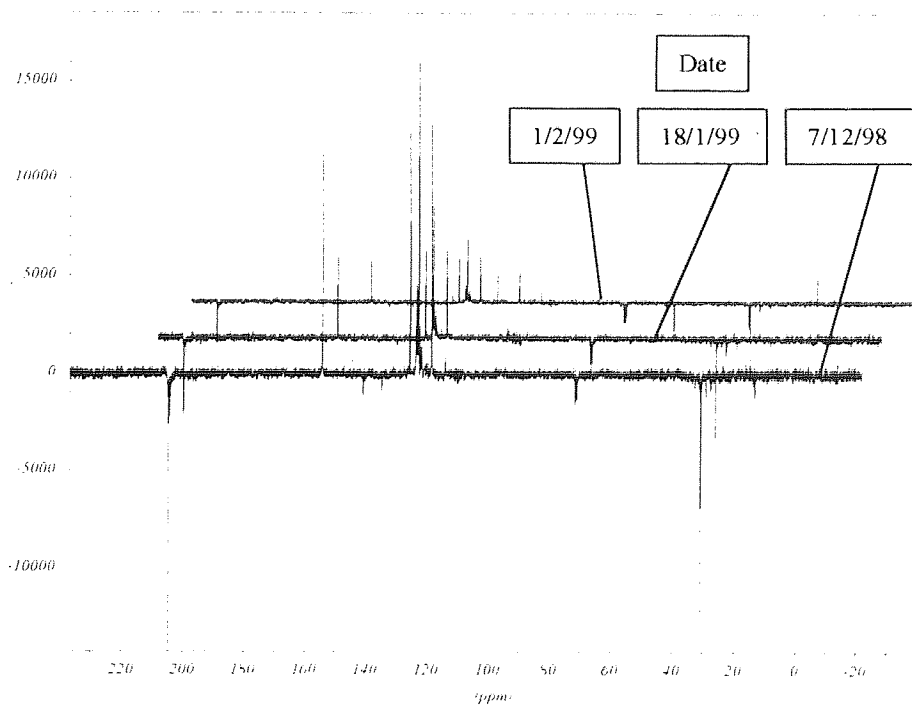


Figure 3.10 Time dependent ^{13}C NMR spectrum of selenoferrole,
 $[\text{Fe}_2(\text{C}_7\text{H}_6\text{Se})(\text{CO})_6]$ (35)

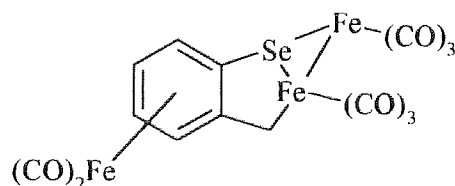
Once again the room temperature NMR spectra (^1H and ^{13}C) for (35) appear too simple to be consistent with the static structure determined by X-ray methods (see section 3.4.1). One suggestion for the simplicity of the NMR spectra is that (35) is fluxional in solution at room temperature. On comparing the methylene resonance for compound (35) [$\delta = 3.78$, see table 3.7] with the methylene resonances observed in the time dependent ^1H NMR study [$\delta = 3.76$, 3.78 and 3.77, see figure 3.9] these resonances are in good agreement.

The reaction between $[\text{Fe}_3(\text{CO})_{12}]$ and five membered heterocyclic ring compounds where the heteroatom is either tellurium and selenium may follow the reaction pathway shown below.

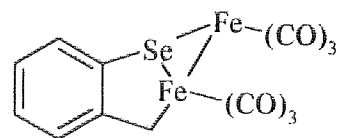


Where A = Starting material

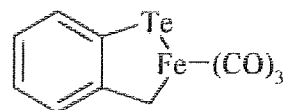
B = Chalcogenaferrole, e.g. (36)



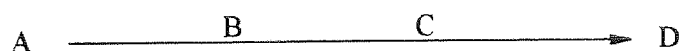
C = Chalcogenaferrole, e.g. (35)



D = Chalcogenaferrole, e.g. (33)



When (A) is the tellurium heterocyclic compound (tellurophthalide) the reaction pathway taken would be as follows,



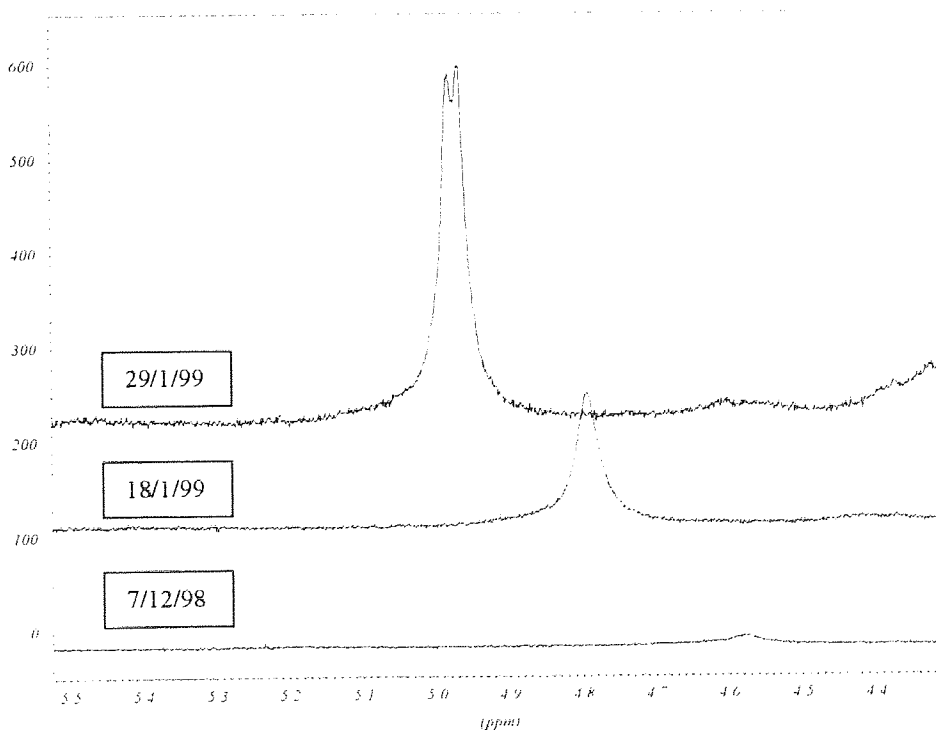
where the starting material may go through the intermediate compounds (B) and (C) resulting in (D), which is compound (33) (see above).

When (A) is the selenium heterocyclic compound (2-selenaphthalide) the reaction pathway taken would be as follows,

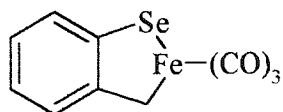


where (B) is compound (36) (see above), which is an intermediate compound in the formation of (C), compound (35) (see above).

There is evidence to suggest that compound (35) undergoes decomposition from (C) to (D) over a period of time. The evidence come from the analysis of the time dependent ^1H NMR spectra of (35) (see figure 3.9) and the ^1H NMR spectrum of (33) (see figure 3.1). The time dependent ^1H NMR spectrum of (35) shows a resonance at about 4.5ppm which increases in intensity over time and splits into a doublet (see below).



One can conclude that this resonance may correspond to the selenium analogue (see below) of compound (33),



because the methylene protons of (33) were observed at approximately 4.4 and 4.0ppm (see table 3.2).

The ^1H and ^{13}C NMR spectra of (35) become more complex over a period of time (see figure 3.9 and 3.10). This suggests that compound (35) decomposes to a mixture of compounds and that (D) may be contained in this mixture.

3.4 X-ray crystallography

3.4.1 X-ray crystallography of products (33), (34), (35) and (36).

3.4.1.1 Crystallographic analysis for products (33), (34), (35) and (36).

Suitable crystals of products (33), (35) and (36) were obtained from boiling hexane. Crystals of (34) were obtained from slow evaporation of a solution of (34) in acetone. The crystal structures of compounds (33), (34), (35) and (36) were established by Dr T.A. Hamor at the University of Birmingham, and are shown in figures 3.11, 3.12, 3.13 and 3.14 respectively. The crystal parameters and experimental data are listed in Table 3.10. Cell dimensions and intensity data for all four structures were measured on a Rigaku R-Axis II area detector diffractometer at 293(2)K using graphite-monochromated Mo-K α radiation, $\lambda = 0.7107 \text{ \AA}$. Conventional absorption corrections were not applied since, on average, each unique reflection intensity is the mean of three intensities measured at different orientations of the crystal, thus minimising absorption effects. The structures were determined²⁹ by direct methods and refined³⁰ by least-squares on F^2 using anisotropic thermal parameters for non-hydrogen atoms. Hydrogen atoms were placed in calculated positions riding on their respective bonding atoms. Diagrams were drawn with ORTEP³¹; thermal ellipsoids are at the 30% probability level. Atom co-ordinates are listed in tables 3.11 to 3.14. Selected bond lengths and angles are in table 3.15.

Table 3.10 Crystallographic data for products **(33)**, **(34)**, **(35)** and **(36)**.

Compound	33	34	35	36
Formula	C ₂₀ H ₁₂ O ₆ Fe ₂ Te ₂	C ₈ H ₆ O ₂	C ₁₃ H ₆ O ₆ Fe ₂ Se	C ₁₅ H ₆ O ₈ Fe ₃ Se
<i>M</i>	715.2	134.1	448.8	560.7
Cryst sys	monoclinic	monoclinic	monoclinic	monoclinic
Space grp	<i>P</i> 2 ₁ / <i>n</i>	<i>P</i> 2 ₁ / <i>c</i>	<i>P</i> 2 ₁ / <i>n</i>	<i>P</i> 2 ₁ / <i>n</i>
<i>a</i> , Å	10.863(2)	7.760(2)	9.479(2)	8.264(1)
<i>b</i>	7.245(2)	10.799(3)	15.339(3)	15.591(2)
<i>c</i>	14.380(3)	8.234(3)	10.637(2)	13.628(2)
β, deg	105.49(2)	112.88(2)	97.73(1)	97.34(1)
<i>U</i> , Å ³	1090.6(4)	635.7(3)	1532.5(5)	1741.5(4)
<i>Z</i>	2	4	4	5
μ(MoKα), mm ⁻¹	3.985	0.101	4.290	4.597
Rflns collected [<i>I</i> > σ(<i>I</i>)]	5937	2740	8792	10382
unique rflns	1888	966	2680	2899
<i>R</i> (<i>int</i>)	0.0583	0.0598	0.0929	0.0478
<i>R</i> , <i>wR</i> 2 ^a	0.0579, 0.1060	0.0986, 0.2246	0.0741, 0.1422	0.040, 0.101
obsd rflns [<i>I</i> > 2σ(<i>I</i>)]	1781	772	2190	2733
<i>R</i> , <i>wR</i> 2 ^a obsd data	0.0533, 0.1042	0.0739, 0.1944	0.0564, 0.1307	0.037, 0.098

$$^a wR2 = [\sum w(F_o^2 - F_c^2)^2 / \sum w(F_o^2)^2]^{1/2}$$

Table 3.11 Atomic coordinates ($\times 10^4$) and equivalent isotropic displacement parameters ($\text{\AA}^2 \times 10^3$) for (33). $U(\text{eq})$ is defined as one third of the trace of the orthogonalized U_{ij} tensor.

	x	y	z	$U(\text{eq})$
Te(1)	4603(1)	2287(1)	-119(1)	50(1)
Fe(1)	3220(1)	-643(2)	-283(1)	47(1)
O(1)	982(6)	1474(11)	-162(5)	79(2)
O(2)	2696(7)	-445(12)	-2396(5)	95(2)
O(3)	1987(6)	-4255(10)	-377(5)	84(2)
C(1)	4210(9)	2825(13)	1237(7)	66(2)
C(2)	4069(7)	1019(13)	1736(6)	54(2)
C(3)	4358(8)	1002(16)	2748(7)	68(3)
C(4)	4199(9)	-559(17)	3233(7)	77(3)
C(5)	3763(10)	-2136(16)	2738(8)	76(3)
C(6)	3482(9)	-2127(13)	1737(7)	65(2)
C(7)	3646(7)	-583(11)	1203(6)	48(2)
C(8)	1865(8)	662(13)	-231(6)	56(2)
C(9)	2946(8)	-530(13)	-1577(7)	62(2)
C(10)	2468(8)	-2832(13)	-332(7)	60(2)

Table 3.12 Atomic coordinates ($\times 10^4$) and equivalent isotropic displacement parameters ($\text{\AA}^2 \times 10^3$) for (34). $U(\text{eq})$ is defined as one third of the trace of the orthogonalized U_{ij} tensor.

	x	y	z	$U(\text{eq})$
O(1)	6238(3)	925(2)	7126(3)	63(1)
O(2)	6745(4)	2535(3)	8957(5)	86(1)
C(1)	7321(5)	95(4)	6496(5)	59(1)
C(2)	9299(4)	477(3)	7500(4)	50(1)
C(3)	10960(5)	28(4)	7469(5)	59(1)
C(4)	12596(5)	591(4)	8528(5)	64(1)
C(5)	12576(5)	1574(4)	9627(5)	69(1)
C(6)	10947(5)	2016(4)	9671(5)	63(1)
C(7)	9298(4)	1455(3)	8569(4)	51(1)
C(8)	7370(5)	1741(4)	8306(5)	60(1)

Table 3.13 Atomic coordinates ($\times 10^4$) and equivalent isotropic displacement parameters ($\text{\AA}^2 \times 10^3$) for (35). U(eq) is defined as one third of the trace of the orthogonalized U_{ij} tensor.

	x	y	z	U(eq)
Se(1)	6925(1)	113(1)	7495(1)	72(1)
Fe(1)	6562(1)	1410(1)	8579(1)	57(1)
Fe(2)	6768(1)	1419(1)	6278(1)	56(1)
O(1)	5620(6)	3204(3)	8806(5)	104(2)
O(2)	3813(6)	730(4)	9149(5)	130(2)
O(3)	8211(6)	1133(4)	11082(4)	109(2)
O(4)	6388(6)	3230(3)	5448(4)	100(2)
O(5)	3718(6)	1182(4)	5618(5)	104(2)
O(6)	7835(6)	681(3)	4032(4)	103(2)
C(1)	9017(7)	179(3)	7716(6)	75(2)
C(2)	9350(6)	1116(3)	7571(4)	58(1)
C(3)	10662(7)	1347(4)	7219(5)	76(2)
C(4)	11071(7)	2190(4)	7185(6)	79(2)
C(5)	10176(6)	2842(4)	7480(5)	70(2)
C(6)	8868(6)	2635(3)	7805(4)	59(1)
C(7)	8381(5)	1770(3)	7875(4)	53(1)
C(8)	6005(6)	2505(4)	8718(5)	70(1)
C(9)	4896(7)	997(4)	8914(6)	83(2)
C(10)	7544(6)	1236(4)	10109(5)	72(2)
C(11)	6565(6)	2529(4)	5768(5)	69(1)
C(12)	4923(7)	1274(4)	5885(5)	71(2)
C(13)	7434(7)	978(4)	4906(5)	71(2)

Table 3.14 Atomic coordinates ($\times 10^4$) and equivalent isotropic displacement parameters ($\text{\AA}^2 \times 10^3$) for (36). U(eq) is defined as one third of the trace of the orthogonalized U_{ij} tensor.

	x	y	z	U(eq)
Se(1)	847(1)	1703(1)	7452(1)	43(1)
Fe(1)	-234(1)	1837(1)	8962(1)	39(1)
Fe(2)	-240(1)	3082(1)	7747(1)	38(1)
Fe(3)	2640(1)	3874(1)	8682(1)	38(1)
O(1)	1686(5)	558(2)	10162(3)	83(1)
O(2)	-3051(6)	757(3)	8204(3)	93(1)
O(3)	-1989(4)	2539(2)	10503(3)	66(1)
O(4)	-3493(4)	2562(3)	6885(3)	69(1)
O(5)	-1942(4)	4357(2)	8793(3)	72(1)
O(6)	425(6)	4030(4)	5984(3)	105(2)
O(7)	1197(5)	5577(2)	8694(3)	68(1)
O(8)	4113(6)	4304(3)	6915(3)	89(1)
C(1)	3102(5)	1881(3)	8020(3)	44(1)
C(2)	3111(5)	2528(2)	8819(3)	38(1)
C(3)	4537(5)	2987(3)	9130(3)	43(1)
C(4)	4575(5)	3652(3)	9838(3)	48(1)
C(5)	3141(5)	3810(3)	10252(3)	45(1)
C(6)	1718(5)	3358(2)	9941(3)	40(1)
C(7)	1602(5)	2676(2)	9230(3)	37(1)
C(8)	922(6)	1036(3)	9692(3)	51(1)
C(9)	-1966(7)	1176(3)	8496(4)	59(1)
C(10)	-1297(5)	2269(3)	9895(3)	47(1)
C(11)	-2186(5)	2743(3)	7221(3)	46(1)
C(12)	-1210(6)	3874(3)	8388(3)	51(1)
C(13)	230(6)	3671(4)	6691(4)	62(1)
C(14)	1764(6)	4908(3)	8679(3)	48(1)
C(15)	3495(6)	4125(3)	7597(3)	55(1)

Table 3.15 Selected bond lengths (Å) and angles (°) for compounds **33** - **36**

Compound 33				
Te(1)-Fe(1)	2.575(1)		Fe(1)-C(8)	1.767(10)
Te(1)-Fe(1)*	2.572(1)		Fe(1)-C(9)	1.806(10)
Te(1)-C(1)	2.139(9)		Fe(1)-C(10)	1.777(9)
Fe(1)-C(7)	2.062(8)			
Fe(1)-Te(1)-Fe(1)*	96.78(4)		C(7)-Fe(1)-C(8)	84.5(3)
Fe(1)-Te(1)-C(1)	88.9(2)		C(7)-Fe(1)-C(9)	174.9(4)
Fe(1)*-Te(1)-C(1)	106.0(3)		C(7)-Fe(1)-C(10)	92.0(4)
Te(1)-Fe(1)-C(7)	85.6(2)		C(8)-Fe(1)-Te(1)*	164.7(3)
Te(1)-Fe(1)-C(8)	91.6(3)		C(8)-Fe(1)-C(9)	96.3(4)
Te(1)-Fe(1)-C(9)	89.3(3)		C(8)-Fe(1)-C(10)	95.8(4)
Te(1)-Fe(1)-C(10)	172.0(3)		C(9)-Fe(1)-Te(1)*	98.1(3)
Te(1)-Fe(1)-Te(1)*	83.22(4)		C(9)-Fe(1)-C(10)	93.0(4)
C(7)-Fe(1)-Te(1)*	80.7(2)		C(10)-Fe(1)-Te(1)*	88.9(3)
Compound 34				
O(1)-C(1)	1.455(4)		C(1)-C(2)	1.491(5)
O(1)-C(8)	1.352(4)		C(7)-C(8)	1.459(5)
O(2)-C(8)	1.208(4)			
C(1)-O(1)-C(8)	110.7(3)		O(2)-C(8)-O(1)	121.4(4)
O(1)-C(1)-C(2)	104.2(3)		O(2)-C(8)-C(7)	130.5(4)
O(1)-C(8)-C(7)	108.1(3)			

Table 3.15 Cont Selected bond lengths (Å) and angles (°) for compounds **33 – 36**

Compound 35				
Se(1)-Fe(1)	2.347(1)		Fe(1)-C(9)	1.781(7)
Se(1)-Fe(2)	2.378(1)		Fe(1)-C(10)	1.783(6)
Se(1)-C(1)	1.967(6)		Fe(2)-C(7)	2.194(5)
Fe(1)-Fe(2)	2.482(1)		Fe(2)-C(11)	1.789(5)
Fe(1)-C(7)	2.046(5)		Fe(2)-C(12)	1.757(7)
Fe(1)-C(8)	1.774(6)		Fe(2)-C(13)	1.798(6)
Fe(1)-Se(1)-C(1)	96.3(2)		Se(1)-Fe(1)-Fe(2)	58.93(3)
Fe(2)-Se(1)-C(1)	90.6(2)		C(7)-Fe(2)-Se(1)	78.4(1)
Fe(1)-Se(1)-Fe(2)	63.36(3)		C(7)-Fe(2)-Fe(1)	51.5(1)
Se(1)-Fe(1)-C(7)	82.1(1)		Se(1)-Fe(2)-Fe(1)	57.70(3)
Fe(2)-Fe(1)-C(7)	57.0(1)			
Compound 36				
Se(1)-Fe(1)	2.355(1)		Fe(2)-C(12)	1.764(4)
Se(1)-Fe(2)	2.383(1)		Fe(2)-C(13)	1.791(5)
Se(1)-C(1)	1.945(4)		Fe(3)-C(2)	2.140(4)
Fe(1)-Fe(2)	2.551(1)		Fe(3)-C(3)	2.122(4)
Fe(1)-C(7)	2.001(4)		Fe(3)-C(4)	2.125(4)
Fe(1)-C(8)	1.794(5)		Fe(3)-C(5)	2.129(4)
Fe(1)-C(9)	1.811(5)		Fe(3)-C(6)	2.124(4)
Fe(1)-C(10)	1.769(4)		Fe(3)-C(7)	2.226(4)
Fe(2)-C(7)	2.452(4)		Fe(3)-C(14)	1.765(5)
Fe(2)-C(11)	1.757(5)		Fe(3)-C(15)	1.762(4)
			Fe(3)...Fe(2)	2.836(1)
Fe(1)-Se(1)-C(1)	95.2(1)		Se(1)-Fe(1)-Fe(2)	57.96(2)
Fe(2)-Se(1)-C(1)	99.6(1)		C(7)-Fe(2)-Se(1)	72.5(1)
Fe(1)-Se(1)-Fe(2)	65.15(2)		C(7)-Fe(2)-Fe(1)	47.1(1)
Se(1)-Fe(1)-C(7)	81.6(1)		Se(1)-Fe(2)-Fe(1)	56.90(2)
Fe(2)-Fe(1)-C(7)	63.8(1)			

3.4.1.2 Discussion of the structures of (33), (34), (35) and (36).

The dimeric complex (33) has crystallographic 1 (C_i) symmetry. The central Fe_2Te_2 core is approximately square-shaped, with iron-tellurium distances 2.572(1) and 2.575(1) Å, angle at iron $83.22(4)^\circ$, angle at tellurium, $96.78(4)^\circ$ (see Table 3.15). The Fe-Te bond lengths fall near the lower end of the range, 2.54 - 2.67 Å found^{11,32} in a number of other complexes containing analogous atomic groupings. The coordination geometry at iron is approximately octahedral, with maximum angular deviation, 15.3° , mean deviation 5.5° . The tellurium-carbon bond length, $\text{Te}(1)\text{-C}(1)$, 2.139(9) Å, is slightly shorter than the mean value given³³ for $\text{Te-C}(\text{sp}^3)$ bonds, 2.158 Å, but falls within the range 2.119 - 2.154 Å found³⁴ in a number of more recent structure determinations. The eight-atom grouping, $\text{C}(1) - \text{C}(7)$, $\text{Fe}(1)$ is coplanar to within 0.03 Å (rms deviation 0.019 Å). The tellurium atom which completes a benzotelluraferrole ring system is, however, displaced by 0.83(1) Å. The plane of the Fe_2Te_2 core is oriented at $80.4(1)^\circ$ to this plane, forming a step to the centrosymmetrically related benzotelluraferrole ring, so that the perpendicular distance between these parallel planes is approximately 3.34 Å.

The non-hydrogen atoms of the phthalide (34) are essentially coplanar, with rms atomic deviation 0.014 Å. The maximum deviation of 0.026(2) Å is that of the carbonyl oxygen atom, O(2), and omitting this atom from the calculations gives a significantly better plane, rms deviation 0.009 Å, with O(2) displaced by 0.049(5) Å. Noteworthy is the difference in bond lengths between those at the saturated carbon atom, C(1), and those at the trigonally hybridized C(8). Thus, while O(1)-C(1) at 1.455(4) Å approximates to a C-O single bond, the O(1)-C(8) length of 1.352(4) Å indicates significant double bond character, and, also, C(1)-C(2) is significantly

longer than C(7)-C(8). The O(2)=C(8) formal double bond, 1.208(4)Å, is similar in length to the corresponding bonds in phthalic anhydride, 1.192(4)Å³⁵.

In the benzoselenoferrole moiety of complex (35), the two iron atoms appear to be in chemically identical environments. However, stereochemically they are not identical; Fe(1) lies close [0.18(1)Å] to the plane of the organic residue and may, therefore, be considered to be the iron constituent of the benzoselenoferrole, whereas Fe(2) is displaced by 1.99 Å from this plane and may be considered to be π -bonded to the selenium atom, Fe(1) and C(7). Bond lengths are consistent with this, Fe(1)-C(7) and Fe(1)-Se(1) each being shorter than the corresponding bonds involving Fe(2) (see Table 2). The selenium atom is displaced by 0.72 Å from the organic plane, on the same side as Fe(2). The crystal structure of the analogous μ -{1-2- η -[hydroseleno-1-cyclohexene-1-carbaldehydato(2-)]- μ -Se} bis(tricarbonyliron) has been determined¹². Here the out-of-plane iron atom is bonded to the selenium atom and both unsaturated carbon atoms of the cyclohexene at distances of 2.353(1), 2.214(8) and 2.132(7)Å, respectively, while the in-plane iron is bonded to selenium at 2.327(1)Å and to the carbonyl carbon atom of the selenoferrole ring at 1.990(8)Å. The Fe-Fe distance of 2.631(2)Å is greater than our distance of 2.482(1)Å which is, however, similar to such distances generally found in Fe₂(CO)₆ residues¹². For comparison, in the complex [Cp*(CO)₂Re{ μ - η^6 -SeC₄H₄Fe(CO)₃}Fe(CO)₃] the Fe₂Se triangle has Fe-Se and Fe-Fe distances of 2.357, 2.367 and 2.558 Å³⁶, similar to the values cited above and those measured in complex (36) (see below), although the distinction between the σ -bonded and π -bonded iron atoms is less obvious.

Complex (36) differs from (35) only by the addition of an η^6 -bound $\text{Fe}(\text{CO})_2$ moiety. The selenoferrole ring is more distorted than in (35), with the “in-plane” iron atom, Fe(1), displaced by 0.407(5) Å from the plane of atoms C(1)-C(7). The out-of-plane Fe(2) and the selenium atom are displaced by 2.05 and 0.70 Å, respectively, on the opposite side of the C(1)-C(7) plane, so that the selenoferrole ring [C(1), C(2), C(7), Fe(1), Se(1)] has a half-chair conformation. The Fe-Fe, Fe-Se, Fe-C and Se-C bond distances are similar to those in (35), apart from Fe(2)-C(7), which is longer by 0.26 Å here, and Fe(1)-Fe(2), which is longer by 0.07 Å. The increase in the Fe(2)-C(7) bond length may be a consequence of the presence of the η^6 -bonded Fe(3), which is situated 2.836(1) Å from Fe(2) and 2.226(4) Å from C(7). In a similar situation, an Fe-Fe distance of 2.822 Å has been considered³⁷ to indicate a metal-metal bond. The Fe(3)-C(phenyl) distances are similar to those measured³⁷ previously; apart from the Fe(3)-C(7) distance, they are all in the range 2.12 - 2.14 Å.

In all three iron carbonyl complexes, the Fe-C-O moieties are near linear, with angular ranges of 175.8 - 178.9° in (33), 177.7 - 179.4° in (35) and 175.1 - 179.6° in (36). Fe-CO bond lengths are normal, being 1.77 - 1.81 Å in (33), 1.76 - 1.80 Å in (35) and 1.76 - 1.81 Å in (36). There is some evidence that the Fe-CO bonds in $\text{Fe}(\text{CO})_2$ moieties, having mean lengths 1.763(2) Å³⁷, 1.736(18) Å³⁸ and 1.763(2) Å in (36) are shorter than those in $\text{Fe}(\text{CO})_3$ moieties, having mean lengths, 1.795(12) Å¹², 1.791(4) Å³⁷, 1.783(12) Å in (33), 1.780(6) Å in (35) and 1.781(9) Å in (36).

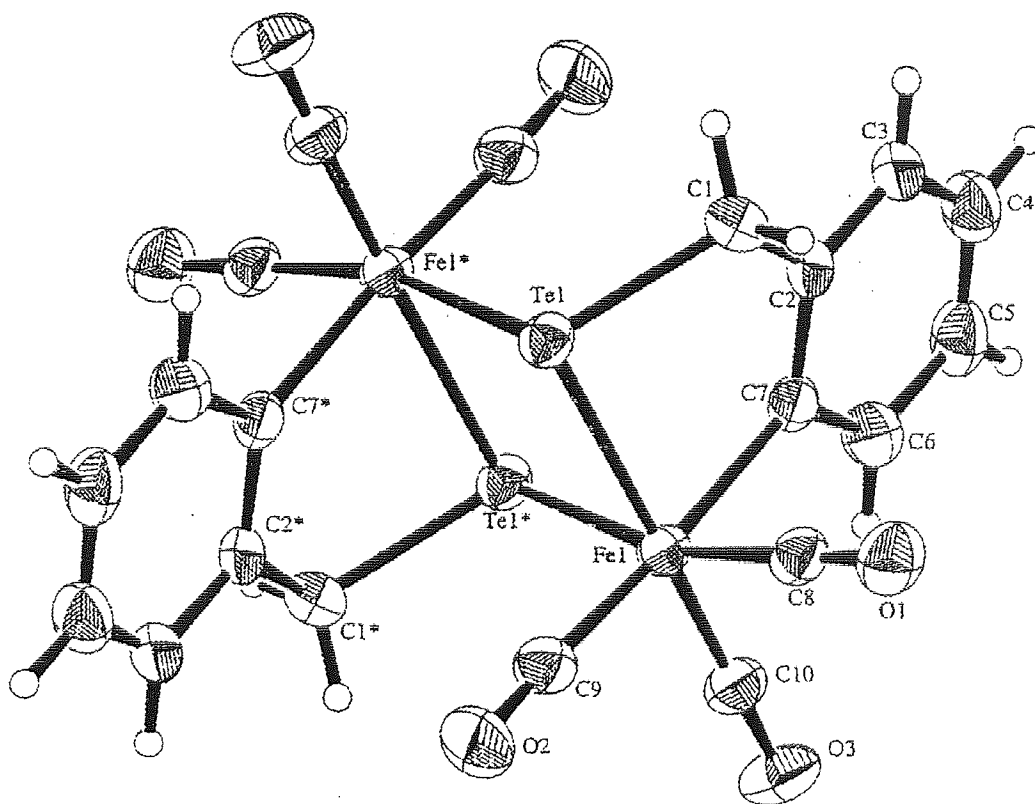


Figure 3.11 The molecular structure of $[\text{Fe}(\text{C}_7\text{H}_6\text{Te})(\text{CO})_3]_2$ (**33**)

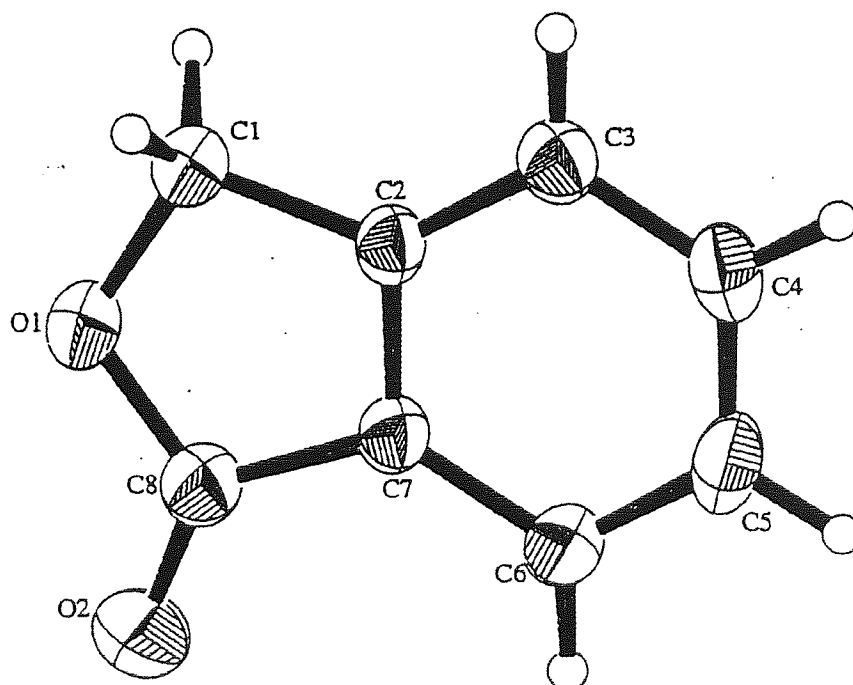


Figure 3.12 The molecular structure of C₈H₆O₂ (34)

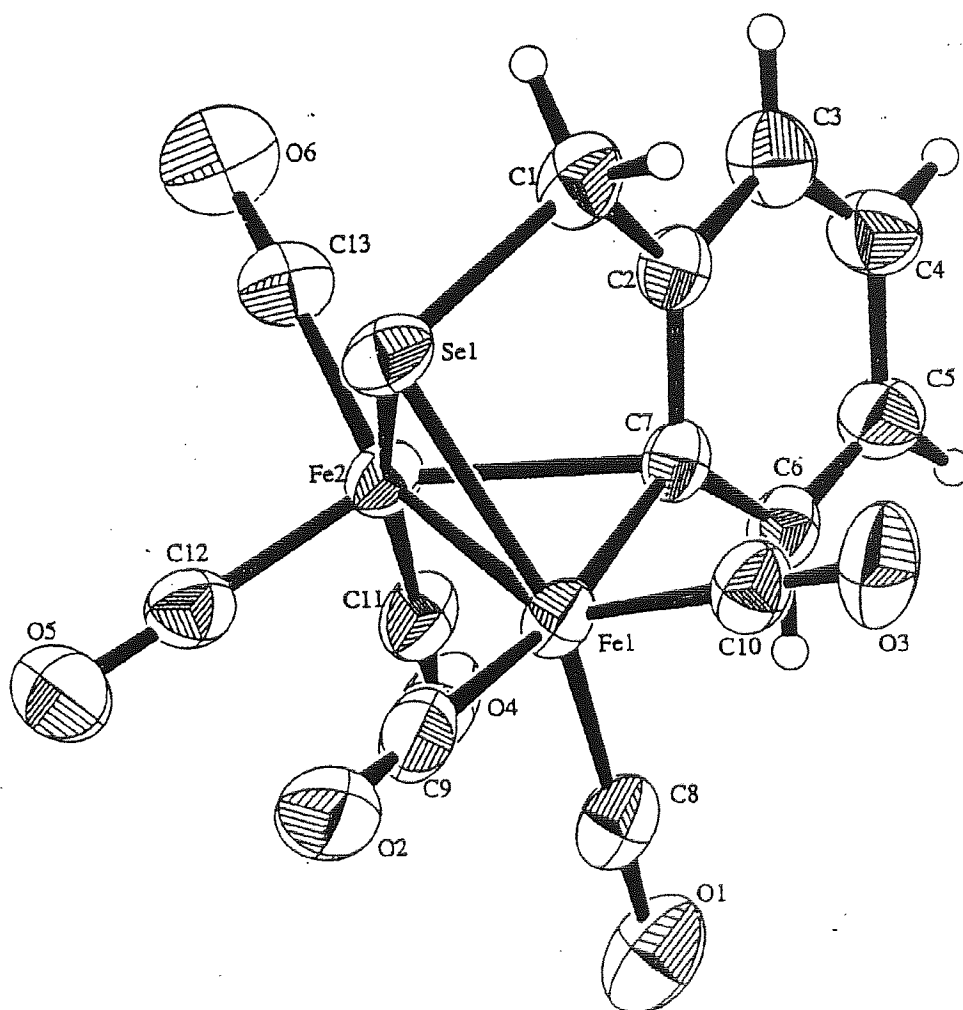


Figure 3.13 The molecular structure of $[\text{Fe}_2(\text{C}_7\text{H}_6\text{Se})(\text{CO})_6]$ (**35**)

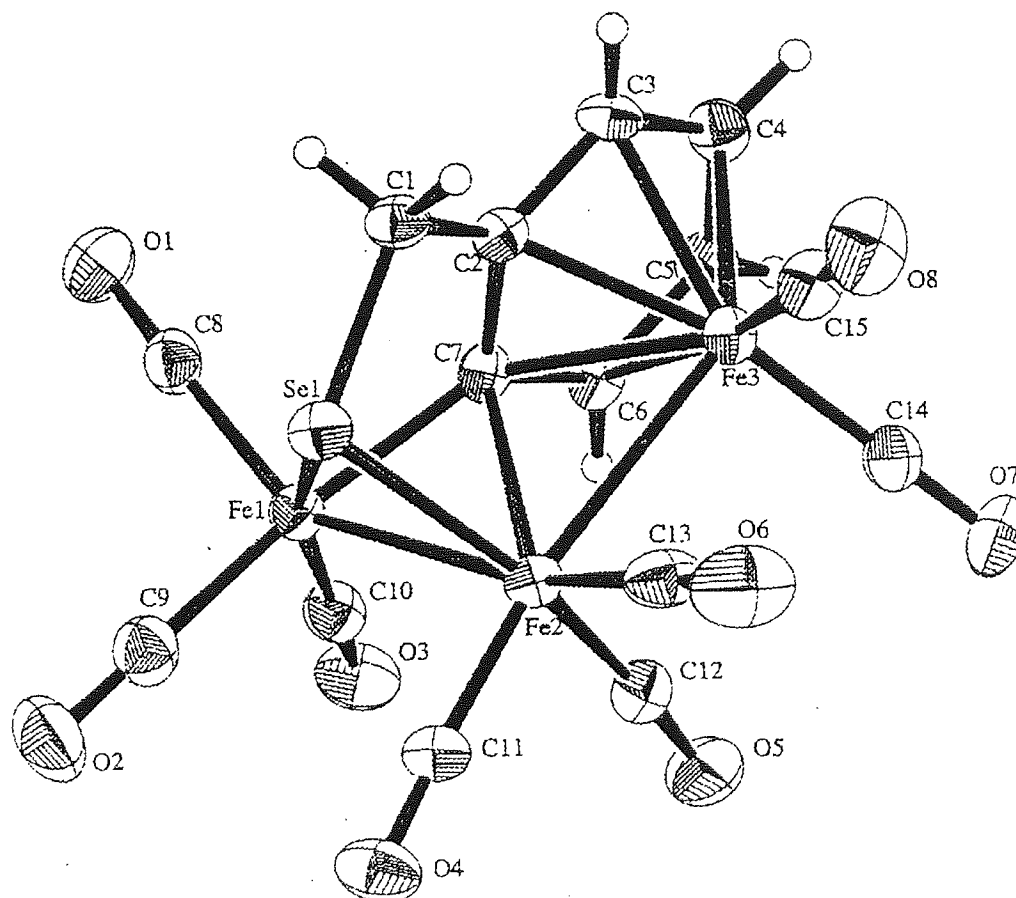


Figure 3.14 The molecular structure of $[\text{Fe}_3(\text{C}_7\text{H}_6\text{Se})(\text{CO})_8]$ (36)

3.4.2 X-ray crystallography of telluraphthalic anhydride (37), 2-selenaphthalic anhydride (38) and 2-selenaphthalide (39)

3.4.2.1 Crystallographic analysis for telluraphthalic anhydride (37), 2-selenaphthalic anhydride (38) and 2-selenaphthalide (39)

Suitable crystals for X-ray analysis were obtained for products (37), (38) and (39), by recrystallising (37) from hexane, slow evaporation of a solution of (38) in hexane : chloroform (1:1) and slow evaporation of a solution of (39) in acetone.

The crystal structures of compounds (37), (38) and (39) were established by Dr T.A Hamor at the University of Birmingham, and are shown in figures 3.15, 3.16 and 3.17 respectively. The crystal parameters and experimental data are listed in table 3.16. Cell dimensions and intensity data for the three structures were measured on a Rigaku R-Axis II area detector diffractometer at 293(2) K using graphite-monochromated Mo-K α radiation, $\lambda=0.7107$ Å. The structures were determined²⁹ by direct methods and refined³⁰ by least-squares on F^2 using anisotropic thermal parameters for non-hydrogen atoms. Hydrogen atoms were placed in calculated positions, riding on their respective bonding atoms. Diagrams were drawn with ORTEP³¹; thermal ellipsoids are at the 30% probability level. Atom co-ordinates are listed in tables 3.17 to 3.19. Selected bond lengths and angles are in table 20.

Table 3.16 Crystallographic data for telluraphthalic anhydride, selenaphthalic anhydride and 2-selenaphthalide.

Compound	Telluraphthalic anhydride (37)	Selenaphthalic anhydride (38)	2-Selenaphthalide (39)
Formula	C ₈ H ₄ O ₂ Te	C ₈ H ₄ O ₂ Se	C ₈ H ₆ OSe
<i>M</i>	259.7	211.1	197.1
Cryst sys	monoclinic	monoclinic	monoclinic
<i>Space Grp</i>	<i>P</i> 2 ₁ / <i>c</i>	<i>P</i> 2 ₁ / <i>n</i>	<i>P</i> 2 ₁ / <i>c</i>
<i>a</i> , Å	8.534(4)	8.529(3)	7.809(4)
<i>b</i>	5.849(4)	5.748(3)	6.403(3)
<i>c</i>	15.528(5)	15.349(4)	15.038(5)
β, deg	100.73(1)	104.07(1)	99.83(2)
<i>U</i> , Å ³	761.5(7)	729.9(5)	740.9(6)
<i>Z</i>	4	4	4
<i>D_c</i>	2.265	1.921	1.767
μ(MoKα), mm ⁻¹	3.84	5.08	4.99
θ range, deg	2.7 - 25.2	2.7 - 25.2	2.6 - 25.2
rfins collected [<i>I</i> > σ(<i>I</i>)]	3763	4086	3531
unique rfins	1283	1254	1216
<i>R</i> (<i>int</i>)	0.0369	0.1204	0.0818
variables refined	100	100	92
Δ/σ(max)	0.001	0.001	0.002
Δρ, e Å ⁻³	0.52, -0.81	0.98, -0.54	0.51, -0.73
<i>R</i> , <i>wR</i> 2 ^a	0.0577, 0.1245	0.0593, 0.1467	0.0989, 0.1724
obsd rfins [<i>I</i> > 2σ(<i>I</i>)]	1173	1184	1035
<i>R</i> , <i>wR</i> 2 ^a obsd data	0.0514, 0.1204	0.0562, 0.1434	0.0768, 0.1551
<i>w</i> (<i>a</i> , <i>b</i>) ^b	0.052, 1.83	0.081, 0.25	0.079, 0

$$^a wR2 = [\sum w(F_o^2 - F_c^2)^2 / \sum w(F_o^2)^2]^{1/2}$$

$$^b w = 1/[\sigma^2(F_o^2) + (aP)^2 + bP] \text{ where } P = (F_o^2 + 2F_c^2)/3$$

Table 3.17 Atomic coordinates ($\times 10^4$) and equivalent isotropic displacement parameters ($\text{\AA}^2 \times 10^3$) for telluraphthalic anhydride (**37**). $U(\text{eq})$ is defined as one third of the trace of the orthogonalized U_{ij} tensor.

	x	y	z	$U(\text{eq})$
Te(1)	8621(1)	-4(1)	7079(1)	55(1)
O(1)	9574(7)	3567(9)	5869(3)	69(2)
O(2)	6478(7)	-3881(10)	6334(3)	72(2)
C(1)	8834(8)	1838(12)	5896(5)	50(2)
C(2)	7914(8)	673(12)	5114(4)	45(2)
C(3)	7859(9)	1528(13)	4277(4)	54(2)
C(4)	7002(11)	356(13)	3568(5)	60(2)
C(5)	6229(9)	-1650(15)	3687(5)	61(2)
C(6)	6290(9)	-2518(13)	4513(5)	57(2)
C(7)	7111(8)	-1357(12)	5231(4)	46(2)
C(8)	7158(9)	-2195(12)	6141(5)	54(2)

Table 3.18 Atomic coordinates ($\times 10^4$) and equivalent isotropic displacement parameters ($\text{\AA}^2 \times 10^3$) for selenaphthalic anhydride (**38**). U(eq) is defined as one third of the trace of the orthogonalized Uij tensor.

	x	y	z	U(eq)
Se(1)	1612(1)	4515(1)	8087(1)	60(1)
O(1)	151(5)	8325(7)	8704(3)	76(1)
O(2)	3613(5)	1077(7)	9085(3)	76(1)
C(1)	1064(5)	6731(8)	8924(3)	52(1)
C(2)	1949(5)	6152(8)	9855(3)	47(1)
C(3)	1865(6)	7503(9)	10586(3)	56(1)
C(4)	2750(6)	6809(10)	11424(3)	60(1)
C(5)	3685(6)	4816(10)	11529(4)	58(1)
C(6)	3761(5)	3468(9)	10807(3)	53(1)
C(7)	2883(5)	4149(7)	9957(3)	45(1)
C(8)	2901(5)	2877(8)	9126(3)	51(1)

Table 3.19 Atomic coordinates ($\times 10^4$) and equivalent isotropic displacement parameters ($\text{\AA}^2 \times 10^3$) for 2-selenaphthalide (**39**). U(eq) is defined as one third of the trace of the orthogonalized U_{ij} tensor.

	x	y	z	U(eq)
Te(1)	3507(1)	193(2)	2057(1)	71(1)
O(1)	1704(10)	3810(10)	1407(4)	79(2)
C(1)	3648(13)	-1697(13)	1048(6)	70(3)
C(2)	2833(10)	-655(12)	197(5)	47(2)
C(3)	2724(12)	-1553(14)	-653(6)	65(2)
C(4)	1952(13)	-485(17)	-1404(7)	75(3)
C(5)	1262(12)	1472(17)	-1325(7)	73(3)
C(6)	1352(11)	2394(15)	-491(6)	61(2)
C(7)	2134(10)	1311(11)	274(5)	43(2)
C(8)	2279(11)	2148(13)	1184(5)	55(2)

3.4.2.2 Discussion of the structures of telluraphthalic anhydride, (37), selenaphthalic anhydride, (38) and 2-selenaphthalide, (39)

The observed tellurium and selenium to sp^2 -hybridized carbon bond lengths are longer than normally accepted values averaging 2.161(6) and 1.945(1) Å respectively, compared with 2.116 and 1.893 Å given in the tabulations of Allen *et al*³³. The Se-C(sp^3) bond in (39) [1.958(9) Å] is, on the other hand, slightly shorter than the accepted³³ value of 1.970 Å. There is little evidence of electron delocalisation in the phthalic anhydrides, (37) and (36); however in (39), a short C(8)-C(7) bond and a relatively long C(8)=O bond appear to indicate some degree of delocalisation.

Although the non-hydrogen atoms of each of the three molecules are essentially coplanar, with rms atomic deviations 0.021 Å (37), 0.035 Å (38) and 0.018 Å (39), closer examination reveals some small but significant deviations from true planarity. In (5), the phenyl ring is planar to within ± 0.008 Å, rms deviation 0.005 Å, with the bonded carbon atoms displaced on opposite sides of the phenyl plane by 0.033 and 0.049 Å, and their respective carbonyl oxygen atoms displaced in the same directions by 0.055 and 0.101 Å. The tellurium atom lies close (0.009 Å) to the phenyl plane. In (38), the phenyl ring is again planar, with rms atomic deviation 0.002 Å. C(1), C(8) and the selenium atom are displaced by, respectively 0.009, 0.032 and 0.130 Å on the same side of this plane, with carbonyl oxygen O(1) lying 0.043 Å on the opposite side of the phenyl plane and O(2) lying close (0.006 Å) to the plane. 2-Selenaphthalide (39) has the eight carbon atoms essentially coplanar (maximum atomic deviation 0.005 Å, rms deviation 0.003 Å) with the selenium and carbonyl oxygen atoms deviating by 0.037 and 0.054 Å on opposite sides of the carbon-atom plane.

The near-planarity of these complexes and of thiophthalic anhydride³⁹ and the parent phthalic anhydride⁴⁰, notwithstanding the differences in bond lengths involving the hetero-atoms [2.161 Å in telluraphthalic anhydride (**37**), 1.945 Å in selenaphthalic anhydride (**38**), 1.801 Å in thiophthalic anhydride³⁹ and 1.395 Å in phthalic anhydride⁴⁰ (see Table 2)] is made possible by the flexibility of valence angles within the five-membered ring. Thus while the C-O-C angle in phthalic anhydride is close to normal at 109.5°, the corresponding angles in thiophthalic anhydride and compounds (**38**) and (**37**) are 92.6(2), 87.3(2) and 81.5(3)°, respectively, correlating with the longer bond lengths. Similarly the angle at selenium in 2-selenaphthalide (**39**) is 87.8(4)°. This large decrease in angle at the heteroatom in going from O to S to Se to Te is accompanied by concomitant increases in the angles C(1)-C(2)-C(7) and C(8)-C(7)-C(2). These angles range from 107.6° in phthalic anhydride to 118.5° in telluraphthalic anhydride (Table 2). There is also a small increase in the angles at the carbonyl carbon atoms. The net result of these bond angle variations is that the sum of the angles within the five-membered ring is, in each case, within 0.2° of 540°, the required value for a planar ring.

There are no abnormal intermolecular contacts. The closest contacts involving tellurium are Te...O, 3.375 Å and Te...Te, 3.828 Å. In the selenium compounds, the closest Se...Se intermolecular distances are 3.889 Å in (**38**) and 4.050 Å in (**39**). In (**38**) there is also an Se...O contact distance of 3.413 Å.

Table 3.20 Selected bond lengths (Å) and angles (°) with e.s.d's in parentheses for compounds **(37)**, **(38)** and **(39)**.

	37	38	39		
	X=Te	X=Se	X=Se	X=S ^a	X=O ^b
X-C(1)	2.166(7)	1.945(5)	1.958(9)	1.801(6)	1.393(5)
X-C(8)	2.155(7)	1.946(5)	1.944(8)	1.801(4)	1.396(4)
C(1)-O	1.198(8)	1.197(6)		1.200(7)	1.192(5)
C(8)-O	1.210(9)	1.209(6)	1.224(10)	1.194(8)	1.192(4)
C(1)-C(2)	1.483(9)	1.483(6)	1.486(11)	1.482(5)	1.471(3)
C(8)-C(7)	1.489(10)	1.473(6)	1.456(10)	1.479(7)	1.466(4)
C(1)...C(8)	2.820(10)	2.687(6)	2.706(11)	2.605(7)	2.277(4)
C(1)-X-C(8)	81.5(3)	87.3(2)	87.8(4)	92.6(2)	109.5(3)
X-C(1)-C(2)	110.5(5)	110.0(3)	108.5(6)	109.8(4)	107.6(3)
X-C(8)-C(7)	110.8(5)	110.3(3)	110.3(6)	109.3(4)	107.6(3)
C(1)-C(2)-C(7)	118.7(6)	116.0(4)	117.0(7)	113.4(5)	107.8(3)
C(8)-C(7)-C(2)	118.4(6)	116.2(4)	116.4(7)	114.7(4)	107.4(3)
Σ(angles)	539.9	539.8	540.0	539.8	539.9

^a Previous work³⁹

^b Previous work⁴⁰

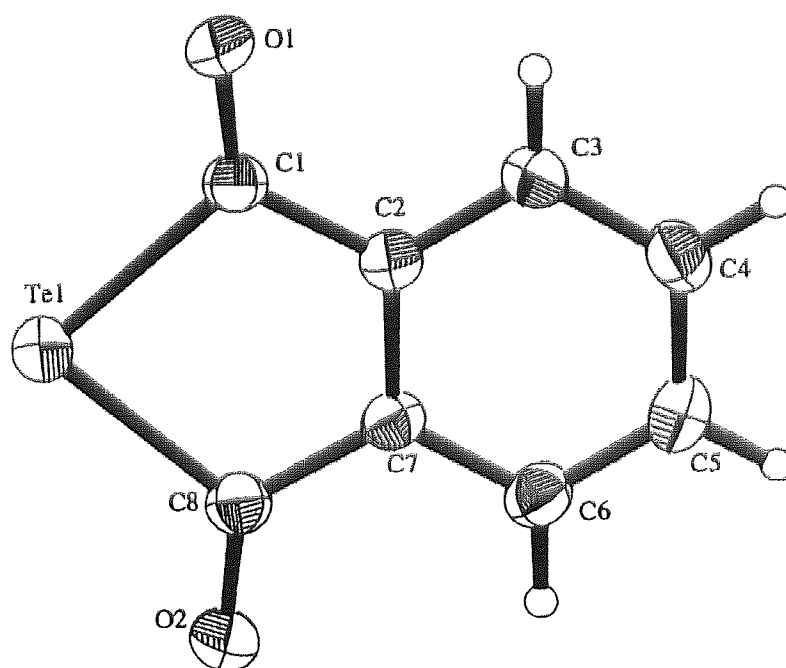


Figure 3.15 The molecular structure of telluraphthalic anhydride (37)

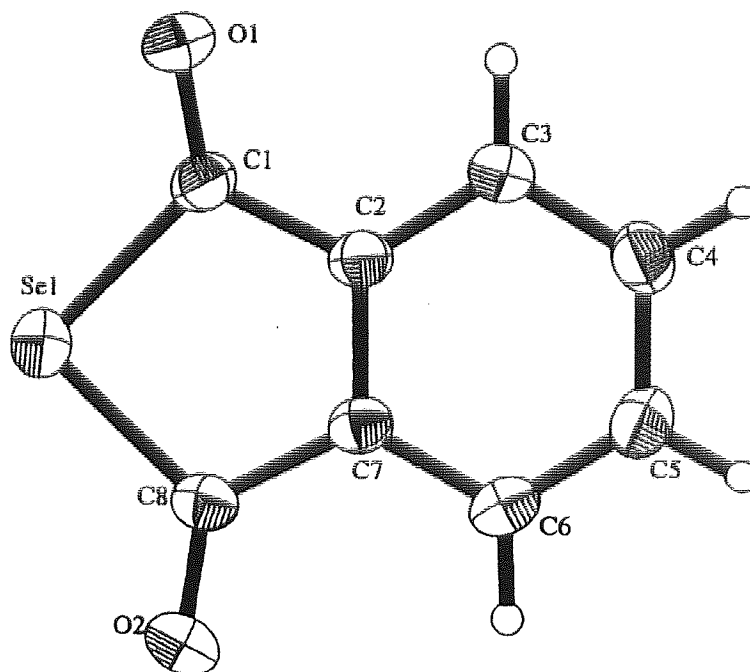


Figure 3.16 The molecular structure of selenaphthalic anhydride (**38**)

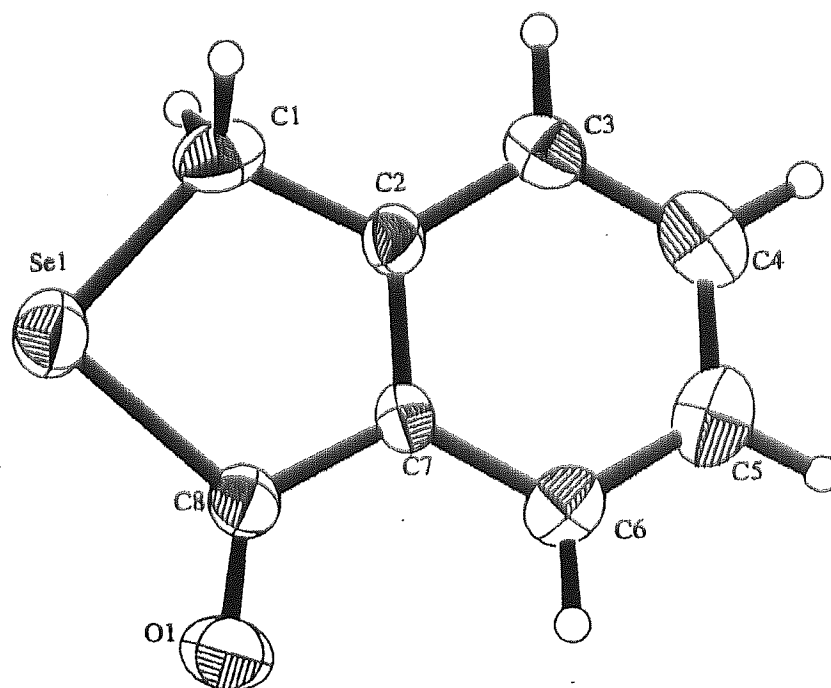


Figure 3.17 The molecular structure of 2-selenaphthalide (39)

3.5 Conclusion

Telluraphthalide reacted with $[\text{Fe}_3(\text{CO})_{12}]$ to give an insertion product, $[\text{Fe}(\text{C}_7\text{H}_4\text{Te})(\text{CO})_3]_2$ (**33**). The initial stage of the reaction is the insertion of an $\text{Fe}(\text{CO})_3$ group into the $\text{Te}-\text{C}(\text{O})$ bond. It is then assumed that two rapid steps occur, i.e. the reverse of a carbonyl insertion reaction. Dimerisation of the product occurred satisfying the 18-electron rule, which requires tellurium to function as a Lewis base.

The reaction of $[\text{Fe}_3(\text{CO})_{12}]$ with telluraphthalic anhydride gives an unexpected product (phthalide, **34**). The origin of this product may be the subject of further investigation. The initial step is insertion of a multi iron moiety into $\text{Te}-\text{C}(\text{O})$, followed by the formation of a carbene by backside attack on one carbonyl group. The loss of FeTe is then possible. The carbene may extract protons from the solvent (toluene).

2-Selenaphthalide reacted with $[\text{Fe}_3(\text{CO})_{12}]$ to give two insertion products (**35**), $[\text{Fe}_2(\text{C}_7\text{H}_6\text{Se})(\text{CO})_6]$, and (**36**), $[\text{Fe}_3(\text{C}_7\text{H}_6\text{Se})(\text{CO})_8]$. The relative yields suggest that (**36**) is an intermediate compound in the formation of (**35**). The initial step of the reaction is the insertion of a iron moiety into the $\text{Se}-\text{C}(\text{O})$ bond. Product (**36**) suggests that the iron moiety is not a simple $\text{Fe}(\text{CO})_3$ unit [as observed in the formation of (**33**)] but a more complex iron species, which may contain all three or two of the iron atoms of the initial $[\text{Fe}_3(\text{CO})_{12}]$. The next step of the reaction is a reverse of a carbonyl insertion giving (**36**). The loss of the η^6 -bound $\text{Fe}(\text{CO})_2$ moiety must occur giving compound (**35**).

The reaction of the selenaphthalic anhydride with $[\text{Fe}_3(\text{CO})_{12}]$ afforded only unreacted starting material and an unidentifiable red product.

The reaction of selenium analogues with $[\text{Fe}_3(\text{CO})_{12}]$ gave products, which may be considered as intermediate compounds of a complex reaction sequence when compared with the tellurium reaction products.

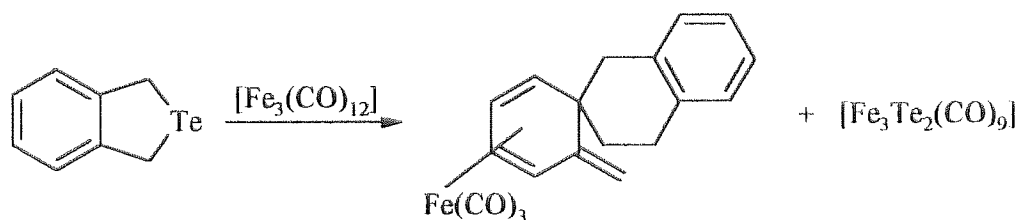
The use of the selenium analogue has produced novel compounds.

CHAPTER FOUR

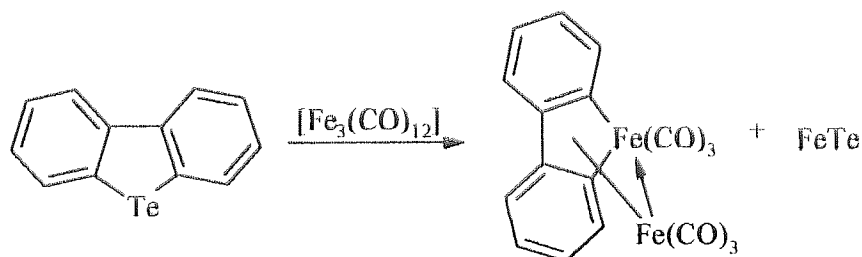
**THE REACTIONS OF SIX MEMBERED HETEROCYCLIC
SYSTEMS CONTAINING EITHER TELLURIUM OR SELENIUM
AS THE HETEROATOM WITH TRIIRON DODECACARBONYL**

4.1 Introduction

The reaction of 2-telluraindane³ with triiron dodecacarbonyl gave three compounds. One of the compounds was a cluster compound, $[\text{Fe}_3\text{Te}_2(\text{CO})_9]$, the second was $[\text{Fe}(\text{CO})_3(\text{C}_{16}\text{H}_{16})]$ (see below) and the third was not identified.

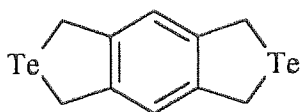


The reaction of dibenzotellurophene³ with triiron dodecacarbonyl gave a dibenzoferrole, $[\text{Fe}_2(\text{C}_{12}\text{H}_8)(\text{CO})_6]$ (see below).

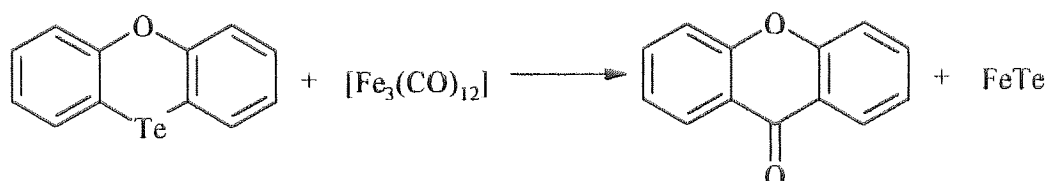


Therefore, it is reasonable to assume that 2-selenaindane and dibenzoselenophene will react with iron carbonyl, thus maintaining the theme where directly related compounds of tellurium and selenium heterocycles are compared.

Currently, cases where there has only been one tellurium^{3,11,20} or selenium atom (see chapter three) within the starting heterocycle (e.g. 2-telluraphthalide, telluraphthalic anhydride) have been considered. It could therefore be interesting to react a compound with two tellurium atoms within the molecule, to see if one or both of the tellurium atom sites would interact with triiron dodecacarbonyl. The compound chosen was 1,3,7,9-tetrahydrobenzo[1,2-c;4,5-c']ditellurophene. This compound was chosen because the molecule is very similar to 2-telluraindane (see below).



Phenoxtellurine reacted with iron carbonyl resulting in the removal of the tellurium from the heterocyclic ring to eventually yield a carbonyl insertion product (see below).



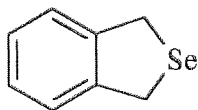
It has been shown in chapter three that selenium analogues can give materials that can be considered models for intermediate stages of the reaction sequence. Therefore it is reasonable to react the selenium analogue of phenoxtellurine, which is phenoxselenine.

To maintain the theme of reactions of directly related tellurium and selenium heterocycles with iron carbonyl, related 3,5-naphtho-1-telluracyclohexane and 3,5-naphtho-1-selenacyclohexane compounds were reacted. These compounds were considered because they had the heteroatom contained within a six-membered ring rather than within a five-membered ring.

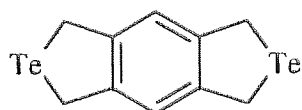
4.2 Experimental

4.2.1 Reactions of tellurium and selenium heterocycles

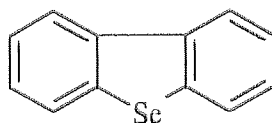
4.2.2 Preparation of heterocyclic tellurium and selenium compounds



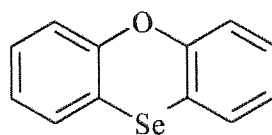
1,3-Dihydrobenzo[c]selenophene⁴¹



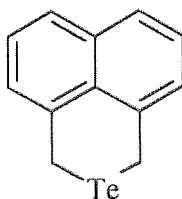
1,3,7,9-Tetrahydrobenzo[1,2c;4,5c']ditellurophene⁴²



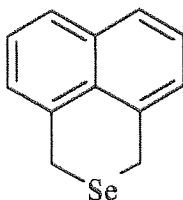
Dibenzoselenophene⁴³



Phenoxselenine⁴⁴



3,5-Naphtho-1-telluracyclohexane⁴⁵



3,5-Naphtho-1-selenacyclohexane⁴⁵

The above heterocycles were prepared using literature methods^{41,42,43,44,45}. The analyses of the above materials were in good agreement with the literature values^{41,42,43,44,45}. Also the x-ray structures of 3,5-naphtho-1-telluracyclohexane and 3,5-naphtho-1-selenacyclohexane have been determined (see section 4.4.1).

4.2.3 Standard procedure for reaction of triron dodecacarbonyl with heterocyclic compounds

Heterocyclic compound and $[\text{Fe}_3(\text{CO})_{12}]$ (molar ratio 1:1) were refluxed, with stirring, in the dark, in toluene (25 cm³) for 4.5 h. The reaction mixture was cooled to room temperature and filtered to give a filtrate and a residual black solid which adhered to the sides of the flask. The solvent was removed from the filtrate *in vacuo* to give a solid. The solid was chromatographed on a column of silica gel.

4.2.3.1 1,3-Dihydrobenzo[c]selenophene

The standard procedure was followed.

1,3-Dihydrobenzo[c]selenophene = 1g, 5.52 mmol

$[\text{Fe}_3(\text{CO})_{12}]$ = 2.78g, 5.52 mmol

Elution of the reaction product with hexane afforded starting material (1,3-dihydrobenzo[c]selenophene).

4.2.3.2 1,3,7,9-Tetrahydrobenzo[1,2c;4,5c']ditellurophene

The standard procedure was followed.

1,3,7,9-Tetrahydrobenzo[1,2c;4,5c']ditellurophene = 0.3g, 0.87 mmol

[Fe₃(CO)₁₂] = 0.84g, 1.67 mmol

Elution of the reaction product with chloroform afforded starting material (1,3,7,9-tetrahydrobenzo[1,2c;4,5c']ditellurophene).

4.2.3.3 Dibenzoselenophene

The standard procedure was followed.

Dibenzoselenophene = 1g, 4.3 mmol

[Fe₃(CO)₁₂] = 2.18g, 4.3 mmol

Elution of the reaction product with chloroform afforded starting material (dibenzoselenophene).

4.2.3.4 Phenoxselenine

The standard procedure was followed.

Phenoxselenine = 0.2g, 0.81 mmol

[Fe₃(CO)₁₂] = 0.41g, 0.81 mmol

Elution of the reaction product with chloroform afforded starting material (phenoxselenine).

4.2.3.5 3,5-Naphtho-1-telluracyclohexane

The standard procedure was followed.

3,5-Naphtho-1-telluracyclohexane = 0.16g, 0.56 mmol

[Fe₃(CO)₁₂] = 0.28g, 0.56 mmol

Elution of the reaction product with chloroform afforded starting material (3,5-naphtho-1-telluracyclohexane).

4.2.3.6 3,5-Naphtho-1-selenacyclohexane

The standard procedure was followed.

3,5-Naphtho-1-selenacyclohexane = 1g, 4.29 mmol

[Fe₃(CO)₁₂] = 2.17g, 4.29 mmol

Elution of the reaction product with chloroform afforded starting material (3,5-naphtho-1-selenacyclohexane).

4.3 Results and discussion

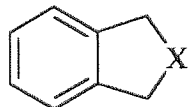
It is unfortunate that 1,3-dihydrobenzo[c]selenophene, 1,3,7,9-tetrahydrobenzo[1,2c;4,5c']ditellurophene, dibenzoselenophene, phenoxselenine, 3,5-naphtho-1-telluracyclohexane and 3,5-naphtho-1-selenacyclohexane do not react with triiron dodecacarbonyl under the conditions employed. One can notice that five membered heterocyclic ring (see chapter three) compounds react with triiron dodecacarbonyl, but six membered heterocyclic ring compounds do not. This may be due to differing degrees of ring strain.

Ring strain may be due to a number of factors: angle strain, torsional strain and steric strain. Angle strain arises due to the expansion or compression of bond angles. Torsional strain arises due to the eclipsing of bonds on neighbouring atoms. Steric strain arises due to the repulsive interactions when atoms approach each other too closely.

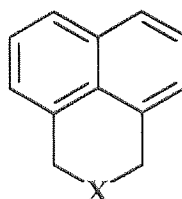
On examination of the reactions of five membered heterocyclic ring compounds with triiron dodecacarbonyl, one notices that the intermediates are six membered rings, which then form five membered ring products (see chapter three). However when a six membered heterocyclic ring compound is reacted with triiron dodecacarbonyl there is no reaction.

If one considers the analogous carbon chemistry, cyclopropane and cyclobutane are highly strained, but cyclopentane is less strained than the three and four membered rings. Cyclohexane is strain free, but rings containing seven to thirteen carbons have ring strain.

One can suggest that the five membered tellurium and selenium heterocyclic compounds have more ring strain than six membered rings. Of the molecules below, (41) will have less strain than (40).



40



41

Where X = Se or Te

This is due to the bond angles around the sp^2 carbons in (41) being larger than in (40) and to the conformation of the heterocyclic ring. It can be seen in section 4.4 that the conformation of the heterocyclic ring of (41) is a half chair, therefore reducing the ring strain within the molecule. The strain within a ring system decreases as the C – X bond length decreases (where X = tellurium or selenium); therefore selenium heterocyclic compounds have less strain than their tellurium analogues.

An additional factor in the lack of reactions of the selenium heterocyclic compounds with iron carbonyl may be the higher carbon – selenium bond strength compared with the tellurium – carbon strength.

4.4 X-ray crystallography

4.4.1 Crystallographic analysis for 1,8-bis(bromomethyl)naphthalene, (42), 1,1-diiodo-3,5-naphthotelluracyclohexane, (43), 3,5-naphtho-1-telluracyclohexane, (44) and 3,5-naphtho-1-selenacyclohexane, (45).

Suitable crystals for X-ray analysis were obtained for products (42), (43), (44) and (45), by recrystallising (42) from hexane, recrystallising (43) from 2-methoxyethanol, slow evaporation of a solution of (44) in ether and slow evaporation of a solution of (45) in pet. ether (40-60).

The crystal structures of compounds (42), (43), (44) and (45) were established by Dr T.A. Hamor at the University of Birmingham and are shown in figures 4.1, 4.2, 4.3 and 4.4 respectively. The crystal parameters and experimental data are listed in table 4.1. Cell dimensions and intensity data for the three structures were measured on a Rigaku R-AXIS II area detector diffractometer at 293(2) K using graphite-monochromated Mo-K α radiation, $\lambda=0.7107$ Å. The structures were determined²⁹ by direct methods and refined³⁰ by least-squares on F^2 using anisotropic thermal parameters for non-hydrogen atoms. Hydrogen atoms were placed in calculated positions, riding on their respective bonding atoms. Diagrams were drawn with ORTEP³¹; thermal ellipsoids are at the 30% probability level. Atom co-ordinates are listed in tables 4.2 to 4.5. Selected bond lengths and angles are in tables 4.6 to 4.9.

Table 4.1 Crystallographic data for products (42), (43), (44) and (45).

Compound	42	43	44	45
Formula	C ₁₂ H ₁₀ Br ₂	C ₁₂ H ₁₀ TeI ₂	C ₁₂ H ₁₀ Te	C ₁₂ H ₁₀ Se
<i>M</i>	314.02	535.6	281.80	233.16
Cryst sys	Monoclinic	Monoclinic	Monoclinic	Monoclinic
Space grp	C2/c	P2 ₁ /c	P2 ₁ /c	P2 ₁ /a
<i>a</i> , Å	23.561(3)	11.835(7)	12.5638(14)	14.656(2)
<i>b</i>	7.6540(11)	8.839(5)	4.7203(4)	9.1572(11)
<i>c</i>	12.4771(11)	13.432(7)	16.872(2)	15.353(2)
β, deg	95.918(9)	109.16(2)	93.559(3)	106.831(5)
<i>U</i> , Å ³	2238.1(5)	1327.3(13)	998.7(2)	1972.1(4)
<i>Z</i>	8	4	4	8
D _c (Mg m ⁻³)	1.864	2.680	1.874	1.571
μ(MoKα), mm ⁻¹	7.200	6.860	2.926	3.754
Rflns collected [I>σ(I)]	5778	23146	5393	20421
unique rflns	1835	2403	1613	3518
<i>R</i> (int)	0.0575	0.0582	0.0238	0.0671
Variables	137	137	128	289
Δρ (max +ve)(eÅ ⁻³)	0.411	0.990	0.659	1.517
Δρ (max -ve)(eÅ ⁻³)	-0.737	-1.308	-0.935	-0.704
<i>R</i>	0.0467	0.0445	0.0478	0.0719
<i>wR</i> 2 ^a	0.1086	0.1111	0.1401	0.1464
<i>w</i> (a.b) ^b	0.054, 1.402	—	0.092, 1.12	0.058, 4.72

$$a_w R2 = [\sum w(F_o^2 - F_c^2)^2 / \sum w(F_o^2)]^{1/2}$$

$$b_w = 1/[\sigma^2(F_o^2) + (aP)^2 + bP] \text{ where } P = (F_o^2 + 2F_c^2)/3$$

Table 4.2 Atomic coordinates ($\times 10^4$) and equivalent isotropic displacement parameters ($\text{\AA}^2 \times 10^3$) for 1,8-bis(bromomethyl)naphthalene, (42). U(eq) is defined as one third of the trace of the orthogonalized Uij tensor.

	x	y	z	U(eq)
Br(1)	1521(1)	7912(1)	41(1)	70(1)
Br(2)	942(1)	3337(1)	-2408(1)	68(1)
C(1)	1775(3)	4262(10)	328(5)	58(2)
C(2)	2262(3)	3863(12)	1011(6)	72(2)
C(3)	2268(5)	2618(14)	1822(7)	87(3)
C(4)	1771(4)	1815(11)	2017(6)	75(2)
C(5)	1259(3)	2150(9)	1361(5)	57(2)
C(6)	756(4)	1311(10)	1604(6)	72(2)
C(7)	260(4)	1547(11)	992(8)	75(2)
C(8)	247(3)	2609(10)	70(6)	61(2)
C(9)	722(3)	3500(8)	-202(5)	49(2)
C(10)	1253(3)	3342(8)	486(5)	47(2)
C(11)	1835(3)	5697(10)	-443(6)	62(2)
C(12)	621(3)	4531(10)	-1199(4)	55(2)

Table 4.3 Atomic coordinates ($\times 10^4$) and equivalent isotropic displacement parameters ($\text{\AA}^2 \times 10^3$) for **1,1-diiodo-3,5-naphthotelluracyclohexane, (43)**. $U(\text{eq})$ is defined as one third of the trace of the orthogonalized U_{ij} tensor.

	x	y	z	$U(\text{eq})$
I(1)	7245(1)	4982(1)	6001(1)	60(1)
I(2)	4299(1)	5276(1)	1944(1)	59(1)
Te(1)	5890(1)	3686(1)	4049(1)	45(1)
C(1)	7273(5)	943(7)	5379(5)	45(1)
C(2)	7274(7)	-52(7)	6139(5)	53(2)
C(3)	8345(7)	-651(8)	6847(5)	59(2)
C(4)	9403(7)	-157(8)	6795(5)	58(2)
C(5)	10584(6)	1450(8)	6024(6)	56(2)
C(6)	10635(6)	2510(9)	5313(7)	60(2)
C(7)	9592(6)	3051(9)	4566(6)	55(2)
C(8)	8476(6)	2526(7)	4511(5)	45(1)
C(9)	8374(5)	1482(6)	5282(5)	41(1)
C(10)	9464(6)	911(7)	6047(5)	46(1)
C(11)	6048(6)	1405(7)	4652(6)	49(2)
C(12)	7434(6)	3094(8)	3615(5)	51(2)

Table 4.4 Atomic coordinates ($\times 10^4$) and equivalent isotropic displacement parameters ($\text{\AA}^2 \times 10^3$) for, 3,5-naphtho-1-telluracyclohexane, (**44**). U(eq) is defined as one third of the trace of the orthogonalized Uij tensor.

	x	y	z	U(eq)
Te(1)	4810(1)	7734(1)	-934(1)	65(1)
C(1)	3076(6)	8427(16)	-2241(4)	59(2)
C(2)	2938(7)	9212(20)	-3020(4)	84(2)
C(3)	2147(11)	11088(30)	-3280(7)	117(4)
C(4)	1439(11)	12168(24)	-2777(11)	119(6)
C(5)	829(10)	12546(21)	-1430(13)	120(6)
C(6)	929(9)	11744(27)	-638(11)	125(5)
C(7)	1725(6)	9945(18)	-359(5)	81(2)
C(8)	2443(5)	8824(15)	-851(4)	59(2)
C(9)	2348(5)	9511(13)	-1680(4)	56(2)
C(10)	1543(6)	11364(20)	-1955(6)	86(2)
C(11)	3990(6)	6457(16)	-2025(4)	65(2)
C(12)	3280(6)	6871(19)	-485(4)	70(2)

Table 4.5 Atomic coordinates ($\times 10^4$) and equivalent isotropic displacement parameters ($\text{\AA}^2 \times 10^3$) for 3,5-naphtho-1-selenacyclohexane, (45). U(eq) is defined as one third of the trace of the orthogonalized Uij tensor.

	x	y	z	U(eq)
Se(1)	10412(1)	3355(1)	1309(1)	76(1)
Se(2)	10234(1)	2843(1)	-3354(1)	84(1)
C(1)	9527(4)	2281(6)	-499(4)	50(1)
C(2)	9246(6)	2665(8)	-1404(4)	71(2)
C(3)	8392(8)	2188(10)	-1999(9)	86(3)
C(4)	7812(6)	1319(10)	-1701(6)	83(2)
C(5)	8044(4)	889(6)	-790(5)	58(2)
C(6)	7416(5)	5(8)	-451(7)	78(2)
C(7)	7622(6)	-347(9)	417(8)	88(3)
C(8)	8470(6)	132(8)	1033(6)	76(2)
C(9)	9112(4)	959(6)	771(4)	53(1)
C(10)	8911(3)	1386(5)	-166(4)	42(1)
C(11)	10463(5)	2825(8)	94(6)	69(2)
C(12)	10014(6)	1384(8)	1460(5)	70(2)
C(13)	9713(4)	2491(6)	-5291(4)	55(2)
C(14)	9687(7)	3194(9)	-6077(6)	80(2)
C(15)	8937(9)	3022(13)	-6854(7)	101(3)
C(16)	8196(8)	2186(12)	-6881(5)	91(3)
C(17)	8174(4)	1399(7)	-6072(5)	65(2)
C(18)	7411(6)	506(11)	-6073(8)	96(3)
C(19)	7375(6)	-181(10)	-5328(10)	96(3)
C(20)	8106(7)	-43(8)	-4507(7)	86(3)
C(21)	8905(4)	830(6)	-4456(4)	56(2)
C(22)	8941(4)	1560(6)	-5257(4)	46(1)
C(23)	10572(5)	2728(9)	-4476(5)	76(2)
C(24)	9678(6)	914(9)	-3588(5)	75(2)

Table 4.6 Selected bond lengths (Å) and angles (°) for 1,8-bis(bromomethyl)naphthalene, (**42**).

Compound (42)				
Br(1)-C(11)	1.970(8)		C(1)-C(11)	1.476(10)
Br(2)-C(12)	1.979(6)		C(8)-C(9)	1.382(9)
C(1)-C(2)	1.390(10)		C(9)-C(10)	1.448(9)
C(1)-C(10)	1.448(9)		C(9)-C(12)	1.471(9)
C(2)-C(1)-C(10)	117.9(7)		C(10)-C(9)-C(12)	126.9(6)
C(2)-C(1)-C(11)	115.8(7)		C(9)-C(10)-C(1)	124.9(6)
C(10)-C(1)-C(11)	126.2(6)		C(1)-C(11)-Br(1)	112.1(5)
C(8)-C(9)-C(10)	119.0(6)		C(9)-C(12)-Br(2)	110.8(5)
C(8)-C(9)-C(12)	114.1(6)			

Table 4.7 Selected bond lengths (Å) and angles (°) for 1,1-diiodo-3,5-naphthotelluracyclohexane, (**43**).

Compound (43)				
I(1)-Te(1)	2.8286(13)		C(1)-C(2)	1.348(9)
I(2)-Te(1)	3.0011(14)		C(1)-C(9)	1.432(8)
Te(1)-C(12)	2.157(6)		C(7)-C(8)	1.379(9)
Te(1)-C(11)	2.158(6)		C(8)-C(9)	1.421(9)
C(12)-Te(1)-C(11)	84.2(3)		C(9)-C(1)-C(11)	124.0(6)
C(12)-Te(1)-I(1)	94.4(2)		C(7)-C(8)-C(9)	119.2(6)
C(11)-Te(1)-I(1)	94.4(2)		C(7)-C(8)-C(12)	116.8(6)
C(12)-Te(1)-I(2)	89.5(2)		C(9)-C(8)-C(12)	124.0(6)
C(11)-Te(1)-I(2)	89.9(2)		C(8)-C(9)-C(1)	125.4(6)
I(1)-Te(1)-I(2)	174.44(2)		C(1)-C(11)-Te(1)	116.2(4)
C(2)-C(1)-C(9)	120.8(6)		C(8)-C(12)-Te(1)	114.2(4)
C(2)-C(1)-C(11)	115.2(6)			

Table 4.8 Selected bond lengths (Å) and angles (°) for 3,5-naphtho-1-telluracyclohexane, (44).

Compound (44)				
Te(1)-C(11)	2.140(7)		C(1)-C(11)	1.508(11)
Te(1)-C(12)	2.149(8)		C(7)-C(8)	1.370(10)
C(1)-C(2)	1.366(10)		C(8)-C(9)	1.434(9)
C(1)-C(9)	1.446(10)		C(8)-C(12)	1.502(11)
C(11)-Te(1)-C(12)	81.7(3)		C(7)-C(8)-C(12)	117.3(7)
C(2)-C(1)-C(9)	119.2(8)		C(8)-C(9)-C(1)	122.7(6)
C(2)-C(1)-C(11)	116.5(7)		C(1)-C(11)-Te(1)	110.7(4)
C(7)-C(8)-C(9)	119.1(7)		C(8)-C(12)-Te(1)	111.0(5)

Table 4.9 Selected bond lengths (Å) and angles (°) for 3,5-naphtho-1-selenacyclohexane, (45).

Compound (45)				
Se(1)-C(12)	1.931(8)		C(9)-C(10)	1.437(8)
Se(1)-C(11)	1.948(8)		C(9)-C(12)	1.486(9)
Se(2)-C(23)	1.928(8)		C(13)-C(14)	1.359(10)
Se(2)-C(24)	1.935(8)		C(13)-C(22)	1.430(8)
C(1)-C(2)	1.376(9)		C(13)-C(23)	1.512(9)
C(1)-C(10)	1.419(8)		C(20)-C(21)	1.401(10)
C(1)-C(11)	1.419(8)		C(21)-C(22)	1.414(8)
C(8)-C(9)	1.356(9)		C(21)-C(24)	1.480(10)
C(12)-Se(1)-C(11)	88.8(3)		C(14)-C(13)-C(22)	119.7(7)
C(23)-Se(2)-C(24)	89.3(3)		C(14)-C(13)-C(23)	118.0(7)
C(2)-C(1)-C(10)	118.4(6)		C(22)-C(13)-C(23)	122.2(6)
C(2)-C(1)-C(11)	118.9(6)		C(20)-C(21)-C(24)	119.3(7)
C(10)-C(1)-C(11)	122.7(6)		C(22)-C(21)-C(24)	123.1(6)
C(8)-C(9)-C(12)	119.1(7)		C(21)-C(22)-C(13)	122.9(5)
C(10)-C(9)-C(12)	121.6(5)		C(13)-C(23)-Se(2)	112.3(4)
C(1)-C(10)-C(9)	123.4(5)		C(21)-C(24)-Se(2)	112.7(5)

4.4.1.1 Discussion of the structures of 1,8-bis(bromomethyl)naphthalene, (42), 1,1-diiodo-3,5-naphthotelluracyclohexane, (43), 3,5-naphtho-1-telluracyclohexane, (44) and 3,5-naphtho-1-selenacyclohexane, (45).

There is nothing unusual seen in the crystal and molecular structures of (42), (43), (44) and (45). All four crystal structures show a planar naphthalene ring system. The three structures (43), (44) and (45) are very similar to each other as the selenium or tellurium atoms are out of the planar ring system. The only distinction of (43) from (44) and (45) is that there are two iodide atoms attached to the tellurium and these iodide atoms are above and below the planar ring system.

Bromine to sp^3 -hybridized carbon bond lengths for (42) [1.970(8) and 1.979(6)] are in good agreement with the accepted values, when compared with 1.966 Å given in the tabulations of Allen *et al*³³. The bond angles C(1)-C(11)-Br(1) and C(9)-C(12)-Br(2) are 112.1(5) and 110.8(5) respectively, hence positioning the bromines as far as possible from each other.

The Te-I bond in (43) [averaging 2.9148 Å] is slightly shorter than that given by Allen *et al*³³, of 2.926(9) Å. On comparing the Te-I bond length in (43) with that in 2-phenylazophenyl-(C,N')tellurium(II) iodide (see section 5.4.1), the bond length is longer than 2.877(1). It is in good agreement with the measured value in 2-(2'-pyridyl)phenyltellurium(II) iodide,⁴⁶ 2.917(1) Å and slightly shorter than that in 1-iodo-2-p-tolyl-1-tellura-2-azaindene⁴⁷, 2.936(1) Å, but falls well within the rather broad range of lengths which have been found previously for such bonds⁴⁸.

Tellurium to sp^3 -hybridized carbon bond lengths for (44) are shorter than normally accepted values, 2.140(7) Å, compared with 2.158 Å given in the tabulations of Allen *et al*³³. However the value for (43), 2.158(6), is in good agreement when compared with the value found by Allen *et al*³³. The Se-C(sp^3) bond in (45) [averaging 1.935 Å]

is, on the other hand, slightly shorter than the accepted³³ value of 1.970 Å and also shorter on comparing within the value of 1.958(9) Å in 2-selenophthalide (see section 3.4.2).

The bond angles C(11)-Te(1)-C(12) for (43) and (44) are 84.2(3) and 81.7(3)° respectively, which is in good agreement with telluraphthalic anhydride, 81.5(3)° (see section 3.4.2). However the bond angles C(12)-Se(1)-C(11) are 88.8(3) and 89.3(3)° which are larger than the one found in selenaphthalic anhydride, [87.3(2)°] and 2-selenaphthalide, [87.8(4)°]. The average C-C-Te and C-C-Se angles are 116.2(4) for (43), 110.85 for (44) and 112.5° for (45) respectively. On comparing the bond angles of the tellurium and selenium molecules, one observed that the tellurium molecular structures are more strained than the selenium ones.

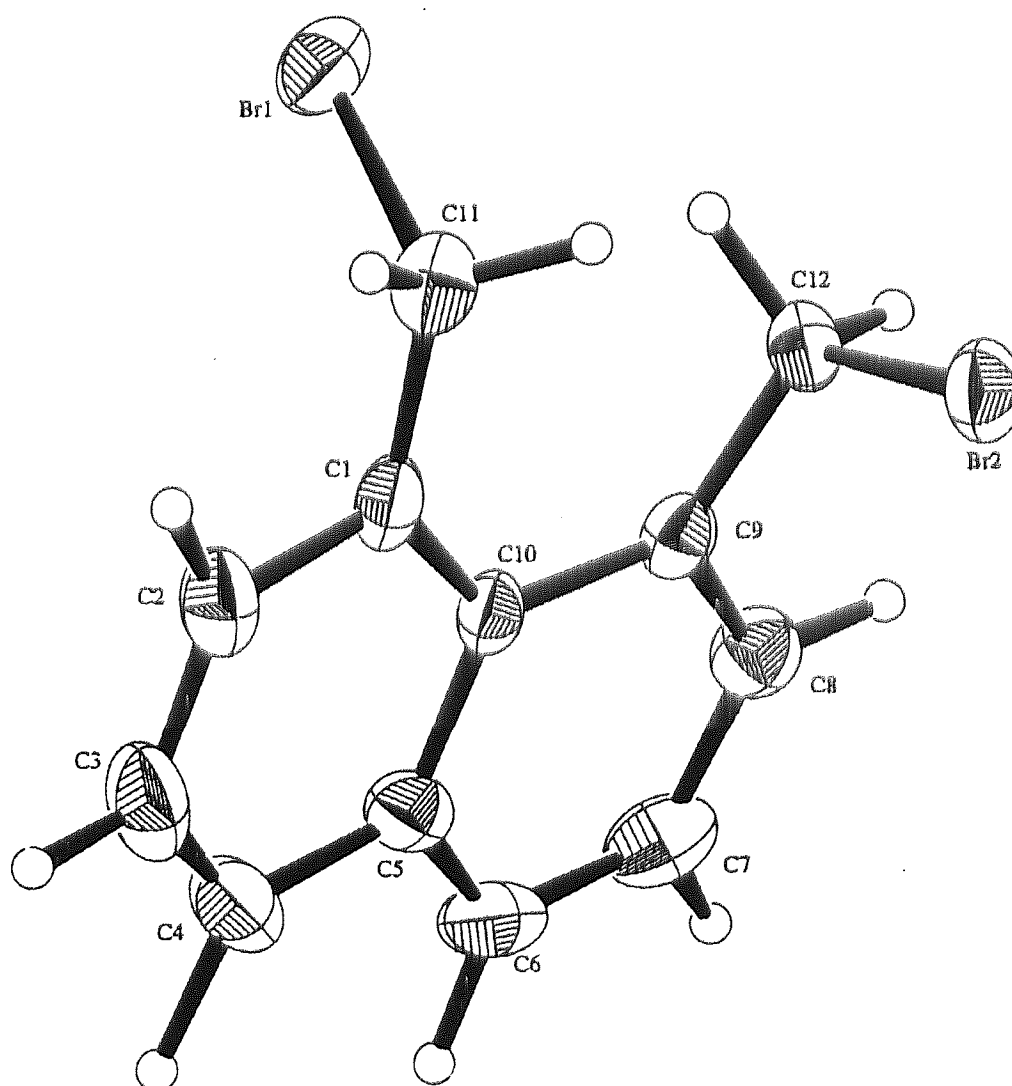


Figure 4.1 The molecular structure of 1,8-bis(bromomethyl)naphthalene, (42).

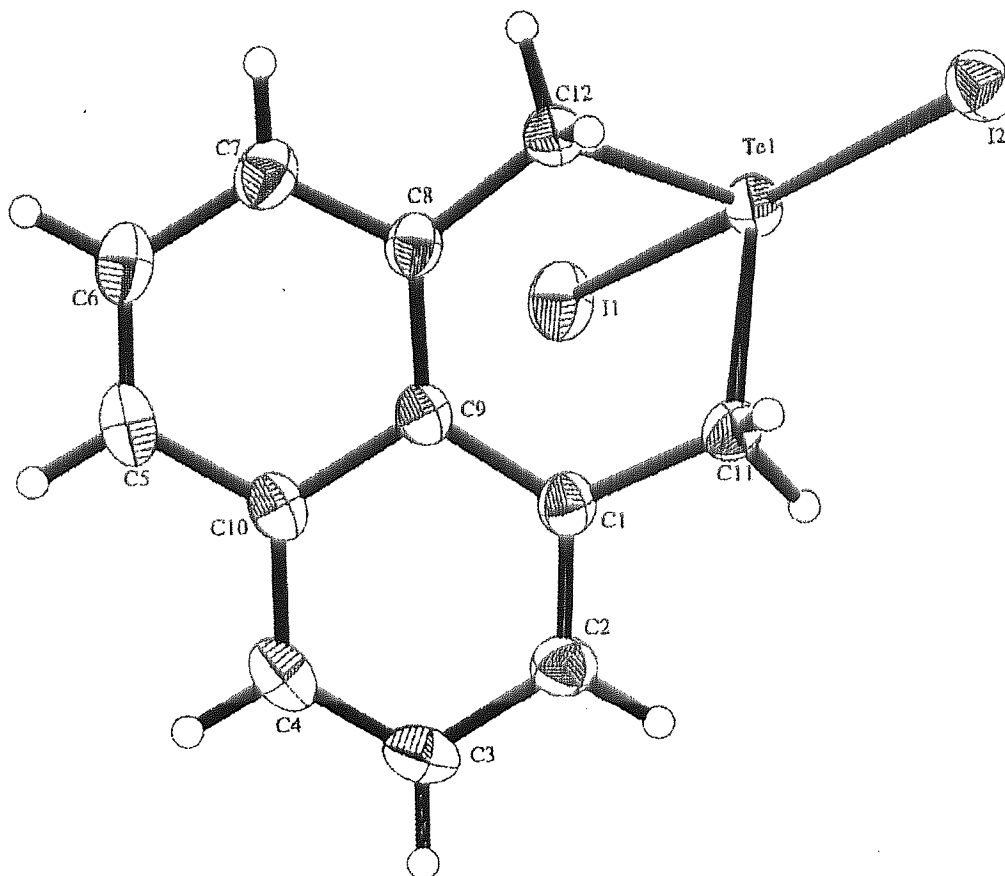


Figure 4.2 The molecular structure of 1,1-diiodo-3,5-naphthotelluracyclohexane, (43).

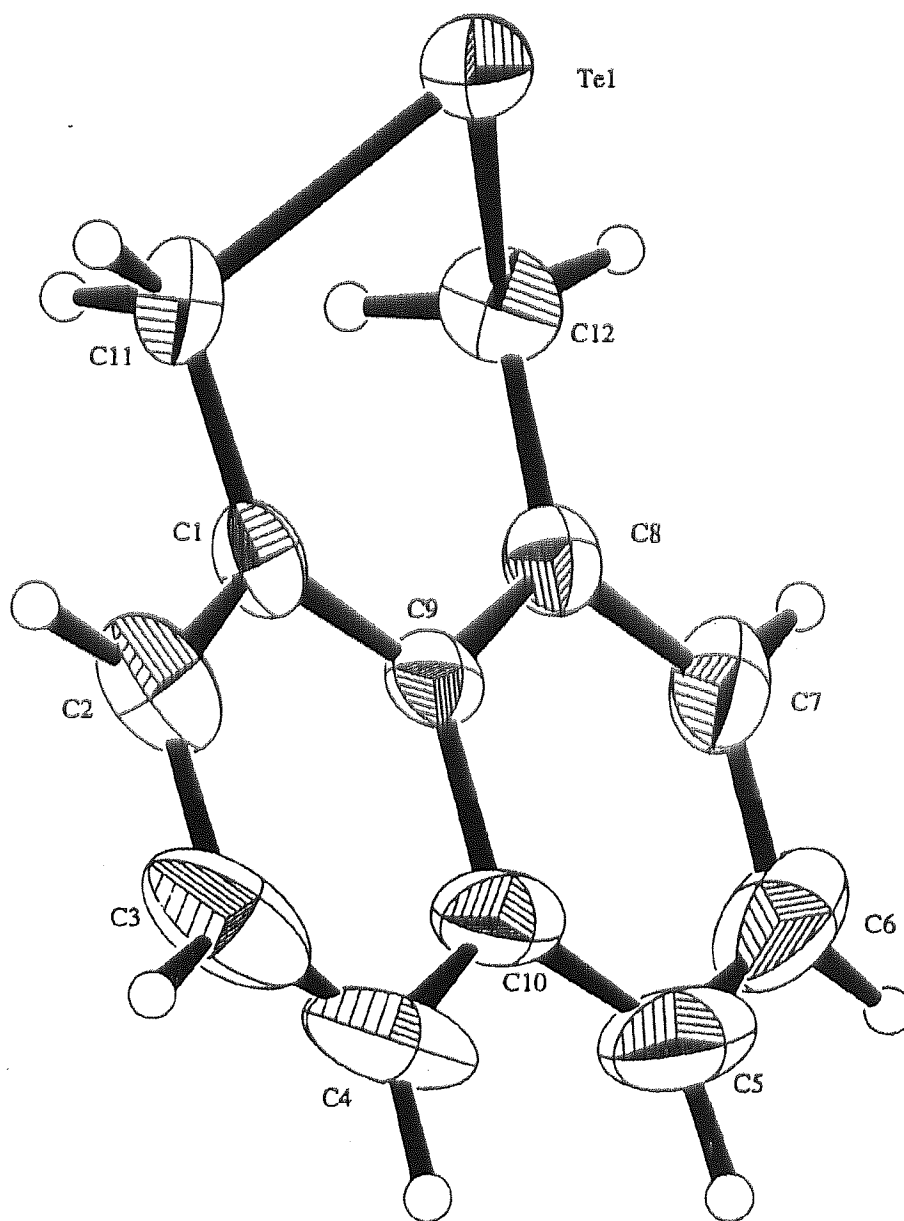


Figure 4.3 The molecular structure of 3,5-naphtho-1-telluracyclohexane, (44).

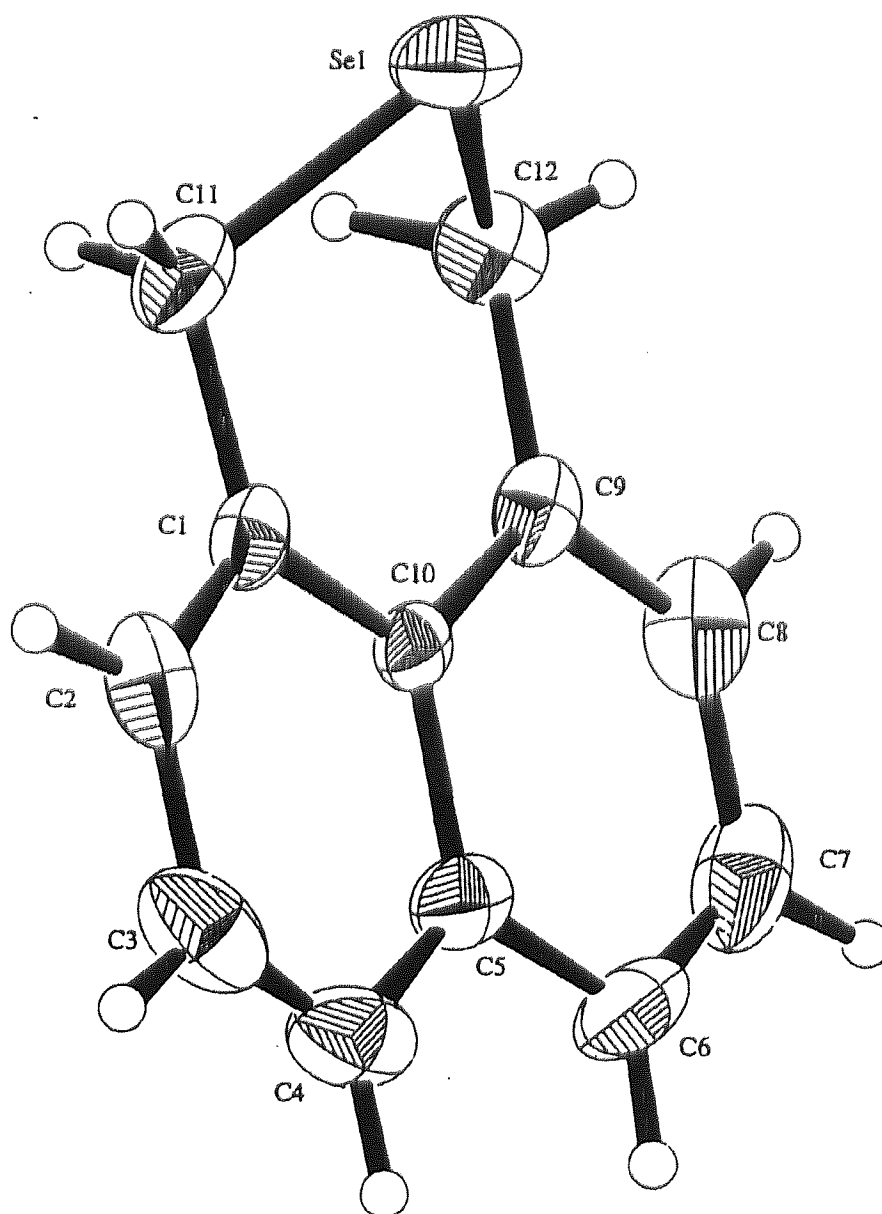


Figure 4.4 The molecular structure of 3,5-naphtho-1-selenacyclohexane, (45).

4.4.2 Crystallographic analysis for 2,2,8,8-tetraiodo-1,3,7,9-tetrahydrobenzo[1,2-*c*;4,5-*c'*]ditellurophene, (46).

$\text{C}_{10}\text{H}_{10}\text{I}_4\text{Te}_2.2\text{C}_3\text{H}_7\text{NO}$, $M = 1039.2$, monoclinic, space group $P2_1/a$, $a = 10.691(4)$, $b = 13.327(6)$, $c = 10.761(4)\text{\AA}$, $\beta = 117.82^\circ$, $V = 1356\text{ \AA}^3$, $Z = 2$, $D_c = 2.545\text{ g cm}^{-3}$, $\mu(\text{Mo-K}\alpha) = 6.72\text{ mm}^{-1}$.

The crystal structure of compound (46) was established by Dr T.A. Hamor and Mr Z. Majeed at the University of Birmingham.

Cell dimensions and intensity data were measured on a Rigaku R-Axis II area detector diffractometer. The angular range for data collection was $2 - 25^\circ$. 15340 reflections were measured, using two different orientations of the crystal, resulting in 2433 unique reflections ($R_{\text{int}} 0.0518$). Although the absorption coefficient is relatively large, specific absorption corrections were not applied, since, on average, each unique reflection intensity is the mean of six intensities measured at different orientations of the crystal, thus minimising absorption effects. The structure was determined by direct methods²⁹ and refined by least-squares³⁰ on F^2 using anisotropic thermal parameters for non-hydrogen atoms. Hydrogen atoms were placed in calculated positions, riding on their respective bonding atoms. Final values of R and $wR2$ are 0.0575 and 0.1137 (max. shift /e.s.d. ratios 0.003), where $w = 1/[\sigma^2(F^2) + (0.061P)^2 + 1.81P]$; $P = (Fo^2 + 2Fc^2)/3$. Residual electron density is in the range -0.87 to $+0.74\text{ e \AA}^{-3}$. An extinction coefficient³⁰ refined to 5.8×10^{-3} . The diagram was drawn with ORTEP³¹; thermal ellipsoids are at the 30% probability level. For 2095 observed reflections [$I > 2\sigma(I)$], $R = 0.0414$.

The dimethylformamide (DMF) solvent molecules in the crystal are disordered over two orientations involving a 180° rotation about the O-N axis.

A view of the tetraiodide together with the oxygen atoms of neighbouring DMF molecules is shown in Figure 4.5. Selected geometric parameters are listed in table 4.10 and atom co-ordinates are listed in table 4.11.

Table 4.10 Atomic coordinates ($\times 10^4$) and equivalent isotropic displacement parameters ($\text{\AA}^2 \times 10^3$) for, $\text{C}_{10}\text{H}_{10}\text{Te}_2\text{I}_4 \cdot 2\text{DMF}$, (**46**). $U(\text{eq})$ is defined as one third of the trace of the orthogonalized U_{ij} tensor.

	x	y	z	$U(\text{eq})$
I(1)	-416(1)	3560(1)	-1017(1)	81(1)
I(2)	-2473(1)	432(1)	-5321(1)	86(1)
Te(1)	-1467(1)	2014(1)	-3225(1)	55(1)
O(1)	-4519(6)	2494(5)	-4403(6)	74(2)
N(1)	-5783(8)	2410(6)	-6765(7)	75(2)
C(1)	-2298(7)	1210(6)	-2048(7)	57(2)
C(2)	-1103(7)	581(5)	-981(7)	48(1)
C(3)	215(7)	573(5)	-980(7)	50(2)
C(4)	436(7)	1181(6)	-2041(8)	60(2)
C(5)	1294(7)	-18(5)	2(7)	50(2)
C(6)	-4828(13)	2838(10)	-5546(15)	48(3)*
C(7)	-6456(37)	1538(24)	-6661(37)	160(14)*
C(8)	-6174(49)	2940(37)	-8093(23)	191(23)*
C(6')	-5416(21)	2083(16)	-5474(22)	83(5)*
C(7')	-6695(38)	1671(29)	-7836(39)	169(17)*
C(8')	-5300(74)	3175(26)	-7214(55)	237(30)*

* Disordered atoms of DMF molecule; site occupancy 0.5

Table 4.11 Selected bond lengths (Å) and angles (°) for C₁₀H₁₀Te₂I₄.2DMF, (46).

Compound (46)				
Te - I(1)	2.943(1)		Te - C(4)	2.139(7)
Te - I(2)	2.904(1)		Te ... O(1)	2.966(6)
Te - C(1)	2.143(7)		Te ... O(1)''	2.973(6)
I(1) - Te - I(2)	177.85(3)		I(2) - Te ... O(1)''	84.7(2)
I(1) - Te - C(1)	88.9(2)		C(1) - Te - C(4)	86.0(3)
I(1) - Te - C(4)	89.1(2)		C(1) - Te ... O(1)	71.6(3)
I(1) - Te ... O(1)	97.1(2)		C(1) - Te ... O(1)''	158.2(3)
I(1) - Te ... O(1)''	96.3(2)		C(4) - Te ... O(1)	156.5(3)
I(2) - Te - C(1)	89.5(2)		C(4) - Te ... O(1)''	73.0(3)
I(2) - Te - C(4)	89.4(2)		O(1) ... Te ... O(1)''	128.3(3)
I(2) - Te ... O(1)	83.7(2)			

4.4.2.1 Discussion of the structure of 2,2,8,8-tetraiodo-1,3,7,9-tetrahydrobenzo[1,2-*c*;4,5-*c'*]ditellurophene, (46).

The structure consists of discrete molecules of the tetraiodide and dimethylformamide (DMF) in the ratio 1:2. Each molecule of the tetraiodide is however linked to four DMF molecules by relatively weak Te...O interactions, and each DMF molecule is similarly linked to two molecules of the tetraiodide, forming an infinite network. The tellurium atom thus forms four strong bonds, Te-C, 2.143(7), and 2.139(7) Å, and Te-I, 2.943(1) and 2.904(1) Å, and two weaker, secondary⁴⁹ bonds to oxygen atoms at 2.966(6) and 2.973(6) Å. These Te to O distances are much longer than normal bonded distances of ca. 2.13 Å^{33,50} but are also much shorter than the accepted van der Waals distance of 3.58 Å⁵¹. The carbon atom skeleton of the tetraiodide is planar to within ±0.005 Å and the two neighbouring oxygen atoms are close to this plane (atomic deviations 0.11 and 0.05 Å on the same side of the plane). The tellurium atom is displaced by 0.13 Å on the opposite side of the plane from the two oxygen atoms. The Te-I bonds are normal to the plane, forming with the bonding carbon atoms and the two DMF oxygen atoms a very distorted octahedral coordination about tellurium. However, if we consider the tellurium lone pair of electrons to be sterically active and occupying the coordination site in the plane of the organic residue bisecting the large (128.3°) O...Te...O angle the geometry can be described as *pseudo*-7- coordinate pentagonal bipyramidal. Previously we have described⁵² a somewhat similar tellurium bonding situation in the crystal structure of 1,3-dihydro-2,2-diiodo-2- tellurolo[3,4-*b*]-quinoxaline-2,3-bis(iodomethyl)-quinoxaline, involving secondary bonding to two iodine atoms, in terms of octahedral coordination; but also in this structure, by invoking a stereochemically active lone pair, a pentagonal bipyramidal description of the bonding about tellurium appears to be valid. Nevertheless, a survey⁵³ of R₂TeI₂

structures shows that in all other cases, where two secondary bonds are formed, the bonding geometry does not conform to a *pseudo*-pentagonal bipyramidal model, and is best described as octahedral, implying a stereochemically inactive lone pair of electrons.

Tellurium to sp^3 -hybridized carbon bond lengths (table 4.11) are in good agreement with normally accepted values, e.g. 2.158 Å given in the tabulations of Allen *et al*³³, or 2.136 - 2.145 Å in two crystalline modifications of 1,1-diiodo-3,4-benzo-1 tellura-cyclopentane^{54,55}. The Te-I lengths compare with previously determined values in the range 2.886 - 2.928 Å^{52,53,54}, and 2.926 Å given by Allen *et al*³³.

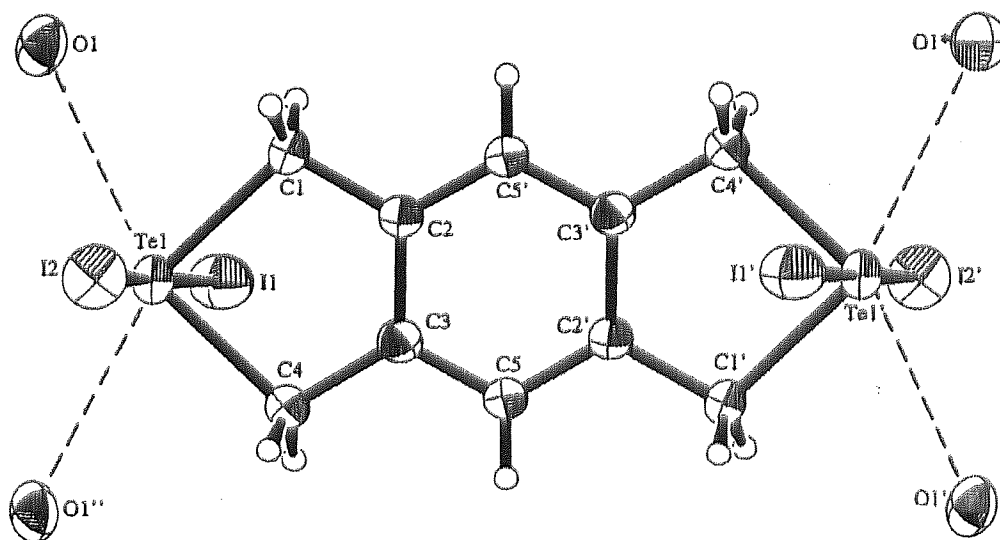


Figure 4.5 View of the tetraiodide, together with four weakly-bonded oxygen atoms of neighbouring DMF molecules. Primed atoms are related to the corresponding unprimed atoms by the centre of symmetry at (0,0,0). Atoms O1'' and O1* are related to O1 by the symmetry operations $\frac{1}{2}+x, \frac{1}{2}-y, z$ and $-\frac{1}{2}-x, -\frac{1}{2}+y, -z$, respectively.

4.5 Conclusion

It is unfortunate that 1,3-dihydrobenzo[c]selenophene, 1,3,7,9-tetrahydrobenzo[1,2-c;4,5-c']ditellurophene, dibenzoselenophene, phenoxselenine, 3,5-naphtho-1-telluracyclohexane and 3,5-naphtho-1-selenacyclohexane do not react with triiron dodecacarbonyl. One can notice that five membered heterocyclic compounds react with triiron dodecacarbonyl, but six membered heterocyclic compounds do not. This may be due to ring strain. Another suggestion is that the selenium heterocyclic compound did not react with iron carbonyl due to the higher carbon – selenium bond strength than the tellurium – carbon strength.

On examination of the X-ray crystal structures of the five and six membered heterocyclic compounds (see section 3.4.2 and 4.4.1) one observed that the tellurium molecular structures are more strained than the selenium ones.

The structure of 2,2,8,8-tetraiodo-1,3,7,9-tetrahydrobenzo[1,2-c;4,5-c']ditellurophene consists of discrete molecules of the tetraiodide and dimethylformamide (DMF) in the ratio 1:2. If we consider the tellurium lone pair of electrons to be sterically active and occupying the co-ordination site in the plane of the organic residue bisecting the large (128.3°) O...Te...O angle, the geometry can be described as *pseudo-7-* co-ordinate pentagonal bipyramidal.

CHAPTER FIVE

INTRAMOLECULAR STABILISATION OF

ORGANOSELENIUM(II) AND –TELLURIUM(II) DERIVATIVES

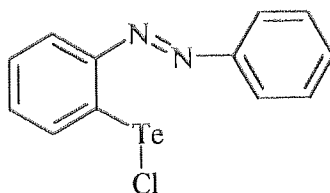
(REX; E = Se, Te; X = ELECTRONEGATIVE GROUP) BY *INTRA-*

MOLECULAR CO-ORDINATION

5.1 Introduction

In general, organoselenium chemistry is much more advanced in many areas than organotellurium chemistry. However the chemistry of intramolecular stabilised organotellurium compounds, where the molecules are stabilised by *intra*-molecular co-ordinate bonds^{16,17,18}, is much more advanced than the corresponding selenium chemistry. Organo-tellurium(II) derivatives have a general formula of RTeX , where in the context of this thesis X = a electronegative group, e.g. halogen.

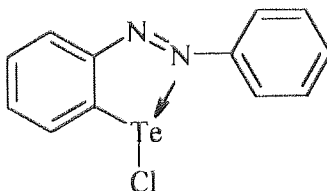
Intra-molecular co-ordination occurs when it is sterically feasible for the acidic and basic centres to interact within the molecule. The co-ordination may only occur when the organic group attached to the tellurium atom has an attached donor group in it, for example phenylazophenyl(C,N')tellurium(II) chloride¹⁹.



Te = Centre of Lewis acidity

N = Centre of Lewis basicity

The molecule shown above may undergo *intra*-molecular co-ordination because the aryl- group has a basic functional group in the *ortho*- position to the tellurium. Therefore, co-ordination will occur between the tellurium and the nitrogen atom, as shown below.



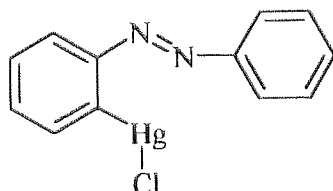
Selenium and tellurium are both in group 16 and one would expect that the elements will have many chemical similarities. It would therefore be reasonable to expect that substituted azobenzenes can be synthesized with selenium, as well as with tellurium and that their chemistries will be similar.

If the *intra*-molecular compounds were considered to be *pseudo*-heterocyclic compounds, reaction of these azobenzene compounds with $[\text{Fe}_3(\text{CO})_{12}]$ might produce interesting and novel compounds.

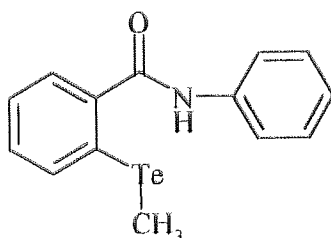
5.2 Experimental

5.2.1 Formation of intramolecular stabilised organotellurium compounds

5.2.1.1 Preparation of intramolecular stabilised organotellurium compounds



(2-Phenylazophenyl-C,N')mercury(II) chloride⁵⁶



2-(Methyltelluro)benzanilide⁵⁷

The above *pseudo*-heterocycles were prepared using literature methods^{56,57}. The analyses of the above materials were in good agreement with the literature values^{56,57}.

5.2.1.2 Attempted synthesis of (2-phenylazophenyl-C,N')tellurium(IV) tribromide

(2-Phenylazophenyl-C,N')mercury(II) chloride (2.4g 5.74 mmol) and tellurium tetrabromide (2.56g 5.74 mmol) were refluxed in sodium dried 1,4-dioxane (20 cm³) for 6 hours under dry nitrogen. On cooling the 2:1 addition compound of dioxane and mercury(II) chloride separated as white plates which were removed by filtration. The filtrate was concentrated on the rotary evaporator, and nitromethane (20 cm³) was added. Evaporation was carried out to dryness and the residue was recrystallised from nitromethane to give reddish brown crystals. Yield 93%, m.p. 171 - 174°C. The reaction product was chromatographed on silica gel and eluted with petroleum ether

and ethylacetate to give two fractions, the analysis of which gave no clear indication as to identity (see CHN, mass spectra and ^{13}C NMR data in tables 5.1, 5.2 and 5.3 respectively). Component 1 was a red solid, m.p. 168-171°C; component 2 was a deep orange solid, m.p. 194-197°C.

5.2.1.3 Synthesis of (2-phenylazophenyl-C,N')tellurium(II) bromide

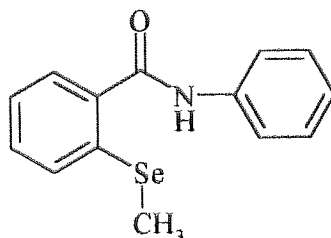
(2-Phenylazophenyl-C,N')tellurium(IV) tribromide (the above material, prior to chromatography) (1.76g, 3.21 mmol) was dissolved in methanol (35 cm³) and heated under reflux. A solution of hydrazine hydrate (0.16g, 3.21 mmol) in methanol (25 cm³) was added slowly to the refluxing solution. The solution was filtered and cooled to afford red crystals. Yield 40%, m.p. 116-118°C

5.2.1.4 Synthesis of (2-phenylazophenyl-C,N')tellurium(II) iodide

Diiodine (0.13g, 5.14 mmol) in chloroform (15cm³) was added dropwise to a solution of (2-phenylazophenyl-C,N')tellurium(II) bromide (0.2g, 5.14 mmol) in chloroform (15cm³). The solution changed colour from red to a very dark red/black and was stirred for 3 h. Then the solvent, together with excess diiodine, was removed on the rotary evaporator. The product remaining was red in colour and was recrystallised from nitrobenzene. M.p. 149-151 °C.

5.2.2 Formation of intramolecular stabilized organoselenium compounds

5.2.2.1 Preparation of intramolecular stabilized organoselenium compounds



2-(Methylseleno)benzanilide⁵⁷

The above *pseudo*-heterocycle was prepared using literature methods⁵⁷. The analyses of the above material were in good agreement with the literature values⁵⁷.

5.2.2.2 Attempted synthesis of (2-phenylazophenyl-*C,N'*)selenium(IV) trichloride

Azobenzene (10.0 g, 55 mmol), selenium(IV) tetrachloride (11.036 g, 5 mmol), anhydrous aluminium chloride (6.6 g, 5 mmol) and 1,2-dichlorobenzene (50 cm³), were heated under argon to approximately 120°C for 1 ½ hours. The reaction mixture was then cooled to 80 °C and methanol (56 cm³) was added until the vigorous reaction ceased. The reaction mixture was then cooled. The resulting precipitate was washed with approximately 100 cm³ of methanol and all filtrates were retained. The precipitate was analysed by ¹H and ¹³C NMR spectroscopy; no signal was obtained therefore the precipitate was assumed to be inorganic and discarded. The filtrates (red/orange colour) were combined and evaporated on the rotary evaporator, resulting in an orange/brown powder, which was recrystallised from methanol.

Yield 88%, m.p. 202-203°C

5.2.2.3 Synthesis of (2-phenylazophenyl-C,N')selenium(II) chloride

(2-Phenylazophenyl-C,N')selenium(IV) trichloride (the above orange/brown powder)(0.5 g, 1.36 mmol) was dissolved in methanol (40 cm³) and heated under reflux. A solution of hydrazine hydrate (0.068 g, 1.36 mmol) in methanol (10 cm³) was added slowly to the refluxing solution and was refluxed for 0.5 hour. The solution was filtered and cooled to afford a brown solid.

Yield 32 %, m.p. 131 - 134°C

5.2.2.4 Synthesis of (2-phenylazophenyl-C,N')selenium(II) chloride

Azobenzene (10g, 55 mmol), selenium(IV) tetrachloride (11.03 g, 5 mmol), anhydrous aluminium chloride (6.6 g, 5 mmol) and 1,2-dichlorobenzene (50 cm³) were heated to 160 °C under argon for 3 hours. The reaction mixture was then cooled to 80 °C and methanol (60 cm³) was added until the vigorous reaction ceased. The mixture was brown/yellow. The reaction mixture was cooled in a freezer for 24 hours, and a brown precipitate formed. The mixture was filtered and the brown precipitate was washed with cold methanol. The brown precipitate was then recrystallised from methanol.

Yield 10%, m.p. 130 - 131°C

5.2.2.5 Synthesis of (2-phenylazophenyl-C,N')selenium(II) chloride : (2-phenylazophenyl-C,N')selenium(II) iodide (1:1)

(2-Phenylazophenyl-C,N')selenium(II) chloride (0.2g, 67.5 mmol) was added to a solution of diiodine (0.085g, 33.7mmol) in AR-grade acetone (40 cm³). A further 100 cm³ of AR-grade acetone was added to the mixture. The mixture was heated and

stirred until the solution turned from red to dark red. The dark red solution was filtered and the solvent removed giving a red solid. The red solid precipitate was then recrystallised from chloroform, giving red crystals.

Yield 15 %, m.p. 86°C

5.2.2.6 Synthesis of (2-phenylazophenyl-C,N')selenium(II) iodide

(2-Phenylazophenyl-C,N')selenium(II) chloride (0.256g, 1.67 mmol) was added to a solution of diiodine (0.212g 1.67 mmol) in AR-grade acetone (200 cm³), which resulted in a red solution. The mixture was then heated for 10 mins. The solvent was removed giving a deep purple crystalline solid. The deep purple solid was recrystallised from acetone and methanol, giving purple/red crystals.

Yield 33 %, m.p. 80°C

5.3 Results and discussion

5.3.1 (2-Phenylazophenyl-*C,N'*)tellurium(IV) tribromide, (*RTeBr*₃), (2-phenylazophenyl-*C,N'*)tellurium(II) bromide, (*RTeBr*) and iodide, (*RTeI*).

The product obtained from the reaction of *RHgCl* with *TeBr*₄ was a reddish brown solid, (m.p. 172 – 174°C). The reduction of ***RTeBr*₃** (the reddish brown solid above) with hydrazine hydrate afforded a red crystalline solid, ***RTeBr*** (m.p. 116 – 118°C). The reaction of ***RTeBr*** with *I*₂ afforded a red crystalline solid, ***RTeI*** (m.p. 149 – 151°C). The yields of the products, ***RTeBr*** and ***RTeI*** were 40% and 83%, respectively. Analytical data; EI and FAB mass spectrum observed peaks; ¹³C and ¹²⁵Te NMR data for the compounds are recorded in tables 5.1, 5.2 and 5.3 respectively.

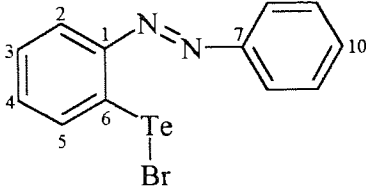
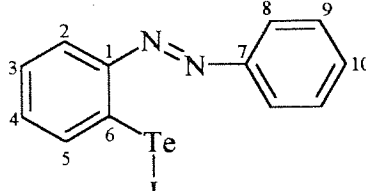
Table 5.1 Analytical data for ***RTeBr*₃**, ***RTeBr*** and ***RTeI***.

Compound	Found (%)			Calculated (%)		
	C	H	N	C	H	N
Crude <i>RTeBr</i>₃	15.3	1.12	2.99	26.3	1.65	5.10
Chromatographed <i>RTeBr</i>₃						
Component 1	22.4	1.84	3.68	26.3	1.65	5.10
Component 2	21.7	1.99	3.49			
<i>RTeBr</i>	36.9	2.41	7.35	37.1	2.33	7.20
<i>RTeI</i>	32.8	2.14	6.51	33.1	2.08	6.43

Table 5.2 Mass spectral data for **RTeBr₃** and **RTeBr** (¹H, ¹²C and ¹³⁰Te).

Fragment	Compound					
	Crude RTeBr ₃		Chromatographed RTeBr ₃ component		RTeBr	
	(EI) m/z	(FAB) m/z	1 (EI) m/z	2 (EI) m/z	(FAB) m/z	(EI) m/z
C ₆ H ₆ ⁺	77		77	77		77
(C ₆ H ₅) ₂ ⁺	152	152	152	152	152	152
(C ₆ H ₆) ₂ N ⁺		165			165	
C ₆ H ₆ Te ⁺	206		206	206		206
C ₁₈ H ₁₃ N ₂ ⁺						257
(C ₆ H ₆) ₂ Te ⁺	282		282	282		282
C ₁₂ H ₉ N ₂ Te ⁺	311	311	311	311	311	311
C ₁₂ H ₉ N ₂ TeBr ⁺	390	391	390	390	391	390
C ₁₂ H ₉ N ₂ TeBrCl ⁺	425			425		
C ₁₂ H ₉ N ₂ TeBr ₂ ⁺	469					
C ₁₂ H ₉ N ₂ TeBr ₃ ⁺		549	550		549	

Table 5.3 ^{13}C and ^{125}Te NMR data collected for **RTeBr** and **RTeI**.

Compound		^{13}C (CDCl_3) δ , ppm	
	C1 – C10	155.3	---
		122.4	148.4
		128.5	128.5
		131.5	130.2
		134.7	132.9
	C1 – C10	148.2	---
		122.5	---
		131.7	128.7
		132.0	130.3
		135.0	133.0

Compound	^{125}Te δ , ppm : vs Me_2Te
(RTeBr)	983.3
(RTeI)	989.9

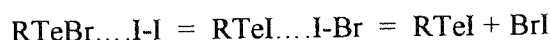
Attempts were made to synthesize **RTeBr₃** by the reaction of 2-phenylazophenyl(C,N')mercury(II) chloride with tellurium tetrabromide, but this gave an impure product. The analytical data for the product (C, 15.3; H, 1.12; N, 2.99) did not agree with the calculated values (C, 26.3; H, 1.65; N, 5.10). The mixture was chromatographed (see experimental section 5.2.1.2) giving two components. The analytical data for the components (see **Chromatographed RTeBr₃** in table 5.1) showed that the separation was not complete. The ^1H , ^{13}C NMR and mass spectra (see **Crude RTeBr₃** and **Chromatographed RTeBr₃** in table 5.2) of the crude product and the two components showed that these were mixtures. The mass spectra (see table 5.2) of the crude product, gave a parent ion of **RTeBr₃** ($\text{C}_{12}\text{H}_9\text{N}_2\text{TeBr}_3^+$, $m/z = 549$),

providing evidence of the formation of **RTeBr₃**. However, the mass spectra also contained fragments having the correct isotopic patterns for mixed tellurium - halide species e.g. $\text{C}_{12}\text{H}_9\text{N}_2\text{TeBrCl}^+$, $m/z = 425$. 2-(2-Pyridyl)phenyltellurium(IV) trichloride¹⁹ was formed as a mixture with mercury derivatives, but on comparing the crude **RTeBr₃** and the separated components no clear evidence has been found to show any mercury derivatives contaminating the mixtures.

Crude **RTeBr₃** was reduced, using hydrazine hydrate and gave pure **RTeBr**. **RTeI** was synthesised by the reaction of **RTeBr** with diiodine. The analytical data (see table 5.1) for **RTeBr** and **RTeI** were in agreement with the calculated values. ¹³C NMR data (see table 5.3) for **RTeBr** and **RTeI** were consistent with the expected carbon environments for both compounds. Both **RTeBr** ($\delta = 983.25$ ppm. vs Me_2Te) and **RTeI** ($\delta = 989.9$ ppm. vs Me_2Te) gave ¹²⁵Te NMR spectra consistent with those expected for Te(II) compounds⁵⁸. Mass spectra (see table 5.2) for **RTeBr** gave a parent ion at $m/z = 390$, which gave further support for the purity of the compound. In addition, a significant feature at $m/z = 257$ corresponded to $\text{C}_{18}\text{H}_{13}\text{N}_2$, which is a fragment derived from R_2Te^+ . The presence of this peak suggests that considerable thermolysis of the material had occurred prior to its passage to the vapour phase, which has been observed previously in azobenzene series⁴⁶. The resulting data for **RTeBr** and **RTeI** are entirely consistent with the structure determined by X-ray crystallography (see section 5.4.1).

It was interesting to note that crystals obtained from the synthesis of **RTeI** diffracted well. Yet when the **RTeI** was synthesized by an alternative method involving the metathesis of **RTeCl** with sodium iodide, the crystals failed to diffract⁴⁶. It is interesting that oxidative addition of diiodine to the monobromide failed to afford a

tellurium(IV) product. Immediate reductive elimination of BrI was possible (see scheme 5.1), but it was believed that the monoiodide arose *via* a labile charge-transfer intermediate, a proposal which can be supported by previous studies of the reactions of diiodine with tellurenyl compounds stabilised by *intra*-molecular co-ordination⁵⁹.



Scheme 5.1 Suggested charge transfer reaction pathway for the formation of **RTeI**.

5.3.2 (2-Phenylazophenyl-*C,N'*)selenium(IV) trichloride, (*RSeCl*₃), (2-phenylazophenyl-*C,N'*)selenium(II) chloride, (*RSeCl*), chloride : iodide (1:1), (*RSeCl/I*) and iodide, (*RSeI*).

The reaction of azobenzene with SeCl₄ afforded a brown crystalline solid, **RSeCl** (m.p. 130 – 131°C). The reaction of **RSeCl** with diiodine (molar ratio 2:1) afforded a red crystalline solid, **RSeCl/I** (m.p. 86°C). The reaction of **RSeCl** with di-iodine (molar ratio 1:1) resulted in a purple crystalline solid, **RSeI** (m.p. 80°C). The yield of the products, **RSeCl**, **RSeCl/I** and **RSeI** were 10%, 15% and 33% respectively. Analytical data; EI and FAB mass spectrum observed peaks; ¹³C, and ⁷⁷Se NMR data for the compounds are recorded in tables 5.4, 5.5 and 5.5 respectively. ⁷⁷Se NMR spectra of **RSeCl**, **RSeCl/I** and **RSeI** are shown in figures 5.1, 5.2 and 5.3, respectively.

Table 5.4 Analytical data for **RSeCl**, **RSeCl/I** and **RSeI**.

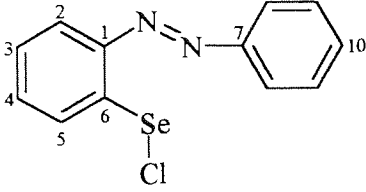
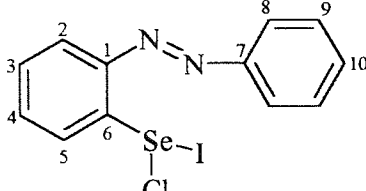
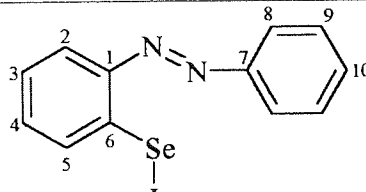
Compound	Found (%)			Calculated (%)		
	C	H	N	C	H	N
RSeCl	48.5	3.23	9.67	48.7	3.07	9.47
RSeCl/I	41.5	2.54	8.09	42.2 *	2.64 *	8.21 *
RSeI	36.9	2.29	7.19	37.24	2.34	7.23

* = CHN calculated on the basis of a (1:1) mixture of **RSeCl** and **RSeI**,
 $C_{24}H_{18}N_4Se_2ICl$.

Table 5.5 Mass spectral data for **RSeCl**, **RSeCl/I** and **RSeI** (1H , ^{12}C and ^{80}Se).

Fragment	Compound		
	RSeCl (EI) m/z	RSeCl/I (EI) m/z	RSeI (EI) m/z
Cl^+	35	35	
$C_6H_6^+$	77	77	77
I^+		127	127
$(C_6H_5)_2^+$	152	152	152
$(C_6H_5)Se^+$	156	156	156
$(C_6H_5)_2Se^+$	232	232	
$C_{18}H_{15}N_2^+$	259	259	259
$C_{12}H_9N_2Se^+$	261	261	261

Table 5.6 ^{13}C and ^{77}Se NMR data collected for **RSeCl**, **RSeCl/I** and **RSeI**.

Compound		^{13}C (CDCl_3) δ , ppm	
	C1 – C10	151.4	144.5
		123.3	146.7
		130.4	128.6
		129.5	130.4
		132.6	132.3
	C1 – C10	151.4	143.8
		122.5	144.3
		131.7	128.6
		129.8	131.7
		132.5	130.2
	C1 – C10	151.5	141.1
		122.7	144.2
		130.2	128.6
		130.1	130.2
		134.2	132.2

Compound	^{77}Se δ , ppm : vs Me_2Se
RSeCl	650.6
RSeCl/I	649.2
RSeI	621.4

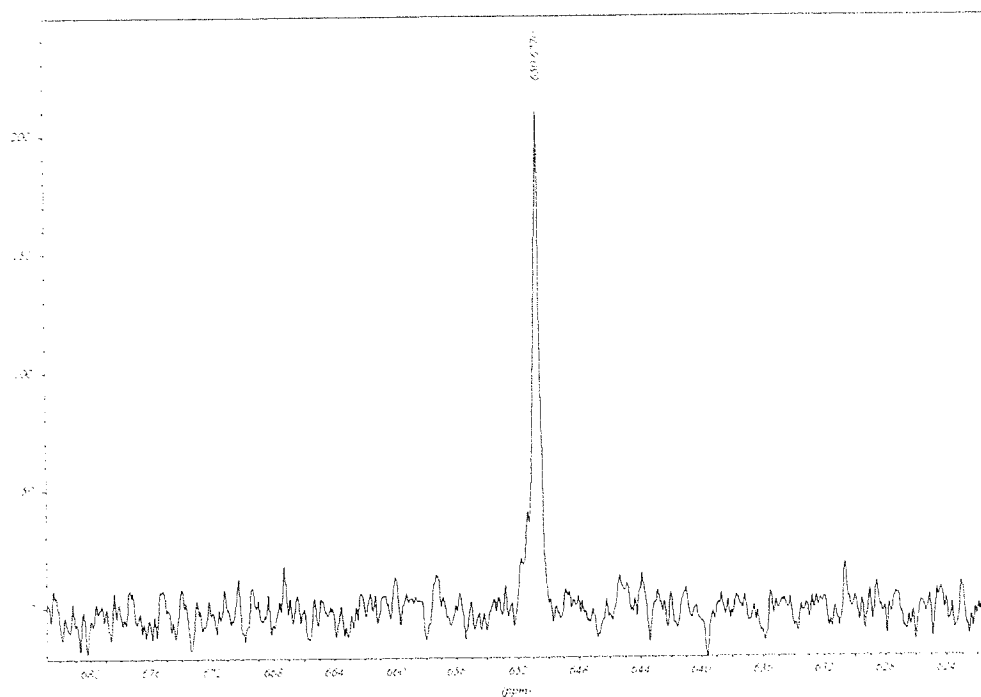


Figure 5.1 ^{77}Se NMR spectrum of **RSeCl**.

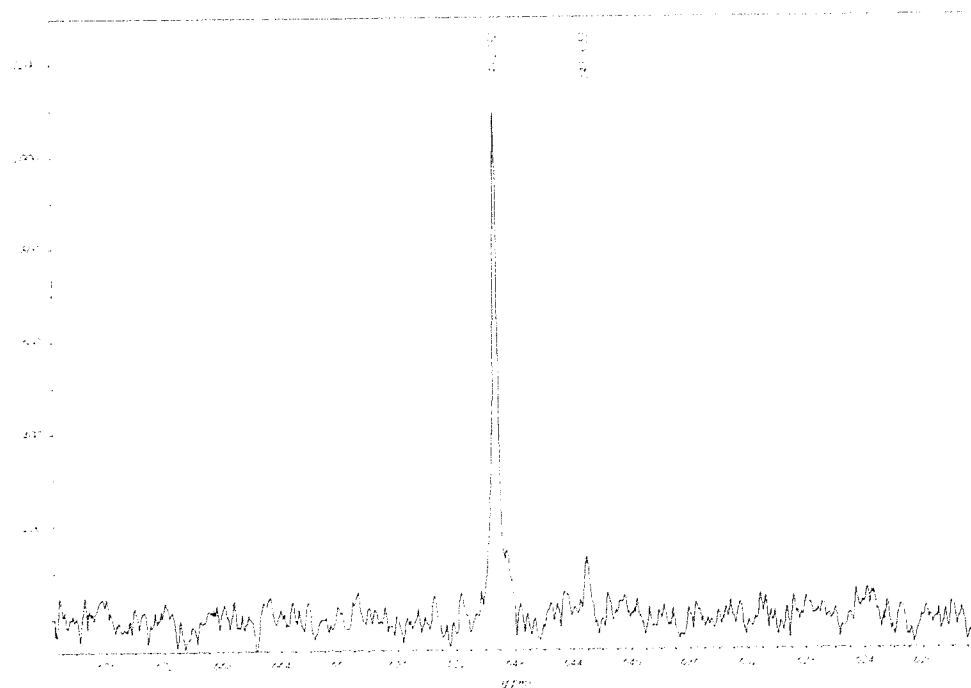


Figure 5.2 ^{77}Se NMR spectrum of **RSeCl/L**.

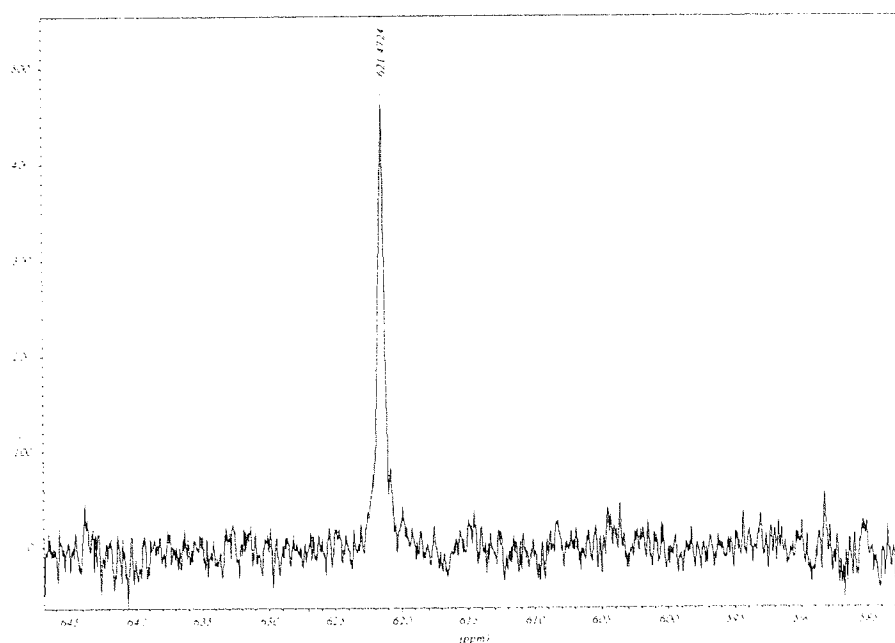


Figure 5.3 ^{77}Se NMR spectrum of **RSeI**.

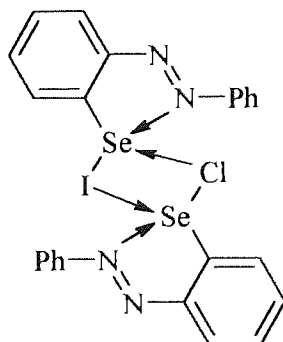
Attempts were made to synthesise **RSeCl₃**, by direct reaction of azobenzene with selenium tetrachloride, but this gave an impure product. The CHN analysis, ^1H and ^{13}C NMR spectra confirmed the product to be a mixture.

RSeCl was prepared by two separate methods. The first method was the reduction of impure **RSeCl₃** with hydrazine hydrate. The second method employed the same reagents and reaction conditions used to synthesise the impure **RSeCl₃**, but extending the reaction time caused the reduction of **RSeCl₃** to **RSeCl**. The second method yielded a brown product that recrystallized readily from methanol producing pure orange/brown crystals.

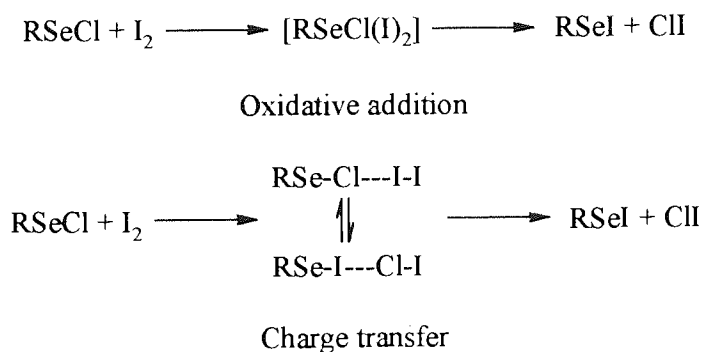
The analytical data obtained for both products were found to be in agreement with the calculated values for **RSeCl** (see table 5.4). The ^{13}C NMR spectra (see table 5.6) for both products were identical and consistent with the expected carbon environments for **RSeCl**. Both products gave a ^{77}Se NMR spectrum ($\delta = 650$ vs Me_2Se) which was consistent with those of selenium(II) compounds⁶⁰.

Synthesis of **RSeCl/I** by metathesis involving diiodine and **RSeCl** worked well. The analytical data obtained for **RSeCl/I** were found to be in good agreement with the calculated values for **RSeCl/I** (see table 5.4). The ^{13}C NMR spectrum for **RSeCl/I** is consistent with the expected carbon environments for **RSeCl/I**. Interestingly the ^{77}Se NMR spectrum of **RSeCl/I** only afforded a single resonance, ($\delta = 649.2$ vs Me_2Se , see figure 5.2) whose chemical shift is consistent with those of selenium(II) compounds⁵⁹. However the ^{77}Se NMR spectrum of **RSeCl/I** is not consistent with the static X-ray structure observed (see section 5.4.2). The X-ray structure obtained displays a random distribution of **RSeCl** and **RSeI** molecules in a ratio of 1:1. If this were the case then one would expect two resonances within the ^{77}Se NMR spectrum for **RSeCl/I**, due to two different selenium environments, one from the **RSeCl** and the other from **RSeI**. On comparison of the ^{77}Se NMR spectra of **RSeCl** ($\delta = 650.6$ vs Me_2Se) and **RSeI** ($\delta = 621.4$ vs Me_2Se) with that of **RSeCl/I** one notices that the resonance observed for **RSeCl/I** is very similar to that for **RSeCl**.

One suggestion for the single resonance is exchange in solution between the molecules of **RSeCl/I**. However if this was the case one would expect an average resonance of about $\delta = 635$. Another suggested reason for the single resonance in the ^{77}Se NMR spectrum is that there is intermolecular co-ordination between the **RSeCl** and **RSeI** molecules in solution (see below).



However if this is the case one would expect a single resonance in the ^{77}Se NMR spectrum. This is due to both selenium atoms being equivalent and it may be fortuitous that the resonance observed has a chemical shift similar to that of **RSeCl**. There are two possible mechanisms for this reaction. The first mechanism is the oxidative addition of I_2 to Se and the second is a charge transfer route (see scheme 5.2).



Scheme 5.2 Reaction pathway suggested for the formation of **RSeCl/I** and **RSeI**.

There is evidence in the literature that selenium iodides are often charge transfer complexes⁶¹. Also with the tellurium iodides charge transfer complexes⁴⁶ can be formed. Therefore the evidence supports the charge transfer route.

The mass spectra (see table 5.5) of both products **RSeCl** and **RSeCl/I** were identical and no parent ions were seen. Other major peaks in both spectra were identical. In addition, a significant feature at $m/e = 259$ corresponded to $\text{C}_{18}\text{H}_{15}\text{N}_2$, which is a fragment derived from R_2Se^+ . The presence of this peak suggests that considerable thermolysis of the materials had occurred prior to passage to the vapour phase. The only difference in the spectra was a peak for Cl^+ in **RSeCl** and I^+ in **RSeCl/I**.

The preparation of **RSeI** was successful by the metathesis of **RSeCl** and diiodide (see experimental section 5.2.2.5). The analytical data for **RSeI** were found to be in agreement with the calculated values (see table 5.4). The ^{13}C NMR spectrum for **RSeI**

is consistent with the expected carbon environments for **RSeI** and the ^{77}Se NMR spectrum ($\delta = 621.4$ vs Me_2Se) is consistent with those of selenium(II) compounds⁵⁹. One would also suggest that the reaction pathway for this reaction is similar to that for the formation of **RTeI**, which is a charge transfer pathway (see scheme 5.2).

5.4 X-ray crystallography

5.4.1 X-ray crystallography for intramolecular stabilized organotellurium compounds.

5.4.1.1 Crystallographic analysis for (2-phenylazophenyl-C,N')tellurium(II) bromide and iodide.

Suitable crystals of **RTeBr** were obtained by recrystallisation from hot methanol and of **RTeI** by recrystallisation from hot chloroform.

Dr T.A. Hamor established the crystal structures of compounds **RTeBr** and **RTeI** at the University of Birmingham.

Data for both structures were measured on a Rigaku R-axis II area detector diffractometer with MoK α radiation at 293(2) K. The structures were determined by direct methods²⁹ and refined³⁰ by full-matrix least squares on F² using anisotropic displacement parameters for the non-hydrogen atoms. Hydrogen atoms were placed in calculated positions. Crystal and refinement data are presented in table 5.7. Atomic coordinates are given in tables 5.8 and 5.9 for **RTeBr** and **RTeI** respectively. Selected geometrical parameters are listed in table 5.10. Hydrogen coordinates, displacement parameters and full lists of bond lengths and angles have been deposited with the Cambridge Crystallographic Data Centre. Fig. 5.4 gives a CHARON⁶² plot of one molecule of **RTeBr** showing the atom numbering. Fig. 5.4 also represents the **RTeI** molecule, the only significant difference being an approximately 0.18 Å longer Te-X bond in **RTeI**.

Table 5.7 Crystal and experimental data for **RTeBr** and **RTel**.

Compound	RTeBr	RTel
Formula	$C_{12}H_9BrN_2Te$	$C_{12}H_9IN_2Te$
M_r	388.7	435.7
Cryst. sys.	triclinic	triclinic
Space grp.	P-1	P-1
a(Å)	7.897(2)	8.011(2)
b(Å)	11.022(2)	11.228(2)
c(Å)	7.537(2)	7.677(2)
α (deg)	105.08(2)	105.81(3)
β (deg)	91.94(1)	91.60(2)
γ (deg)	74.46(2)	73.85(3)
$V(\text{\AA}^3)$	609.8(2)	637.4(2)
Z	2	2
$D_c(\text{g cm}^{-3})$	2.117	2.270
$\mu(\text{MoK}\alpha)(\text{mm}^{-1})$	5.688	4.730
Cryst.size(mm)	0.3 x 0.3 x 0.25	0.2 x 0.2 x 0.15
Data range (θ)(deg)	2.8 - 25.2	2.8 - 25.2
Rfls.measd. [$I > \sigma(I)$]	3649	7145
Unique reflections	1936	2034
R(int)	0.038	0.033
Variables	145	145
Δ/σ (max)	0.001	<0.001
$\Delta\rho$ (max +ve)($\text{e}\text{\AA}^{-3}$)	0.94	1.05
$\Delta\rho$ (max -ve)($\text{e}\text{\AA}^{-3}$)	-1.25	-1.21
R	0.0551	0.0592
wR2a	0.1569	0.1110
w(a.b)b	0.089, 2.69	0.014, 6.12

$$a_w R2 = [\sum w(F_o^2 - F_c^2)^2 / \sum w(F_o^2)]^{1/2}$$

$$b_w = 1/[\sigma^2(F_o^2) + (aP)^2 + bP] \text{ where } P = (F_o^2 + 2F_c^2)/3$$

Table 5.8 Atomic coordinates ($\times 10^4$) and equivalent isotropic displacement parameters ($\text{\AA}^2 \times 10^3$) for **RTeBr**. $U(\text{eq})$ is defined as one third of the trace of the orthogonalized U_{ij} tensor.

	x	y	z	$U(\text{eq})$
Te(1)	8281(1)	6335(1)	3261(1)	49(1)
Br(1)	9112(2)	3708(1)	2463(2)	74(1)
N(1)	6567(9)	8755(7)	1941(10)	48(2)
N(2)	7335(9)	8437(8)	3356(10)	48(2)
C(1)	7067(11)	6400(9)	785(11)	45(2)
C(2)	6865(12)	5349(10)	-629(12)	55(2)
C(3)	6022(13)	5578(10)	-2165(14)	61(2)
C(4)	5375(13)	6819(11)	-2372(13)	61(2)
C(5)	5544(12)	7881(11)	-1019(13)	57(2)
C(6)	6407(11)	7682(8)	577(11)	43(2)
C(7)	7585(11)	9475(8)	4828(12)	48(2)
C(8)	7593(13)	10697(9)	4569(13)	57(2)
C(9)	7885(15)	11643(11)	6091(16)	69(3)
C(10)	8184(14)	11395(12)	7769(15)	76(3)
C(11)	8211(15)	10192(10)	8003(14)	65(3)
C(12)	7900(13)	9219(10)	6557(12)	57(2)

Table 5.9 Atomic coordinates ($\times 10^4$) and equivalent isotropic displacement parameters ($\text{\AA}^2 \times 10^3$) for **RTeI**. U(eq) is defined as one third of the trace of the orthogonalized U_{ij} tensor.

	x	y	z	U(eq)
Te(1)	8209(1)	6405(1)	3218(1)	49(1)
I(1)	9121(1)	3643(1)	2471(1)	71(1)
N(1)	6572(10)	8785(8)	1881(11)	51(2)
N(2)	7277(11)	8503(8)	3282(11)	51(2)
C(1)	7055(12)	6450(9)	781(13)	46(2)
C(2)	6861(13)	5402(10)	-608(14)	54(3)
C(3)	6066(15)	5601(11)	-2141(15)	60(3)
C(4)	5441(14)	6845(12)	-2369(15)	60(3)
C(5)	5619(13)	7890(11)	-1046(14)	56(3)
C(6)	6441(12)	7701(10)	545(13)	48(2)
C(7)	7526(13)	9549(9)	4748(14)	49(2)
C(8)	7600(14)	10718(10)	4474(16)	60(3)
C(9)	7864(17)	11662(12)	5940(19)	74(3)
C(10)	8081(15)	11449(11)	7597(17)	69(3)
C(11)	8053(16)	10285(12)	7863(16)	72(3)
C(12)	7782(15)	9343(11)	6441(14)	60(3)

Table 5.10 Selected bond lengths (Å) and angles (°) with e.s.d's in parentheses for
RTeBr and RTel.

	RTeBr	RTel
Te-C(1)	2.078(8)	2.070(10)
Te...N(2)	2.219(8)	2.252(8)
Te-X	2.698(1)	2.877(1)
N(1)-N(2)	1.290(10)	1.276(11)
N(1)-C(6)	1.382(11)	1.388(13)
N(2)-C(7)	1.423(11)	1.444(13)
C(1)-Te...N(2)	74.7(3)	74.3(3)
C(1)-Te-X	93.4(3)	94.8(3)
N(2)...Te-X	168.1(2)	169.1(2)
N(1)-N(2)...Te	118.2(6)	117.8(7)
C(7)-N(2)...Te	125.1(5)	124.6(6)

5.4.1.2 Discussion of the structures of (2-phenylazophenyl-C,N')tellurium(II) bromide and iodide.

Apart from the tellurium-halogen bond length, there is a close correspondence between both structures, which are isomorphous. The nine-atom moiety, Te, N(1), N(2), C(1)-C(6), is essentially planar, r.m.s. atomic deviations 0.010 Å in **RTeBr**, and 0.015 Å in **RTeI**. The C(7)-C(12) phenyl ring is planar, r.m.s. deviations <0.010 Å and is rotated about the N(2)-C(7) bond, relative to the nine-atom plane, by 22.1(3) and 23.0(3)°, respectively, for the two structures.

The tellurium atom is formally bonded to a halogen atom and to an aromatic carbon atom, with an additional link to the nitrogen atom N(2) *trans* to the halogen. The Te-Br distance is in good agreement with the 2.707(11) Å found⁶³ in 2-(2'-pyridyl)phenyltellurium(II) bromide and is also within the range of distances, 2.632-2.758 Å, in the Te(IV) complex [2-(dimethylaminomethyl)phenyl]tellurium tribromide⁶⁴. Longer Te-Br distances, 2.835(1) Å and 2.969(1) Å, in two crystal modifications of (ethylenethiourea)phenyltellurium(II) bromide⁶⁵ are associated with the stronger *trans*-influence of a sulfur atom, as compared with nitrogen, and the occurrence of N-H...Br hydrogen bonding.

The Te-I bond is slightly shorter than that given by Allen *et al.*³³ of 2.926(9) Å. It is also slightly shorter than that measured in 2-(2'-pyridyl)phenyltellurium(II) iodide,⁴⁶ 2.917(1) Å and in 1-iodo-2-p-tolyl-1-tellura-2-azaindene⁴⁷, 2.936(1) Å, but falls well within the rather broad range of lengths which have been found previously for such bonds⁴⁸.

The Te-C bonds do not show any trend and are all close to 2.07 Å. This is somewhat shorter than generally found previously for tellurium bonded to an aromatic

carbon atom, e.g. 2.116(2) Å, Allen *et al.*³³ and 2.077-2.112 Å in 2-(2'-pyridyl)phenyltellurium(II) halides^{63,46}.

The Te-N interaction (N donating an electron pair to Te) completes a trigonal bipyramidal type of coordination about the central tellurium atom, with two lone pairs and the carbon atom C(1) equatorial, and the more electronegative nitrogen and halogen atoms, axial, in accord with VSEPR theory. The Te-N distances are similar to those observed^{63,46} in the 2-(2'-pyridyl)phenyl tellurium halides and follow the trend noted⁴⁶, that there is a slight increase in this distance as the atomic number of the trans halogen increases.

In each crystal structure there is one relatively short Te...halogen intermolecular contact, approximately *trans* to the bonded carbon atom. The relevant distances are 3.769(1) Å (bromide) and 3.895(1) Å (iodide), and the C(1)-Te...X angles are, respectively, 173.9(3) and 173.0(3)°. These Te...X contacts fall within the category of secondary interactions⁴⁹.

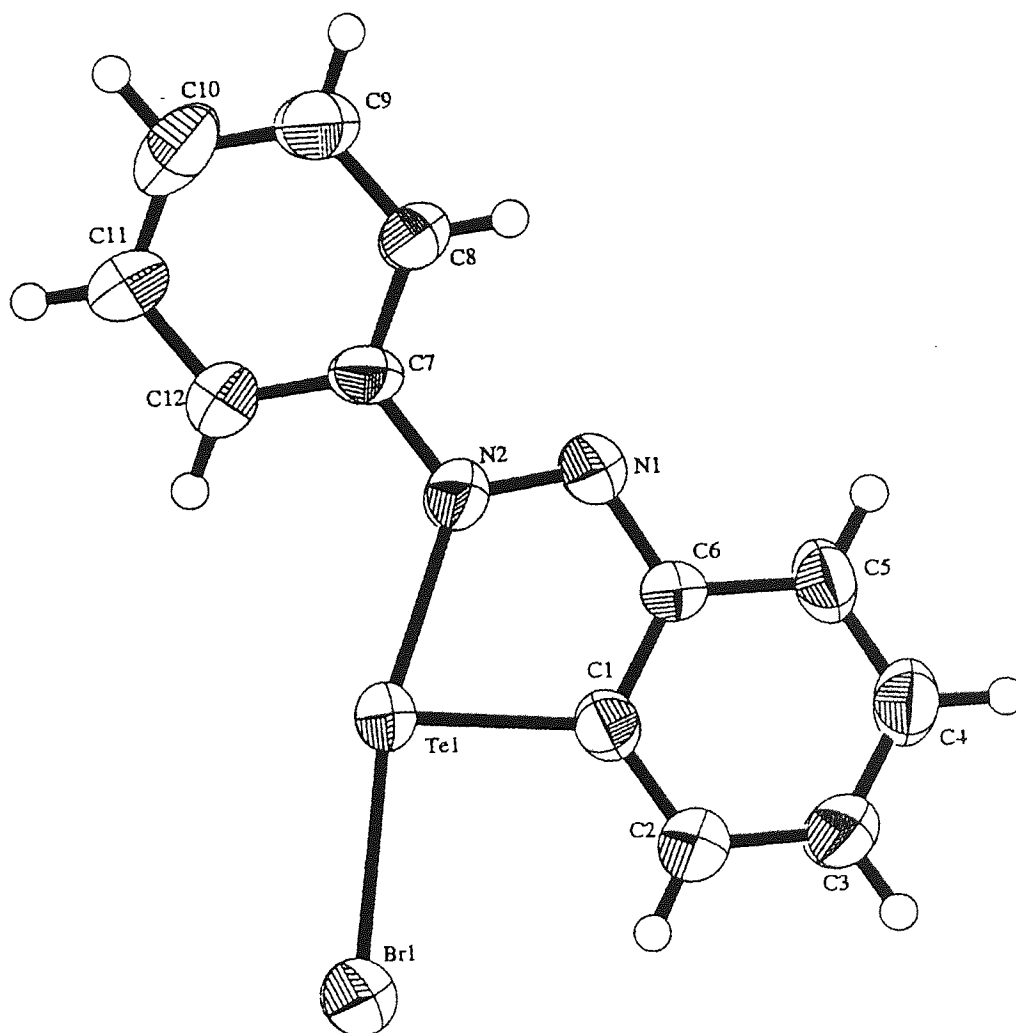


Figure 5.4 The molecular structure of **RTeBr**.

5.4.2 X-ray crystallography for intramolecular stabilized organoselenium compounds.

5.4.2.1 Crystallographic analysis for (2-phenylazophenyl-C,N')selenium(II) chloride, chloriodide and iodide

Suitable crystals of **RSeCl** were obtained by recrystallisation from hot methanol, crystals of **RSeCl/I** were obtained by recrystallisation from hot chloroform and crystals of **RSeI** were obtained by slow evaporation of a solution of **RSeI** in acetone and methanol (1:1).

Dr T.A. Hamor established the crystal structures of compounds **RSeCl** and **RSeCl/I** at Birmingham University.

Dr P. Lowe and Mr Z. Majeed established the crystal structure of compound **RSeI** at Aston University.

Data for **RSeCl** and **RSeCl/I** were measured on a Rigaku R-axis II area detector diffractometer with MoK α radiation at 293(2) K. The structures were determined by direct methods⁶⁶ and refined³⁰ by least-squares using anisotropic thermal parameters for non-hydrogen atoms. Hydrogen atoms were placed in calculated positions riding on their respective bonding atoms. Crystal and refinement data are presented in table 5.11. Atomic coordinates are given in tables 5.12 and 5.13 for **RSeCl** and **RSeCl/I** respectively. Selected geometric parameters are listed in table 5.15. Hydrogen coordinates, displacement parameters and full lists of bond lengths and angles have been deposited with the Cambridge Crystallographic Data Centre. Figure 5.5 gives a ORTEP³¹ plot of one molecule of **RSeCl**, showing the atom numbering. Figure 5.6 gives a ORTEP³¹ plot of one molecule of **RSeCl/I**, showing the atom numbering.

Cell dimensions and intensity data were measured for **RSeI** with an Enraf-Nonius CAD4 diffractometer operating in the ω - 2θ scan mode using MoK α radiation. Three standard reflections were measured every two hours to check the stability of the system. The structure was determined by direct methods⁶⁶ and refined³⁰ by least squares using anisotropic thermal parameters for the heavier atoms. Hydrogen atoms were placed in calculated positions, riding on their respective bonding atoms. Crystal and refinement data are presented in table 5.11. Atomic coordinates are given in table 5.14. Selected geometric parameters are listed in table 5.15. Figure 5.7 gives a ORTEP³¹ plot of one molecule of **RSeI**, showing the atom numbering.

Table 5.11 Crystal and experimental data for **RSeCl**, **RSeCl/I** and **RSeI**.

Compound	RSeCl	RSeCl/I	RSeI
Formula	$C_{12}H_9ClN_2Se$	$C_{12}H_9Cl_{0.5}I_{0.5}N_2Se$	$C_{12}H_9IN_2Se$
M_r	295.62	341.35	387.07
Cryst. sys.	Monoclinic	Monoclinic	Monoclinic
Space grp.	P21/n	P21/n	P21/n
a(Å)	14.862(2)	15.279(2)	4.845(2)
b(Å)	15.485(2)	15.844(2)	18.369(6)
c(Å)	5.0263(2)	5.0162(4)	13.7745(12)
α (deg)	90	90	90
β (deg)	90.277(9)	91.771(7)	91.77(2)
γ (deg)	90	90	90
$V(\text{\AA}^3)$	1156.8(3)	1213.7(3)	1225.3(6)
Z	4	4	4
$D_c(\text{Mg m}^{-3})$	1.697	1.868	2.098
$\mu(\text{MoK}\alpha)(\text{mm}^{-1})$	3.448	4.448	5.557
Cryst.size(mm)	0.35 x 0.20 x 0.12	0.31 x 0.12 x 0.11	0.56 x 0.32 x 0.2
Data range (θ)(deg)	1.90 to 25.19	1.85 to 25.20	2.22 to 24.95
Rfls.measd. [$I > \sigma(I)$]	6253	6463	2956
Unique reflections	1914	2040	2140
R(int)	0.0432	0.0413	0.0369
Variables	145	160	176
$\Delta\rho$ (max +ve)($e\text{\AA}^{-3}$)	0.828	0.561	0.913
$\Delta\rho$ (max -ve)($e\text{\AA}^{-3}$)	-0.827	-0.747	-0.770
R	0.0576	0.0624	0.0424
wR2a	0.1495	0.1547	0.1117
w(a.b)b	0.0725, 1.969	0.0649, 2.64	

$$a_wR2 = [\sum w(F_o^2 - F_c^2)^2 / \sum w(F_o^2)^2]^{1/2}$$

$$b_w = 1/[\sigma^2(F_o^2) + (aP)^2 + bP] \text{ where } P = (F_o^2 + 2F_c^2)/3$$

Table 5.12 Atomic coordinates ($\times 10^4$) and equivalent isotropic displacement parameters ($\text{\AA}^2 \times 10^3$) for **RSeCl**. U(eq) is defined as one third of the trace of the orthogonalized U_{ij} tensor.

	x	y	z	U(eq)
Se(1)	6892(1)	1223(1)	7166(1)	56(1)
Cl(1)	6192(1)	2284(1)	10175(4)	81(1)
N(1)	7561(3)	354(3)	4959(9)	54(1)
N(2)	8424(3)	290(3)	5353(10)	58(1)
C(1)	8054(4)	1388(4)	8554(12)	53(1)
C(2)	8320(4)	1939(4)	10562(12)	58(1)
C(3)	9225(4)	1964(4)	11217(13)	66(2)
C(4)	9865(4)	1464(4)	9935(14)	70(2)
C(5)	9613(4)	906(4)	7995(14)	68(2)
C(6)	8695(3)	866(4)	7276(11)	54(1)
C(7)	7161(3)	-206(4)	3038(11)	53(1)
C(8)	6221(4)	-213(4)	2880(14)	68(2)
C(9)	5814(4)	-762(5)	1069(14)	76(2)
C(10)	6321(5)	-1275(4)	-600(14)	69(2)
C(11)	7248(5)	1248(4)	-430(14)	71(2)
C(12)	7669(4)	-719(4)	1427(13)	64(2)

Table 5.13 Atomic coordinates ($\times 10^4$) and equivalent isotropic displacement parameters ($\text{\AA}^2 \times 10^3$) for **RSeCl/I**. $U(\text{eq})$ is defined as one third of the trace of the orthogonalized U_{ij} tensor.

	x	y	z	$U(\text{eq})$
I(1)	3974(1)	-2351(1)	10639(3)	68(1)
Se(1)	3110(1)	-1184(1)	7168(2)	68(1)
Cl(1)	3870	-2206	10212	60(2)
N(1)	2433(4)	-305(4)	4967(12)	64(2)
N(2)	1612(4)	-235(4)	5396(14)	70(2)
C(1)	2001(5)	-1338(5)	8505(16)	62(2)
C(2)	1751(6)	1889(5)	10483(18)	75(2)
C(3)	884(6)	-1895(6)	11244(18)	80(2)
C(4)	259(6)	-1371(7)	9988(23)	92(3)
C(5)	490(6)	-829(6)	8074(19)	77(2)
C(6)	1363(5)	-798(5)	7301(16)	70(2)
C(7)	2824(5)	229(5)	3085(16)	67(2)
C(8)	2324(6)	754(5)	1468(18)	76(2)
C(9)	2717(7)	1267(6)	-367(20)	86(3)
C(10)	3609(7)	1274(6)	-533(19)	86(3)
C(11)	4105(7)	753(7)	1095(22)	92(3)
C(12)	3732(6)	238(6)	2908(19)	84(3)

Table 5.14 Atomic coordinates ($\times 10^4$) and equivalent isotropic displacement parameters ($\text{\AA}^2 \times 10^3$) for **RSeI**. $U(\text{eq})$ is defined as one third of the trace of the orthogonalized U_{ij} tensor.

	x	y	z	$U(\text{eq})$
I(1)	4498(1)	1433(1)	1890(1)	63(1)
Se(1)	7759(2)	2699(1)	1975(1)	42(1)
N(1)	9502(13)	4078(4)	1265(5)	43(2)
N(2)	9955(13)	3654(3)	1972(4)	40(1)
C(1)	6275(15)	3136(4)	840(5)	39(2)
C(2)	4197(18)	2879(5)	229(6)	47(2)
C(3)	3406(19)	3279(6)	-571(6)	55(2)
C(4)	4617(21)	3932(6)	-789(7)	60(2)
C(5)	6690(20)	4193(5)	-209(6)	52(2)
C(6)	7497(16)	3803(5)	633(5)	43(2)
C(7)	11882(14)	3855(4)	2722(5)	38(2)
C(8)	12198(21)	3434(7)	3526(7)	60(3)
C(9)	14037(18)	3614(6)	4279(7)	61(2)
C(10)	15639(19)	4223(6)	4180(7)	63(2)
C(11)	15366(23)	4645(6)	3368(9)	67(3)
C(12)	13490(19)	4475(5)	2634(7)	56(2)

Table 5.15 Selected bond lengths (Å) and angles (°) with e.s.d's in parentheses for
RSeCl, RSeCl/I and RSeI.

	RSeCl	RSeCl/I	RSeI	X=Cl[a]
Se-C(1)	1.877(5)	1.857(8)	1.881(7)	1.889(4)
Se...N(2)	2.011(5)	2.040(6)	2.051(7)	2.025(3)
Se-Cl	2.466(2)	2.4878(8)		2.475(1)
Se-I		2.837(2)	2.812(2)	
N(1)-N(2)	1.300(6)	1.284(9)	1.262(9)	1.277(5)
N(2)-C(7)	1.426(7)	1.413(10)	1.420(10)	
N(1)-C(6)	1.374(7)	1.370(10)	1.380(10)	1.379(5)
C(1)-Se...N(2)	80.8(2)	80.3(3)	79.5(3)	79.(2)
C(1)-Se-Cl	94.1(2)	96.1(2)		94.26(13)
C(1)-Se-I		96.1(2)	96.8(2)	
N(2)...Se-Cl	174.55(13)	174.8(2)		173.39(10)
N(2)...Se-I		174.8(2)	176.2(2)	
N(1)-N(2)...Se	117.2(4)	116.8(5)	116.9(5)	117.5(3)
C(7)-N(2)...Se	125.1(3)	123.5(5)	123.4(5)	

[a] Previous work⁶⁷

5.4.2.2 Discussion of the structures of (2-phenylazophenyl-C,N')selenium(II) chloride, chloride : iodide (1:1) and iodide.

The crystal structure of **RSeCl/I** was disordered. There was a random distribution of **RSeCl** and **RSeI** molecules throughout the crystal lattice with a ratio of 1:1.

The nine-atom moiety, Se, N(1), N(2), C(1)-C(6), is essentially planar, r.m.s. atomic deviations 0.019 Å in **RSeCl**, 0.012 Å in **RSeCl/I** and 0.024 Å in **RSeI**. The C(7)-C(12) phenyl ring is planar, r.m.s. deviations <0.006 Å and is rotated about the N(2)-C(7) bond, relative to the nine-atom plane, by 7.34(3), 7.82(4) and 6.5(5)° respectively, for the three structures.

The selenium atom is formally bonded to a halogen atom and to an aromatic carbon atom, with an additional link to nitrogen atom N(2) *trans* to the halogen. The Se-Cl distances for **RSeCl** and **RSeCl/I** (see table 5.15) are near the upper end of the range 2.234 - 2.851 Å given in the compilation by Allen *et al.*³³ for this bond and are in good agreement with the mean value of 2.4769 Å, but are slightly shorter than the lengths of 2.475(1) Å measured in 3-chloro-5-methyl-2-p-tolyl-3H-3-selenaindazole⁶⁷. The Se-I bond in **RSeCl/I**, which is 2.837(2) Å and in **RSeI**, which is 2.812(2) Å is slightly longer than that measured in 2,4,6-tri-tert-butylphenyl(iodo)selenide⁶⁸, 2.529(1) Å and longer than expected for a Se-I single bond⁶⁹.

The Se-C bonds do not show any trend and range from 1.85 to 1.88 Å. This is somewhat shorter than generally found previously for selenium bonded to an aromatic carbon atom, e.g. 1.970 Å, Allen *et al.*³³ and 1.889(4) Å in 3-chloro-5-methyl-2-p-tolyl-3H-3-selenaindazole⁶⁷.

The Se-N interaction (N donating an electron pair to Se) completes a trigonal bipyramidal type of coordination about the central selenium atom, with two lone pairs and the carbon atom C (1) equatorial, and the more electronegative nitrogen and

halogen atoms, axial, in accord with VSEPR theory. The Se-N distances are similar to those observed⁶⁷ in 3-chloro-5-methyl-2-p-tolyl-3H-3-selenaindazole and follow the trend noted⁶⁷, that there is a slight increase in this distance as the atomic number of the *trans* halogen increases.

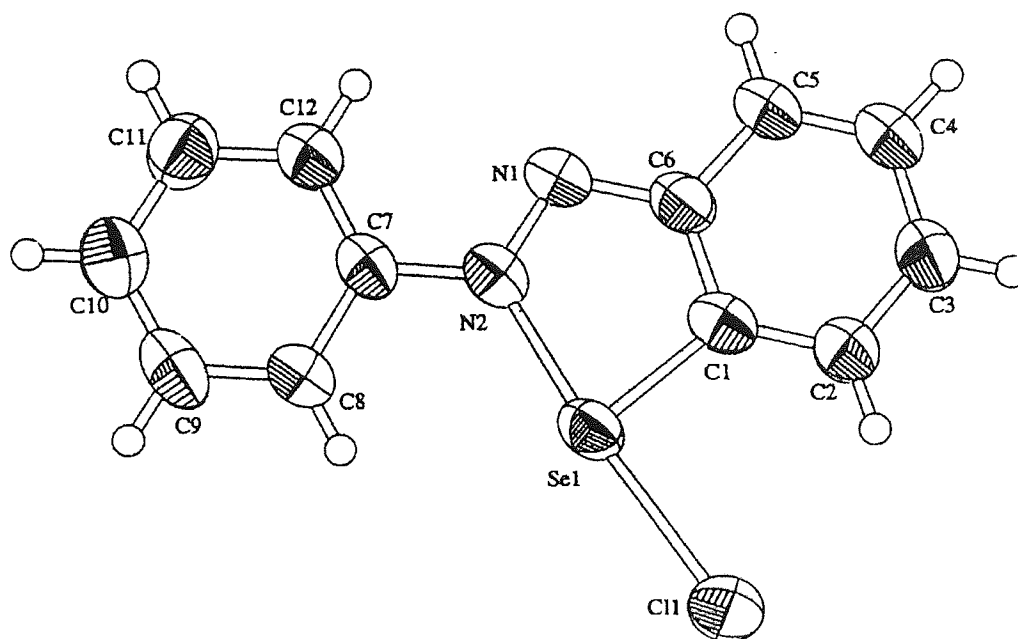


Figure 5.5 The molecular structure of **RSeCl**.

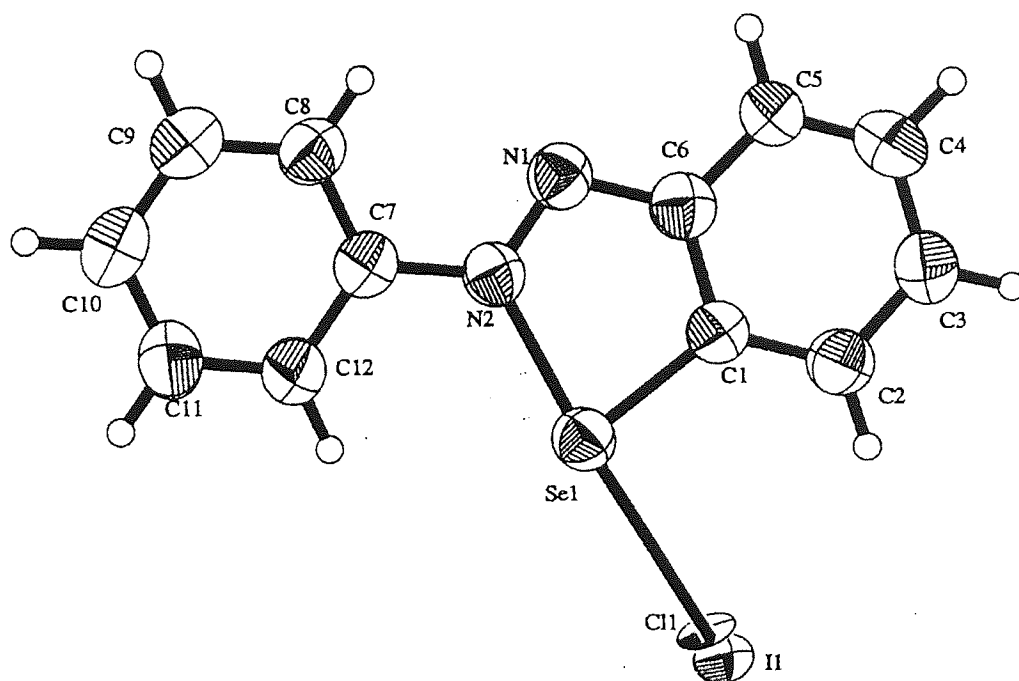


Figure 5.6 The molecular structure of **RSeCl/I**.

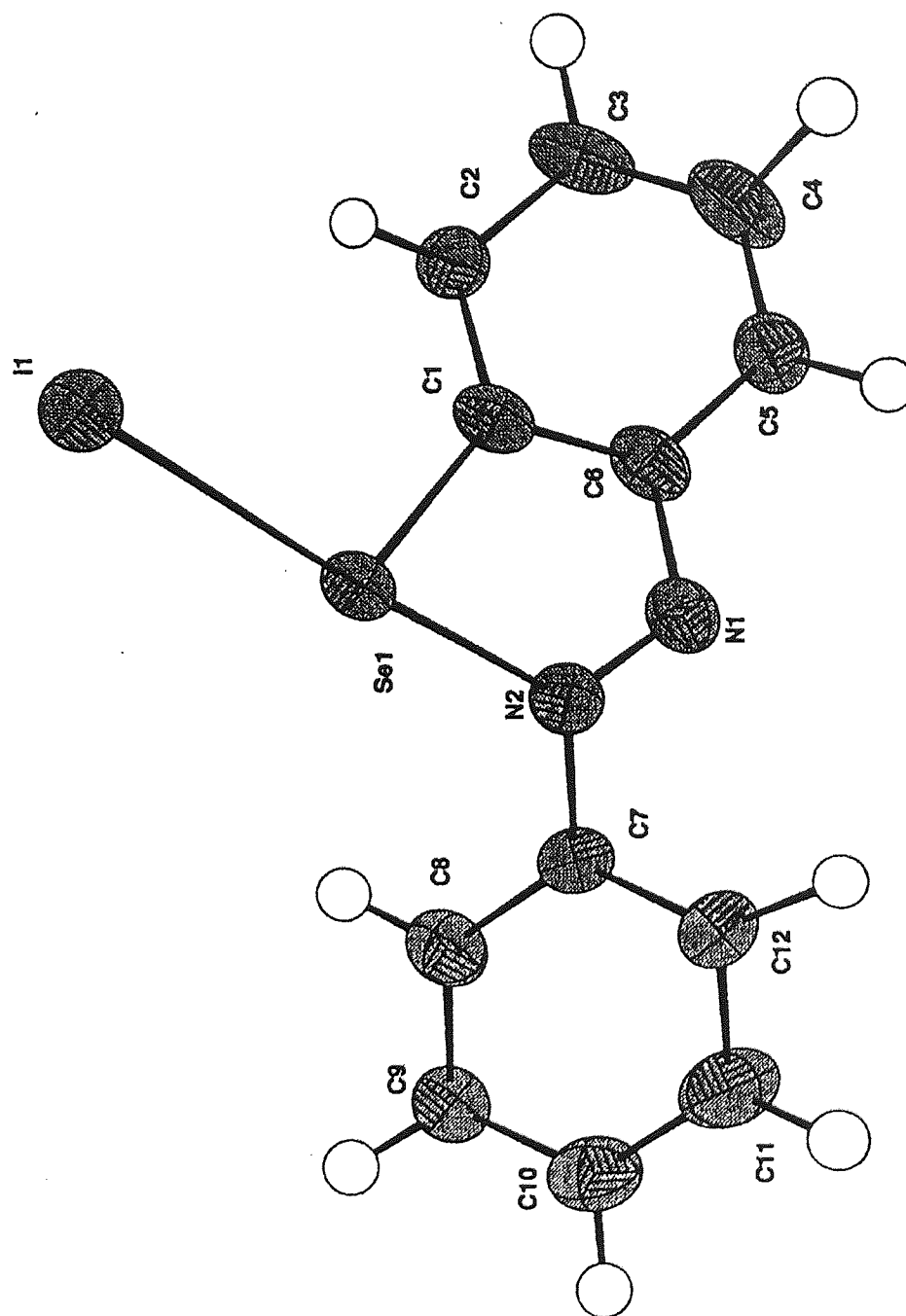


Figure 5.7 The molecular structure of **RSeI**.

5.5 Conclusion

To date attempts to form pure **RTeBr₃** have failed (R = phenylazophenyl).

The direct reduction of impure **RTeBr₃** with hydrazine hydrate afforded pure **RTeBr**, which has been characterised by a number of analytical techniques.

Reaction of **RTeBr** with diiodine leads directly to the related **RTeI**, which again has been characterised by a number of analytical techniques. A reaction pathway is proposed, which involves as a possible intermediate, a labile charge-transfer complex. Directly related organoselenium halides were also prepared. The attempted formation of **RSeCl₃** gave a mixture.

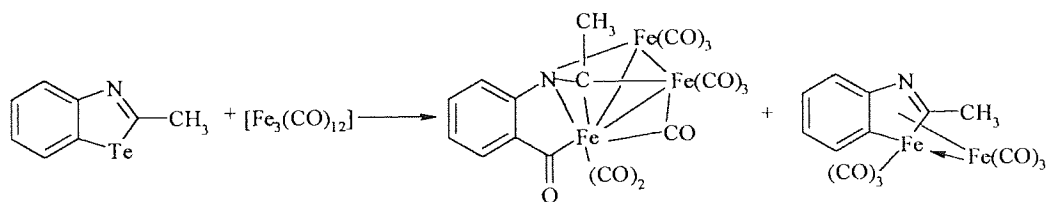
Two methods for the formation of **RSeCl** are presented. The first method is the direct reduction of impure **RSeCl₃** with hydrazine hydrate. The second method, used the same reagents and conditions as for the formation of the impure **RSeCl₃**, but with an extended reaction time.

The formation of **RSeI** is reported. Reaction of **RSeCl** with diiodine (molar ratio 1:1) gave pure **RSeI**, but when a 2:1 molar ratio of **RSeCl** and diiodine was used **RSeCl/I** was formed. The suggested reaction pathway for both products is again *via* a charge transfer complex.

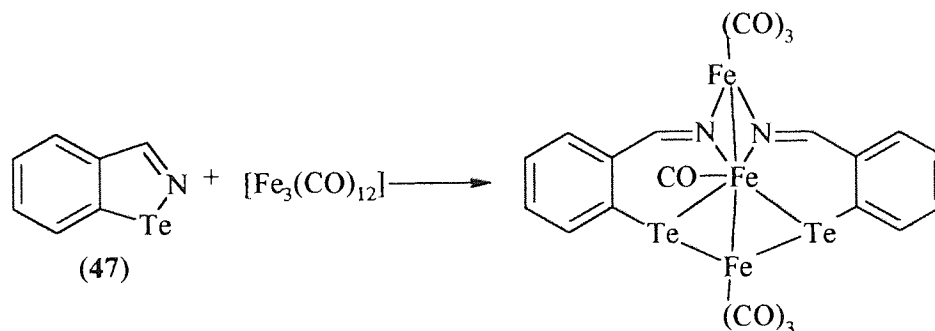
CHAPTER SIX
THE REACTIONS OF NITROGEN-CONTAINING SELENIUM
OR TELLURIUM HETEROCYCLES WITH TRIIRON
DODECACARBONYL

6.1 Introduction

Previous studies on systems where the heterocyclic ring contained both tellurium and nitrogen heteroatoms gave interesting results. The reaction of 2-methylbenzotellurazole¹¹ with triiron dodecacarbonyl yielded three major products. The first product was a known cluster compound $[\text{Fe}_3\text{Te}_2(\text{CO})_9]$, the second and third were detellurated compounds having the formulae $[\text{Fe}_3\{\text{C}_6\text{H}_4(\text{CO})\text{NCCH}_3\}(\text{CO})_9]$ and $[\text{Fe}_2(\text{C}_6\text{H}_4\text{NCCH}_3)(\text{CO})_6]$ (see below).



The reaction of benzisotellurazole¹¹ (47) with triiron dodecacarbonyl afforded the known cluster compound, $[\text{Fe}_3\text{Te}_2(\text{CO})_9]$ and a second compound having the formula $[\text{Fe}_3\{\text{C}_6\text{H}_4(\text{CHN})\text{Te}\}_2(\text{CO})_7]$ (see below).

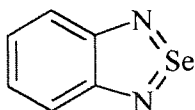


The above reactions show that the presence of the nitrogen in the heterocyclic ring opens the possibility of new pathways for these reactions. These tellurium, nitrogen compounds can be seen as precursors for the formation of novel organometallic compounds. Therefore it is also of interest to investigate the reaction of selenium, nitrogen containing heterocyclic compounds with $[\text{Fe}_3(\text{CO})_{12}]$.

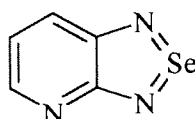
6.2 Experimental

6.2.1 Reactions of nitrogen-containing heterocycles

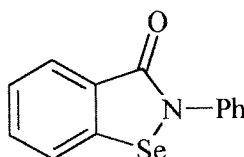
6.2.1.1 Preparation of nitrogen-containing compounds



2,1,3-Benzoselenadiazole⁷⁰



1,2,5-Selenadiazolo[3,4-b]pyridine⁷¹



2-Phenyl-1,2-benzisoselenazol-3(2H)-one⁵⁷

The above heterocycles were prepared using literature methods^{57,70,71}. The analyses of the above materials were in good agreement with the literature values^{57,70,71}.

6.2.1.2 Reaction of triiron dodecacarbonyl with 2,1,3-benzoselenadiazole

2,1,3-Benzoselenadiazole (1.00g, 5.64 mmol) and $[\text{Fe}_3(\text{CO})_{12}]$ (2.7g, 5.64 mmol) were refluxed, with stirring, in the dark, in toluene (50 cm³) for 4.5 h. The reaction mixture was cooled to room temperature and filtered to give a colourless filtrate and a residual black solid which adhered to the sides of the flask. The solvent was removed from the filtrate in *vacuo*. No involatile materials were found.

The reaction was repeated with the addition of anthracene (1.00g, 5.64 mmol). The above method was followed, giving a colourless product. The colourless product was chromatographed on a column of silica gel (pore diameter *ca.* 6 nm). Elution with chloroform and removal of the solvent gave a colourless solid, (observed by TLC on UV-active silica gel TLC plates) which was found to be anthracene.

6.2.1.3 Reaction of triiron dodecacarbonyl with 1,2,5-selenadiazolo[3,4-b]pyridine

1,2,5-Selenadiazolo[3,4-b]pyridine (0.73g, 4 mmol) and $[\text{Fe}_3(\text{CO})_{12}]$ (2.01g, 4 mmol) were refluxed, with stirring, in the dark, in toluene (50 cm³) for 4.5 h. The reaction mixture was cooled to room temperature and filtered to give a pale yellow filtrate and a residual black solid which adhered to the sides of the flask. The solvent was removed from the filtrate in *vacuo* to give a pale yellow solid. The pale yellow compound was found to be the starting material (1,2,5-selenadiazolo[3,4-b]pyridine).

6.2.1.4 Reaction of triiron dodecacarbonyl with 2-phenyl-1,2-benzisoselenazol-3(2H)-one

2-Phenyl-1,2-benzisoselenazol-3(2H)-one (1.09g, 4 mmol) and $[\text{Fe}_3(\text{CO})_{12}]$ (2.01g, 4 mmol) were refluxed, with stirring, in the dark, in toluene (50 cm³) for 4.5 h. The reaction mixture was cooled to room temperature and filtered to give a yellow filtrate and a residual black solid which adhered to the sides of the flask. The solvent was removed from the filtrate in *vacuo* to give a yellow solid. The yellow compound was found to be the starting material (2-phenyl-1,2-benzisoselenazol-3(2H)-one).

6.2.1.5 Reaction of triiron dodecacarbonyl with 2-methylbenzoselenazole

2-Methylbenzoselenazole (1g, 5.1 mmol) and $[\text{Fe}_3(\text{CO})_{12}]$ (2.56g, 5.1 mmol) were refluxed, with stirring, in the dark, with toluene (25 cm³) over 4.5 h. On cooling to room temperature the reaction mixture was filtered to give an orange filtrate and a

residual black solid which adhered to the sides of the flask. The solvent was removed from the filtrate in *vacuo* to give a orange oil. The orange oil was chromatographed on a column of silica gel (pore diameter *ca.* 6 nm) giving a red band followed by another pale yellow band. Elution with dichloromethane/hexane (2:1) and removal of the solvent gave red crystals, (**48**) {0.019g, 0.8 % based on $\text{Fe}_3(\text{CO})_{12}$ }, from the first eluate and pale yellow crystals from the second eluate (unreacted 2-methylbenzoselenazole).

Crystals suitable for X-ray diffraction measurements were grown by cooling a concentrated chloroform/hexane (2:1) solution for (**48**) (see section 6.4.1).

6.2.1.6 Reaction of triiron dodecacarbonyl with (2-phenylazophenyl-C,N')tellurium(II) bromide

(2-Phenylazophenyl-C,N')tellurium(II) bromide (0.15g, 3.9 mmol) and $[\text{Fe}_3(\text{CO})_{12}]$ (0.20g 3.9 mmol) were refluxed, with stirring, in the dark, with toluene (25 cm³) over 4.5 h. On cooling to room temperature, the reaction mixture was filtered to give a orange/red filtrate. The solvent was removed from the filtrate in *vacuo* to give a red solid. The red solid was recrystallised from methanol. The red solid was shown to be unreacted (2-phenylazophenyl-C,N')tellurium(II) bromide.

6.2.1.7 Reaction of triiron dodecacarbonyl with (2-phenylazophenyl-C,N')selenium(II) chloride

(2-Phenylazophenyl-C,N')selenium(II) chloride (1.5g, 3.9 mmol) and $[\text{Fe}_3(\text{CO})_{12}]$ (0.20g 3.9 mmol) were refluxed, with stirring, in the dark, with toluene (25 cm³) over 4.5 h. On cooling to room temperature, the reaction mixture was filtered to give a red filtrate. The solvent was removed from the filtrate in *vacuo* to give a red solid. The

red solid was recrystallised from methanol. The red solid was shown to be unreacted (2-phenylazophenyl-C,N')tellurium(II) chloride.

6.2.1.8 Reaction of triiron dodecacarbonyl with 2-(methyltelluro)benzanilide

2-(Methyltelluro)benzanilide (0.75g, 2.2 mmol) and $[\text{Fe}_3(\text{CO})_{12}]$ (1.12g, 2.2 mmol) were refluxed, with stirring, in the dark, with toluene (25 cm³) for 4.5 h. On cooling to room temperature the reaction mixture was filtered to give a red filtrate and a residual black solid which adhered to the sides of the flask. The solvent was removed from the filtrate in *vacuo* to give a red solid. The red solid was chromatographed on a column of silica gel (pore diameter *ca.* 6 nm) giving a red band followed by another colourless band. Elution with chloroform and removal of the solvent gave a deep red solid, from the first eluate, and a colourless solid from the second eluate (unreacted 2-(methyltelluro)benzanilide).

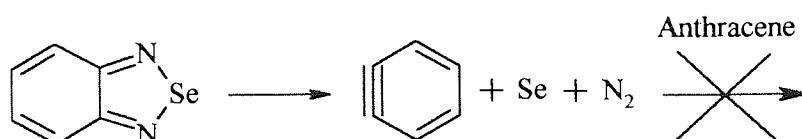
6.2.1.9 Reaction of triiron dodecacarbonyl with 2-(methylseleno)benzanilide

2-(Methylseleno)benzanilide (0.86g, 2.97 mmol) and $[\text{Fe}_3(\text{CO})_{12}]$ (1.5g, 2.97 mmol) were refluxed, with stirring, in the dark, with toluene (25 cm³) for 4.5 h. On cooling to room temperature the reaction mixture was filtered to give a red filtrate and a residual black solid which adhered to the sides of the flask. The solvent was removed from the filtrate in *vacuo* to give a red solid. The red solid was chromatographed on a column of silica gel (pore diameter *ca.* 6 nm) giving a red band followed by another colourless band (observed by TLC on UV-active silica gel TLC plates). Elution with chloroform and removal of the solvent gave a deep red solid from the first eluate, and a colourless solid from the second eluate (unreacted 2-(methylseleno)benzanilide).

6.3 Results and discussion

It is apparent that 2,1,3-benzoselenadiazole, 1,2,5-selenadiazolo[3,4-b]pyridine and 2-phenyl-1,2-benzisoselenazol-3(2H)-one do not react with triiron dodecacarbonyl under the conditions employed.

The reaction of 2,3,1-benzoselenadiazole and triiron dodecacarbonyl was revisited⁷² but no products were isolated. Anthracene was introduced into the reaction to see if any benzyne moiety could be trapped. Unfortunately only anthracene was recovered in these experiments (see below).



Only starting materials were recovered when (2-phenylazophenyl-C,N')tellurium(II) bromide and (2-phenylazophenyl-C,N')selenium(II) chloride were reacted with triiron dodecacarbonyl under the condition employed (see experimental section 5.2.3.1).

6.3.1 Reaction of triiron dodecacarbonyl with 2-methylbenzoselenazole

The products obtained from this reaction (4.5 h) were red crystals and a black solid residue. The black solid was believed to be a mixture of iron oxides. The yield of the red product was 0.019g or 0.8% based on $\text{Fe}_3(\text{CO})_{12}$. Data from the FTIR spectrum in the carbonyl region for the red crystals are recorded in table 6.1. The EI mass spectrum observed peaks are recorded in table 6.2.

Table 6.1 FTIR bands in the carbonyl region for product from reaction of 2-methylbenzselenazole and $[\text{Fe}_3(\text{CO})_{12}]$.

Red crystals KBr, $\nu(\text{CO}) \text{ cm}^{-1}$
2074
2028
1975

The FTIR band pattern for the red crystals in the carbonyl region together with the mass spectrum implies the heterocyclic product, $[\text{Fe}_2\{\text{C}_6\text{H}_4(\text{NCH}_2\text{CH}_3)\text{Se}\}(\text{CO})_6]$ (**47**). This was further confirmed by elemental analysis, mass spectrum:

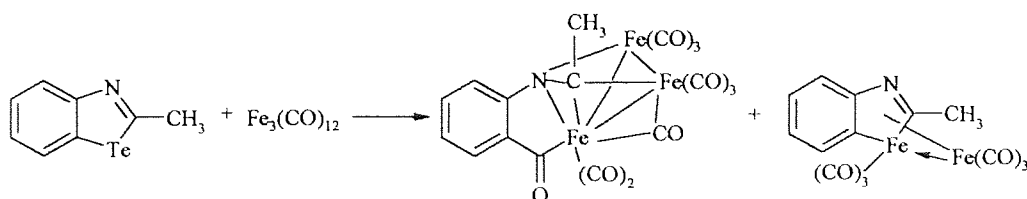
Calculated (%)	C, 35.1	H, 1.88	N, 2.93	$\text{C}_{14}\text{H}_9\text{NO}_6\text{Fe}_2\text{Se}$
Found (%)	C, 34.9	H, 1.85	N, 2.84	

Table 6.2 EI mass spectrum registered peaks for product from reaction of 2-methylbenzselenazole and $[\text{Fe}_3(\text{CO})_{12}]$ (^1H , ^{12}C , ^{56}Fe and ^{80}Se).

Deep red crystals, (48)	
m/z	Fragment
423	$\text{C}_{12}\text{H}_9\text{NO}_4\text{Fe}_2\text{Se}^+$
395	$\text{C}_{11}\text{H}_9\text{NO}_3\text{Fe}_2\text{Se}^+$
310	$\text{C}_{10}\text{H}_9\text{NO}_2\text{FeSe}^+$
282	$\text{C}_9\text{H}_9\text{NOFeSe}^+$
254	$\text{C}_8\text{H}_9\text{NFeSe}^+$

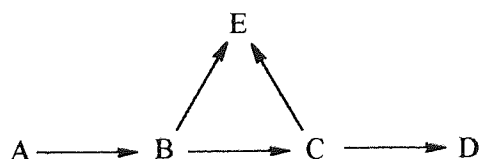
However the spectroscopic analysis of (**48**) is consistent with the static structure of compound (**48**) (see section 6.4).

On comparing with the analogous reaction, where the heterocyclic compound contains tellurium¹¹, one observes that the tellurium reaction product is a ferrole (see below).



The reaction product with the selenium derivative is a selenium containing heterocyclic compound. This gives further evidence that the reactions of selenium analogues with $[\text{Fe}_3(\text{CO})_{12}]$ give compounds that represented intermediates products, when compared with the reaction of tellurium heterocycles with $[\text{Fe}_3(\text{CO})_{12}]$.

The reaction between $[\text{Fe}_3(\text{CO})_{12}]$ and heterocycles containing either selenium or tellurium with nitrogen may follow the reaction pathway shown below.

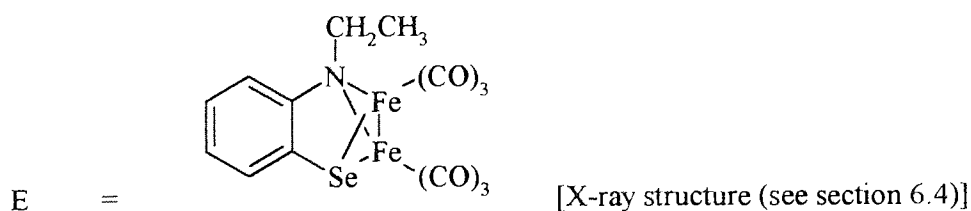


Where A = Starting material

B = Unknown intermediate

C = Chalcogenaferrole (product for the selenium reaction)

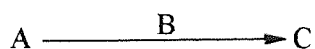
D = Ferrole (product for the tellurium reaction)



If (A) is a tellurium heterocyclic compound then the reaction path taken would be



where the starting material would go through the intermediate compounds (B) and (C) resulting in a ferrole product. However the selenium heterocyclic compounds usually give compound (C). Hence the reaction path taken would be



where (B) is a unknown intermediate.

The product studied by X-ray analysis may be due to a side reaction as shown above forming (E). (E) may be formed in two ways. One possible route is by the decomposition of (B) [unknown intermediate] to (E) or the decomposition of (C) [chalcogenoferrole] to (E).

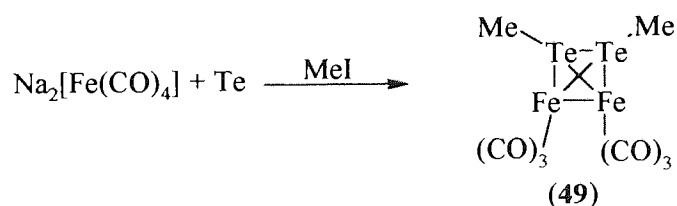
Both of the reaction pathways suggest the product studied by X-ray analysis (E) (in the reaction scheme above) must undergo a transformation that results in the insertion of a second iron into the heterocyclic ring. On inserting the second iron, the carbon attached to the selenium atom is forced to leave resulting in a carbene on the carbon attached to the nitrogen atom. The carbene may be stabilised by the co-ordination⁷³ to the third iron within the triiron triangle. On prolonged heating of this intermediate, the loss of the third iron may occur giving a highly reactive carbene species. The resulting carbene may undergo two possible reactions; one is the decomposition by adventitious moisture. If this is the case the carbene should give a secondary alcohol (which is not observed). The second possibility is that the carbene extracts protons from the solvent (toluene).

It is interesting to note that this is the second time that a possible carbene intermediate has been postulated in the work discussed in this thesis. Therefore at this juncture one must consider that the formation of this carbene cannot be by chance and may play an

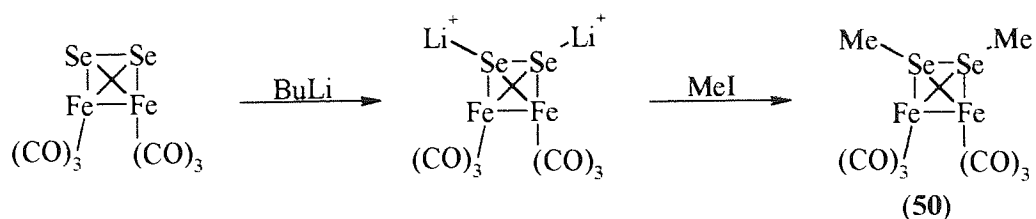
important role in the reaction pathway. Further work may be carried out on these systems to establish the relationship between the carbene and the resulting product. One suggestion is to use deuterated toluene ($C_6H_5CD_3$ or $C_6D_5CD_3$) as the solvent, this will give rise to products that are labelled (C-D₂) and these products may be analysed by NMR or mass spectroscopy. One would use partial and fully deuterated toluene to see if the protons are extracted from the methyl group or the benzene ring.

6.3.2 Reactions of triiron dodecacarbonyl with 2-(methyltelluro)benzanilide or 2-(methylseleno)benzanilide

The reaction of 2-(methyltelluro)benzanilide with $[Fe_3(CO)_{12}]$ (4.5 hours) produced a deep red product, (49) and from the reaction of 2-(methylseleno)benzanilide with $[Fe_3(CO)_{12}]$ a deep red crystalline product, (50), was obtained. Both reactions also produced black solid residues. (49) was found to be $[Fe_2(\mu\text{-TeMe})_2(CO)_6]$ ⁷⁴ and (50) was found to be $[Fe_2(\mu\text{-SeMe})_2(CO)_6]$ ⁷⁵. The analyses of both (49) and (50) were in good agreement with the literature values^{74,75}. Bachman *et al.*⁷⁴ employed a two step synthesis of (49). The first step was the reaction of $Na_2[Fe(CO)_4]$ and tellurium, followed by the reaction with MeI (see scheme 6.1). Mathur *et al.*⁷⁵ synthesised (50) by the reaction of $[Fe_2(\mu\text{-Se})_2(CO)_6]$ with BuLi followed by MeI (see scheme 6.2).



Scheme 6.1 Formation of (49) by Bachman *et al.*



Scheme 6.2 Formation of (50) by Mathur *et al.*

Both the reactions employed by Bachman and Mathur required dry conditions involving Schlenk lines and a vacuum atmosphere dry box. It was surprising (49) and (50) could be formed using less rigorous conditions as indicated in the experimental section (see sections 6.2.1.7 and 6.2.1.8). It also seems that 2-(methyltelluro)benzanilide and 2-(methylseleno)benzanilide maybe a good source of E-Me (where E = tellurium or selenium). They are a more stable source of E-Me than other conventional sources.

The X-ray crystal structures of (49) and (50) have been determined (see section 6.4).

6.4 X-ray crystallography

6.4.1 X-ray crystallography for product (48).

6.4.1.1 Crystallographic analysis for product (48).

Dr P. Lowe and Mr Z. Majeed established the crystal structure of compound (48) at Aston University.

Cell dimensions and intensity data were measured for (48) with an Enraf-Nonius CAD4 diffractometer operating in the ω -2 θ scan mode using MoK α radiation. Three standard reflections were measured every two hours to check the stability of the system. The structures were determined²⁹ by direct methods and refined³⁰ by least-squares on F^2 using anisotropic thermal parameters for non-hydrogen atoms. Hydrogen atoms were placed in calculated positions, riding on their respective bonding atoms. Diagrams were drawn with ORTEP;³¹ thermal ellipsoids are at the 30% probability level. Crystal and refinement data are presented in table 6.3. Atomic co-ordinates are given in table 6.4. Selected geometric parameters are listed in table 6.5. Figure 6.1 gives a ORTEP³¹ plot of one molecule of (48), showing the atom numbering.

Table 6.3 Crystal and experimental data for (48).

Compound	(48)
Formula	$C_{14}H_9Fe_2NO_6Se$
M_r	477.88
Cryst. sys.	Triclinic
Space grp.	P-1
$a(\text{\AA})$	7.782(2)
$b(\text{\AA})$	9.396(2)
$c(\text{\AA})$	12.434(3)
$\alpha(\text{deg})$	77.01(2)
$\beta(\text{deg})$	76.29(2)
$\gamma(\text{deg})$	79.45(2)
$V(\text{\AA}^3)$	852.5(4)
Z	4
$D_c(\text{Mg m}^{-3})$	1.862
$\mu(\text{MoK}\alpha)(\text{mm}^{-1})$	3.864
Data range (θ)(deg)	2.25 to 26.99
Rfls. measd. [$I > \sigma(I)$]	5053
Unique reflections	3686
$R(\text{int})$	0.0284
Variables	254
$\Delta\rho$ (max +ve)($\text{e}\text{\AA}^{-3}$)	0.803
$\Delta\rho$ (max -ve)($\text{e}\text{\AA}^{-3}$)	-0.767
R	0.0345
wR2a	0.0834

Table 6.4 Atomic coordinates ($\times 10^4$) and equivalent isotropic displacement parameters ($\text{\AA}^2 \times 10^3$) for (48). U(eq) is defined as one third of the trace of the orthogonalized U_{ij} tensor.

	x	y	z	U(eq)
Se(1)	9982(1)	3875(1)	1744(1)	52(1)
Fe(1)	8378(1)	3252(1)	3648(1)	38(1)
Fe(2)	6821(1)	4004(1)	2090(1)	41(1)
N(1)	7526(4)	1923(3)	2869(2)	37(1)
C(7)	6096(6)	1042(4)	3464(3)	49(1)
C(8)	5031(7)	663(5)	2706(5)	68(1)
C(6)	9011(5)	1085(4)	2225(3)	44(1)
C(5)	10375(5)	1850(4)	1579(3)	51(1)
C(4)	11871(7)	1176(7)	957(4)	72(1)
C(3)	12020(8)	-294(7)	966(5)	87(2)
C(2)	10728(8)	-1072(6)	1596(5)	85(2)
C(1)	9197(7)	-416(5)	2235(4)	63(1)
C(9)	8746(5)	4963(4)	3895(3)	51(1)
O(1)	8970(5)	6071(3)	4016(3)	76(1)
C(10)	6620(6)	3120(4)	4861(3)	55(1)
O(2)	5525(5)	3077(4)	5654(3)	86(1)
C(11)	10132(5)	2038(4)	4269(3)	48(1)
O(3)	11217(5)	1306(3)	4660(3)	75(1)
C(12)	6617(6)	5967(4)	1804(3)	57(1)
O(4)	6464(6)	7214(3)	1662(3)	88(1)
C(13)	6518(6)	3714(4)	768(3)	57(1)
O(5)	6309(6)	3520(4)	-63(3)	90(1)
C(14)	4556(6)	4174(4)	2855(4)	55(1)
O(6)	3135(5)	4373(4)	3336(3)	83(1)

Table 6.5 Selected bond lengths (Å) and angles (°) for compound (**48**).

Compound 48				
Se(1)-C(5)	1.920(4)		C(7)-C(8)	1.526(6)
Se(1)-Fe(2)	2.3797(9)		C(6)-C(5)	1.380(6)
Se(1)-Fe(1)	2.3975(9)		C(6)-C(1)	1.389(5)
Fe(1)-C(10)	1.778(4)		C(5)-C(4)	1.370(6)
Fe(1)-C(9)	1.787(4)		C(4)-C(3)	1.362(8)
Fe(1)-C(11)	1.815(4)		C(3)-C(2)	1.341(8)
Fe(1)-N(1)	2.022(3)		C(2)-C(1)	1.390(7)
Fe(1)-Fe(2)	2.4296(9)		C(9)-O(1)	1.134(4)
Fe(2)-C(12)	1.783(4)		C(10)-O(2)	1.139(5)
Fe(2)-C(14)	1.791(5)		C(11)-O(3)	1.120(5)
Fe(2)-C(13)	1.801(4)		C(12)-O(4)	1.133(4)
Fe(2)-N(1)	2.017(3)		C(13)-O(5)	1.141(5)
N(1)-C(6)	1.452(4)		C(14)-O(6)	1.130(5)
N(1)-C(7)	1.464(5)			
C(5)-Se(1)-Fe(2)	93.09(12)		C(12)-Fe(2)-C(14)	87.63(19)
C(5)-Se(1)-Fe(1)	91.31(11)		C(12)-Fe(2)-C(13)	99.51(17)
Fe(2)-Se(1)-Fe(1)	61.14(3)		C(14)-Fe(2)-C(13)	100.6(2)
C(10)-Fe(1)-C(9)	89.93(18)		C(12)-Fe(2)-N(1)	157.40(15)
C(10)-Fe(1)-C(11)	98.49(18)		C(14)-Fe(2)-N(1)	95.98(15)
C(9)-Fe(1)-C(11)	99.05(17)		C(13)-Fe(2)-N(1)	101.70(14)
C(10)-Fe(1)-N(1)	96.25(15)		C(12)-Fe(2)-Se(1)	89.83(16)
C(9)-Fe(1)-N(1)	156.21(14)		C(14)-Fe(2)-Se(1)	158.31(13)
C(11)-Fe(1)-N(1)	102.70(14)		C(13)-Fe(2)-Se(1)	101.04(15)
C(10)-Fe(1)-Se(1)	161.69(14)		N(1)-Fe(2)-Se(1)	78.60(8)
C(9)-Fe(1)-Se(1)	88.89(13)		C(12)-Fe(2)-Fe(1)	104.30(13)
C(11)-Fe(1)-Se(1)	99.74(12)		C(14)-Fe(2)-Fe(1)	100.06(13)
N(1)-Fe(1)-Se(1)	78.08(8)		C(13)-Fe(2)-Fe(1)	148.90(12)
C(10)-Fe(1)-Fe(2)	103.56(14)		N(1)-Fe(2)-Fe(1)	53.10(8)
C(9)-Fe(1)-Fe(2)	103.29(12)		Se(1)-Fe(2)-Fe(1)	59.79(3)
C(11)-Fe(1)-Fe(2)	148.40(12)		C(6)-N(1)-C(7)	112.4(3)
N(1)-Fe(1)-Fe(2)	52.93(8)		C(6)-N(1)-Fe(2)	115.2(2)
Se(1)-Fe(1)-Fe(2)	59.07(3)		C(7)-N(1)-Fe(2)	117.7(2)

Table 6.5 Cont. Selected bond lengths (Å) and angles (°) for compound (**48**).

C(6)-N(1)-Fe(1)	111.6(2)		C(3)-C(4)-C(5)	119.3(5)
C(7)-N(1)-Fe(1)	120.9(2)		C(2)-C(3)-C(4)	120.0(5)
Fe(2)-N(1)-Fe(1)	73.97(9)		C(3)-C(2)-C(1)	121.8(5)
N(1)-C(7)-C(8)	114.8(4)		C(6)-C(1)-C(2)	118.9(5)
C(5)-C(6)-C(1)	117.8(4)		O(1)-C(9)-Fe(1)	177.6(3)
C(5)-C(6)-N(1)	116.5(3)		O(2)-C(10)-Fe(1)	177.1(4)
C(1)-C(6)-N(1)	125.7(4)		O(3)-C(11)-Fe(1)	178.9(4)
C(4)-C(5)-C(6)	122.1(4)		O(4)-C(12)-Fe(2)	177.6(4)
C(4)-C(5)-Se(1)	125.5(4)		O(5)-C(13)-Fe(2)	179.1(5)
C(6)-C(5)-Se(1)	112.3(3)		O(6)-C(14)-Fe(2)	175.6(4)

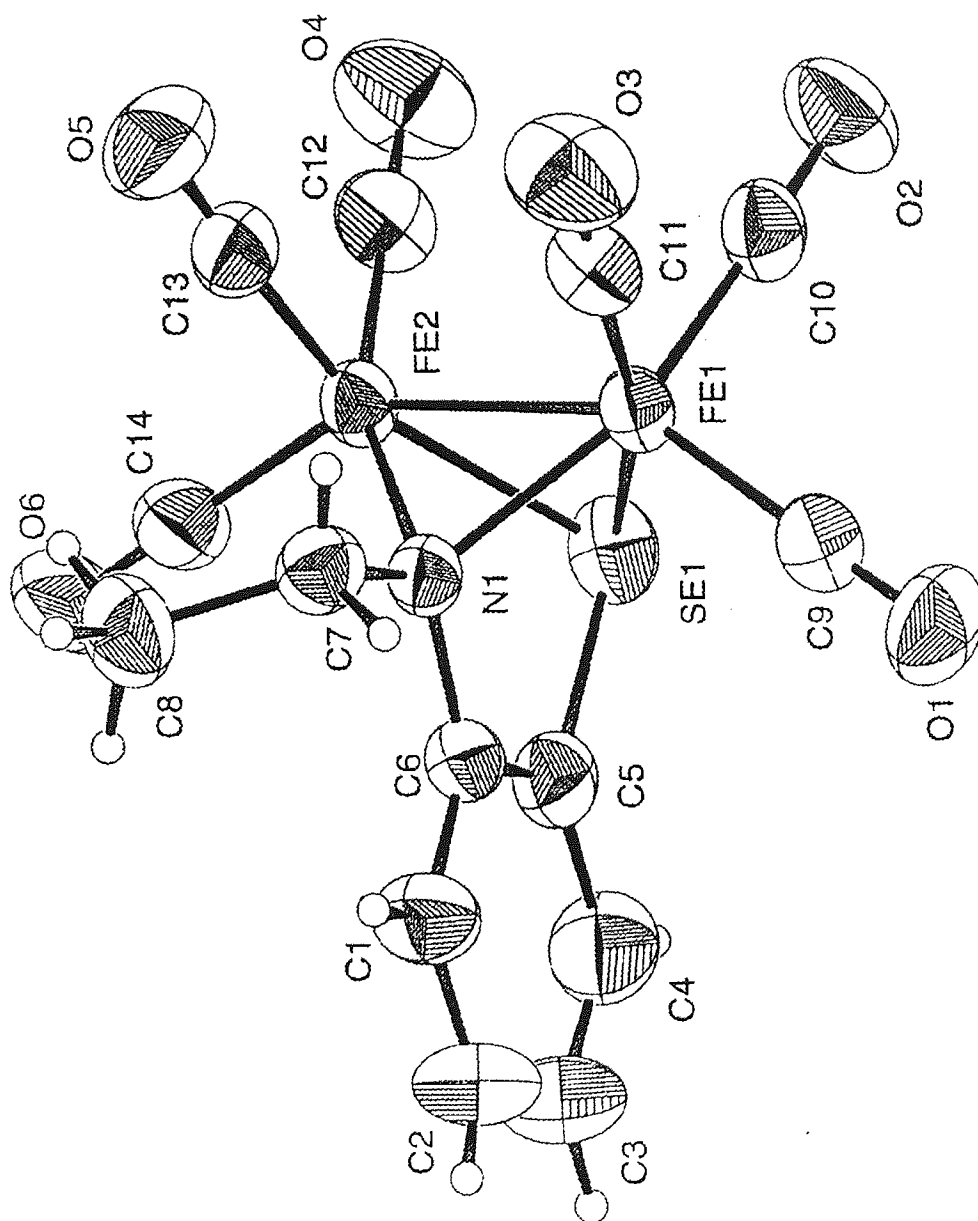


Figure 6.1 The molecular structure of $[\text{Fe}_2\{\text{C}_6\text{H}_4(\text{NCH}_2\text{CH}_3)\text{Se}\}(\text{CO})_6]$, (48).

6.4.2 Discussion of the structure (48)

In (48) (figure 6.4) both iron atoms, Fe(1) and Fe(2), form part of a benzoferrazole system. The Fe-Fe distance of 2.4296(9) Å is in good agreement with the Fe-Fe distance found for μ -{1-2- η -[hydroseleno-1-cyclohexene-1-carbaldehydato(2-)]- μ -Se} bis(tricarbonyliron)¹², 2.482(1) Å. The Se-Fe distances for Se(1)-Fe(1) and Se(1)-Fe(2) are 2.3795(9) and 2.3797(9) Å respectively, which are in good agreement with those in the compounds described in chapter 3 [Se(1)-Fe(1) and Se(1)-Fe(2) bond distances for compound (35) are 2.347(1) and 2.378(1) respectively; Se(1)-Fe(1) and Se(1)-Fe(2) bond distances for compound (36) are 2.355(1) and 2.383(1) respectively].

The Se(1)-C(5) bond distance is 1.920(4) Å. This is somewhat shorter than generally found previously for selenium bonded to an aromatic carbon atom, e.g. 1.970 Å, Allen *et al*³³. The sp² carbon has a bonding distance of 1.452(4) Å to the nitrogen [C(6)-N(1)], compared with 1.416 Å given in the tabulations of Allen *et al*³³. The sp³ has a bonding distance of 1.464(5) Å carbon to the nitrogen [C(7)-N(1)], compared with 1.469 Å given in the tabulations of Allen *et al*³³.

6.4.2.1 Crystallographic analysis for [Fe₂(μ -TeMe)₂(CO)₆], (49), and [Fe₂(μ -SeMe)₂(CO)₆], (50).

Suitable crystals of (49) and (50) were obtained from slow evaporation of chloroform (1 week). Dr P. Lowe established the crystal structures of compounds (49) and (50) at Aston University.

Crystals of (49) and (50) were glued to the end of a thin glass fibre. All measurements were made on a Siemens P4S diffractometer using MoK α radiation equipped with an incident beam graphite monochromator. Cell dimensions and an orientation matrix for

data collection, obtained from a least-squares refinement of the setting angles of 25 - 50 accurately centred reflections in the range $20 < 2\theta < 25^\circ$, corresponded to an orthorhombic cell for (49) and triclinic cell for (50) cell. These are listed with other relevant crystal data in table 6.6. Atomic coordinates are given in tables 6.7 and 6.8 for (49) and (50) respectively. Selected geometric parameters are listed in tables 6.9 and 6.10 for (49) and (50) respectively. Figures 6.2 and 6.3 give a plot of one molecule of (49) and (50) respectively, showing the atom numbering.

The structures were solved by direct methods using the SHELXTL package of computer programs⁷⁶. Neutral atom scattering factors were used⁷⁷ with corrections for real and imaginary anomalous dispersion⁷⁷. All structures were refined by full-matrix least-squares methods based on F^2 using SHELXL-93⁷⁸. This is a full-matrix least-squares refinement package that uses all data and refines on F^2 rather than the traditional F . The various parameters used in this refinement process are defined as follows:

$$R_1 = \sum |F_o - F_c| / \sum F_o$$

$$wR_2 = \{ \sum [w(F_o^2 - F_c^2)^2] / \sum [w(F_o^2)^2] \}^{1/2}$$

where $w = 1/[s^2(F_o) + (aP)^2 + bP]$ and a and b are variable parameters whose optimal values are usually suggested by the program during the refinement process. The goodness-of-fit parameter (S) is based on F^2 and defined as:

$s = \{ \sum [w(F_o^2 - F_c^2)^2] / [n - p] \}^{1/2}$, where n is the number of reflections and p is the total number of parameters refined) and used all unique data. Non-hydrogen atoms were refined anisotropically while hydrogen atoms were located in difference Fourier syntheses and refined isotropically.

Table 6.6 Crystal and experimental data for (49) and (50).

Compound	49	50	Previous work
Formula	C ₈ H ₆ O ₆ Fe ₂ Te ₂	C ₈ H ₆ O ₆ Fe ₂ Se ₂	[Fe ₂ (μ-SeMe) ₂ (CO) ₆]
<i>M</i> _r	565.04	467.75	467.74
Cryst. sys.	Orthorhombic	Triclinic	Orthorhombic
Space grp.	Pnma	P1	PC2 _{1n}
<i>a</i> (Å)	21.008(2)	8.0842(12)	7.202(1)
<i>b</i> (Å)	10.9075(13)	12.1275(17)	10.544(1)
<i>c</i> (Å)	6.3888(9)	14.536(2)	18.344(3)
α(deg)	90	87.606(11)	
β(deg)	90	78.362(10)	
γ(deg)	90	81.151(10)	
<i>V</i> (Å ³)	1464.0	1379.1	1392.9(3)
<i>Z</i>	4	4	4
<i>D</i> _c (Mg m ⁻³)	2.944	2.253	2.23 (g cm ⁻³)
μ(MoK _α)(mm ⁻¹)	6.865	7.393	60.60 (cm ⁻¹)
Cryst.size(mm)	0.16 x 0.66 x 0.26	0.04 x 1.00 x 0.40	
Data range (θ)(deg)	2.69 to 27.49	2.60 to 25.0	
Rfls.measd.[<i>I</i> >σ(<i>I</i>)]	1773	3864	
Unique reflections	1773	3551	
<i>R</i> (int)	0.0000	0.0580	
Variables	97	342	
Δρ (max +ve)(eÅ ⁻³)	0.742	1.237	
Δρ (max -ve)(eÅ ⁻³)	-0.575	-0.820	
<i>R</i>	0.0290	0.0593	0.041
wR2a	0.0758	0.1568	0.067

$$a_w R^2 = [\sum w(F_o^2 - F_c^2)^2 / \sum w(F_o^2)^2]^{1/2}$$

$$b_w = 1/[\sigma^2(F_o^2) + (aP)^2 + bP] \text{ where } P = (F_o^2 + 2F_c^2)/3$$

Table 6.7 Atomic coordinates ($\times 10^4$) and equivalent isotropic displacement parameters ($\text{\AA}^2 \times 10^3$) for $\text{C}_8\text{H}_6\text{O}_6\text{Fe}_2\text{Te}_2$, (**49**). $U(\text{eq})$ is defined as one third of the trace of the orthogonalized U_{ij} tensor.

	x	y	z	$U(\text{eq})$
Te(1)	4710(1)	2500	1600(1)	41(1)
Te(2)	3215(1)	2500	207(1)	46(1)
Fe	3774(1)	1296(1)	3096(1)	36(1)
O(12)	4514(2)	732(4)	6850(6)	75(1)
O(11)	3927(2)	-1048(4)	890(7)	82(1)
O(13)	2576(2)	846(5)	5268(8)	90(2)
C(13)	3038(2)	1032(4)	4392(8)	53(1)
C(12)	4224(2)	971(4)	5382(7)	47(1)
C(11)	3872(2)	-131(4)	1714(8)	53(1)
C(2)	2203(3)	2500	798(19)	75(3)
C(1)	5468(3)	2500	3842(15)	64(2)

Table 6.8 Atomic coordinates ($\times 10^4$) and equivalent isotropic displacement parameters ($\text{\AA}^2 \times 10^3$) for $\text{C}_8\text{H}_6\text{O}_6\text{Fe}_2\text{Se}_2$, (**50**). $U(\text{eq})$ is defined as one third of the trace of the orthogonalized U_{ij} tensor.

	x	y	z	$U(\text{eq})$
Fe(11)	1181(2)	2293(1)	686(1)	45(1)
Fe(12)	3806(2)	1984(1)	1456(1)	49(1)
Fe(21)	-421(2)	7864(1)	3682(1)	48(1)
Fe(22)	-2045(2)	6239(1)	3606(1)	50(1)
Se(11)	1021(2)	2745(1)	2290(1)	52(1)
Se(12)	3087(2)	3631(1)	577(1)	49(1)
Se(21)	769(2)	5974(1)	3939(1)	55(1)
Se(22)	-2347(2)	7258(1)	5019(1)	58(1)
O(111)	-273(15)	231(9)	1218(10)	94(4)
O(112)	2687(14)	1517(10)	-1222(8)	85(3)
O(113)	-1958(13)	3704(10)	351(10)	92(4)
O(121)	6078(13)	2855(12)	2514(9)	95(4)
O(122)	6390(15)	957(9)	-85(9)	96(4)
O(123)	3533(15)	-189(9)	2361(10)	98(4)
O(211)	-2900(12)	9747(8)	3265(9)	84(3)
O(212)	1463(13)	7814(9)	1742(8)	82(3)
O(213)	1696(12)	9136(9)	4545(8)	78(3)
O(221)	-806(14)	5655(10)	1631(8)	84(3)
O(222)	-3292(15)	4155(9)	4286(10)	101(4)
O(223)	-5203(13)	7456(10)	3180(10)	90(4)
C(11)	-8(17)	1642(13)	3154(10)	66(4)
C(12)	4580(16)	3628(11)	-666(10)	62(3)
C(21)	2545(18)	5401(13)	2862(13)	79(5)
C(22)	-4449(18)	8316(15)	5258(13)	82(5)
C(111)	306(17)	1045(12)	1010(12)	69(4)
C(112)	2086(16)	1811(11)	-472(11)	60(3)
C(113)	-734(17)	3168(11)	467(11)	64(4)
C(121)	5207(16)	2495(13)	2129(11)	65(4)
C(122)	5379(18)	1374(11)	484(12)	65(4)
C(123)	3632(16)	650(12)	2016(11)	66(4)
C(211)	-1976(16)	9004(10)	3441(10)	57(3)
C(212)	752(16)	7844(10)	2505(11)	60(3)
C(213)	883(16)	8641(11)	4225(11)	63(4)
C(221)	-1273(17)	5869(12)	2398(11)	61(3)
C(222)	-2788(19)	4952(12)	4026(12)	72(4)
C(223)	-3971(17)	7000(11)	3350(10)	59(3)

Table 6.9 Selected bond lengths (Å) and angles (°) with e.s.d's in parentheses for
(49).

Compound 49				
Te(1)-C(1)	2.142(7)		Te(1)-Fe	2.5511(6)
Te(1)-Fe#1	2.5511(6)		Te(2)-C(2)	2.159(7)
Te(2)-Fe#1	2.5518(7)		Te(2)-Fe	2.5518(7)
Fe-C(12)	1.776(5)		Fe-C(13)	1.777(5)
Fe-C(11)	1.800(5)		Fe-Fe#1	2.6271(11)
O(12)-C(12)	1.149(5)		O(11)-C(11)	1.137(6)
O(13)-C(13)	1.139(6)			
C(1)-Te(1)-Fe	108.8(2)		C(1)-Te(1)-Fe#1	108.8(2)
Fe-Te(1)-Fe#1	61.98(3)		C(2)-Te(2)-Fe#1	109.1(3)
C(2)-Te(2)-Fe	109.1(3)		Fe#1-Te(2)-Fe	61.96(3)
C(12)-Fe-C(13)	92.7(2)		C(12)-Fe-C(11)	99.8(2)
C(13)-Fe-C(11)	100.8(2)		C(12)-Fe-Te(1)	90.0(2)
C(13)-Fe-Te(1)	158.2(2)		C(11)-Fe-Te(1)	100.0(2)
C(12)-Fe-Te(2)	160.53(14)		C(13)-Fe-Te(2)	91.1(2)
C(11)-Fe-Te(2)	98.2(2)		Te(1)-Fe-Te(2)	79.58(2)
C(12)-Fe-Fe#1	101.51(14)		C(13)-Fe-Fe#1	99.3(2)
C(11)-Fe-Fe#1	149.8(2)		Te(1)-Fe-Fe#1	59.010(13)
Te(2)-Fe-Fe#1	59.020(14)		O(13)-C(13)-Fe	178.0(5)
O(12)-C(12)-Fe	178.4(4)		O(11)-C(11)-Fe	178.1(5)

Symmetry transformations used to generate equivalent atoms:

#1 x, -y + 1/2, z

Table 6.10 Selected bond lengths (Å) and angles (°) with e.s.d's in parentheses for
(50).

Compound 50				
Fe(11)-C(111)	1.774(14)		Fe(11)-C(112)	1.778(16)
Fe(11)-C(113)	1.814(13)		Fe(11)-Se(12)	2.3836(19)
Fe(11)-Se(11)	2.391(2)		Fe(11)-Fe(12)	2.564(2)
Fe(12)-C(123)	1.793(4)		Fe(12)-C(122)	1.798(17)
Fe(12)-C(121)	1.827(14)		Fe(12)-Se(12)	2.385(2)
Fe(12)-Se(11)	2.396(2)		Fe(21)-C(212)	1.780(15)
Fe(21)-C(211)	1.793(13)		Fe(21)-C(213)	1.823(14)
Fe(21)-Se(21)	2.3912(19)		Fe(21)-Se(22)	2.399(2)
Fe(21)-Fe(22)	2.549(2)		Fe(22)-C(223)	1.783(14)
Fe(22)-C(221)	1.792(16)		Fe(22)-C(222)	1.797(14)
Fe(22)-Se(21)	2.391(2)		Fe(22)-Se(22)	2.392(2)
Se(11)-C(11)	1.959(12)		Se(12)-C(12)	1.959(14)
Se(21)-C(21)	1.968(15)		Se(22)-C(22)	1.945(14)
O(111)-C(111)	1.160(17)		O(112)-C(112)	1.148(17)
O(113)-C(113)	1.136(15)		O(121)-C(121)	1.129(16)
O(122)-C(122)	1.115(18)		O(123)-C(123)	1.122(18)
O(211)-C(211)	1.134(15)		O(212)-C(212)	1.140(17)
O(213)-C(213)	1.130(15)		O(221)-C(221)	1.130(17)
O(222)-C(222)	1.128(17)		O(223)-C(223)	1.130(15)
C(111)-Fe(11)-C(112)	92.3(7)		C(111)-Fe(11)-C(113)	98.5(6)
C(112)-Fe(11)-C(113)	99.8(7)		C(111)-Fe(11)-Se(12)	158.9(5)
C(112)-Fe(11)-Se(12)	92.3(4)		C(113)-Fe(11)-Se(12)	101.0(4)
C(111)-Fe(11)-Se(11)	92.0(6)		C(112)-Fe(11)-Se(11)	159.1(4)
C(113)-Fe(11)-Se(11)	99.8(5)		Se(12)-Fe(11)-Se(11)	76.80(6)
C(111)-Fe(11)-Fe(12)	101.4(5)		C(112)-Fe(11)-Fe(12)	101.4(4)
C(113)-Fe(11)-Fe(12)	150.2(5)		Se(12)-Fe(11)-Fe(12)	57.50(6)
Se(11)-Fe(11)-Fe(12)	57.71(6)		C(123)-Fe(12)-C(122)	92.0(6)
C(123)-Fe(12)-C(121)	99.6(7)		C(122)-Fe(12)-C(121)	99.6(6)
C(123)-Fe(12)-Se(12)	159.1(4)		C(122)-Fe(12)-Se(12)	92.6(4)
C(121)-Fe(12)-Se(12)	99.7(5)		C(123)-Fe(12)-Se(11)	91.4(4)
C(122)-Fe(12)-Se(11)	156.8(4)		C(121)-Fe(12)-Se(11)	102.5(5)
Se(12)-Fe(12)-Se(11)	76.68(7)		C(123)-Fe(12)-Fe(11)	101.6(4)
C(122)-Fe(12)-Fe(11)	99.4(4)		C(121)-Fe(12)-Fe(11)	150.9(5)
Se(12)-Fe(12)-Fe(11)	57.45(6)		Se(11)-Fe(12)-Fe(11)	57.53(6)
C(212)-Fe(21)-C(211)	92.7(6)		C(212)-Fe(21)-C(213)	99.2(7)
C(211)-Fe(21)-C(213)	98.8(6)		C(212)-Fe(21)-Se(21)	91.4(4)
C(211)-Fe(21)-Se(21)	157.8(4)		C(213)-Fe(21)-Se(21)	102.1(4)
C(212)-Fe(21)-Se(22)	156.8(4)		C(211)-Fe(21)-Se(22)	92.5(4)
C(213)-Fe(21)-Se(22)	102.2(5)		Se(21)-Fe(21)-Se(22)	75.68(7)
C(212)-Fe(21)-Fe(22)	99.1(4)		C(211)-Fe(21)-Fe(22)	100.0(4)
C(213)-Fe(21)-Fe(22)	153.0(5)		Se(21)-Fe(21)-Fe(22)	57.80(6)
Se(22)-Fe(21)-Fe(22)	57.73(6)		C(223)-Fe(22)-C(221)	91.6(6)
C(223)-Fe(22)-C(222)	99.8(6)		C(221)-Fe(22)-C(222)	98.3(7)
C(223)-Fe(22)-Se(21)	156.8(4)		C(221)-Fe(22)-Se(21)	92.8(4)
C(222)-Fe(22)-Se(21)	102.1(5)		C(223)-Fe(22)-Se(22)	91.9(5)
C(221)-Fe(22)-Se(22)	157.5(4)		C(222)-Fe(22)-Se(22)	103.0(6)

Table 6.10 Cont. Selected bond lengths (Å) and angles (°) with e.s.d's in parentheses
for **(50)**.

Se(21)-Fe(22)-Se(22)	75.81(7)		C(223)-Fe(22)-Fe(21)	99.0(4)
C(221)-Fe(22)-Fe(21)	99.5(4)		C(222)-Fe(22)-Fe(21)	153.6(5)
Se(21)-Fe(22)-Fe(21)	57.79(6)		Se(22)-Fe(22)-Fe(21)	57.99(7)
C(11)-Se(11)-Fe(11)	111.7(5)		C(11)-Se(11)-Fe(12)	111.4(5)
Fe(11)-Se(11)-Fe(12)	64.76(7)		C(12)-Se(12)-Fe(11)	111.6(4)
C(12)-Se(12)-Fe(12)	111.6(4)		Fe(11)-Se(12)-Fe(12)	65.06(6)
C(21)-Se(21)-Fe(21)	111.5(5)		C(21)-Se(21)-Fe(22)	113.1(5)
Fe(21)-Se(21)-Fe(22)	64.41(6)		C(22)-Se(22)-Fe(22)	112.1(6)
C(22)-Se(22)-Fe(21)	109.8(6)		Fe(22)-Se(22)-Fe(21)	64.27(7)
O(111)-C(111)-Fe(11)	179.6(17)		O(112)-C(112)-Fe(11)	178.7(12)
O(113)-C(113)-Fe(11)	178.1(13)		O(121)-C(121)-Fe(12)	176.5(14)
O(122)-C(122)-Fe(12)	176.2(13)		O(123)-C(123)-Fe(12)	179.5(17)
O(211)-C(211)-Fe(21)	176.9(12)		O(212)-C(212)-Fe(21)	177.7(14)
O(213)-C(213)-Fe(21)	178.6(14)		O(221)-C(221)-Fe(22)	178.6(13)
O(222)-C(222)-Fe(22)	178.3(15)		O(223)-C(223)-Fe(22)	178.1(12)

6.4.3.2 Crystallographic discussion for $[\text{Fe}_2(\mu\text{-TeMe})_2(\text{CO})_6]$, (49), and $[\text{Fe}_2(\mu\text{-SeMe})_2(\text{CO})_6]$, (50).

The original structural determination of (49)⁷⁴ was carried out at a temperature of -80°C, whereas the data collection for the present structure was carried out at room temperature. The crystal structures are virtually identical.

The original structural determination of (50)⁷⁵ was carried out on crystals grown by slow evaporation of a solution (50) in hexane / dichloromethane at -10°C. The crystals were orthorhombic with a space group of $\text{PC2}_1\text{n}$, whereas, by contrast those obtained from chloroform were actually triclinic with a space group of P1 .

Both crystal structures contain four molecules in the unit cell. The present crystal structure has similar bond lengths and angles to those of the previous structure, the only difference being the crystal system and space group for compound (50). This shows that compound (50) exhibits polymorphism.

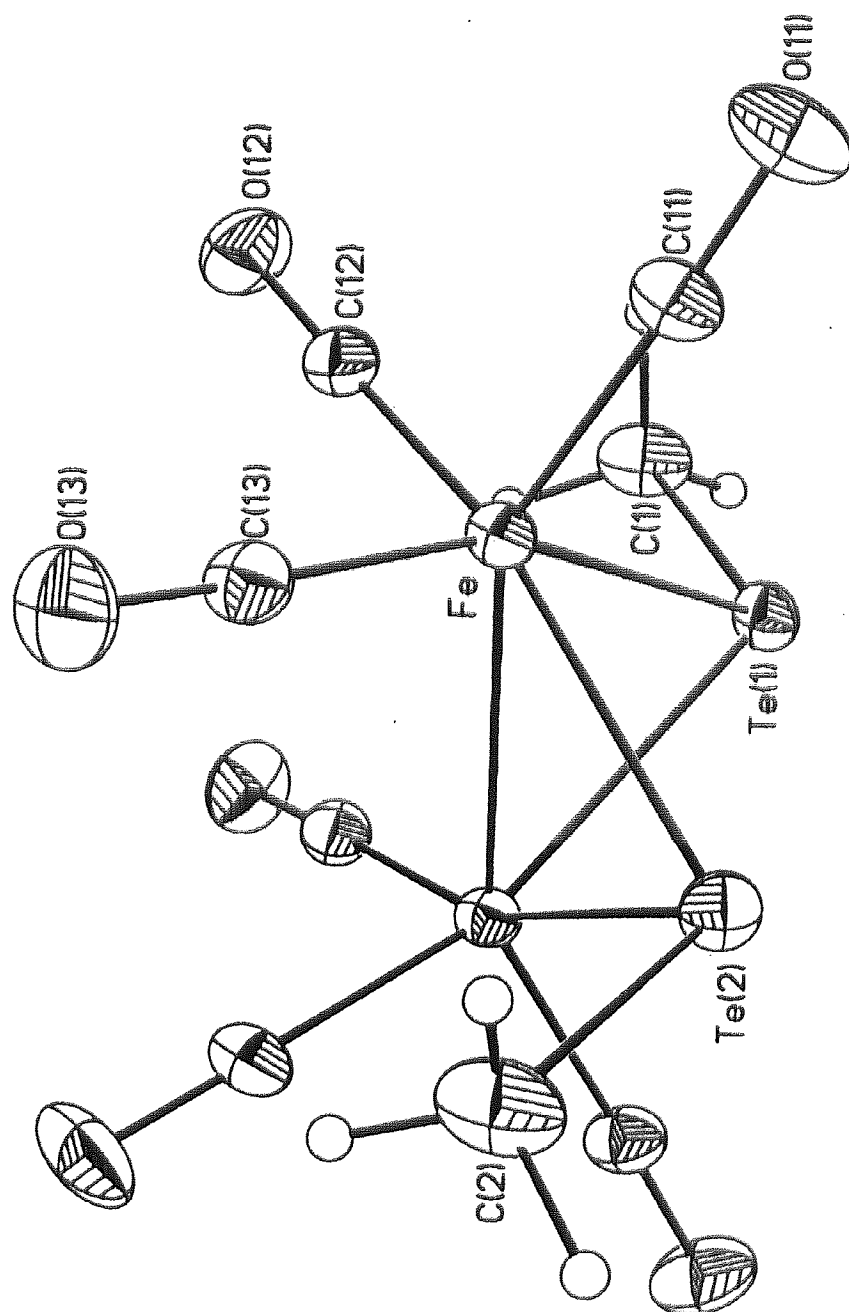


Figure 6.2 The molecular structure of $[\text{Fe}_2(\mu\text{-TeMe})_2(\text{CO})_6]$, (49).

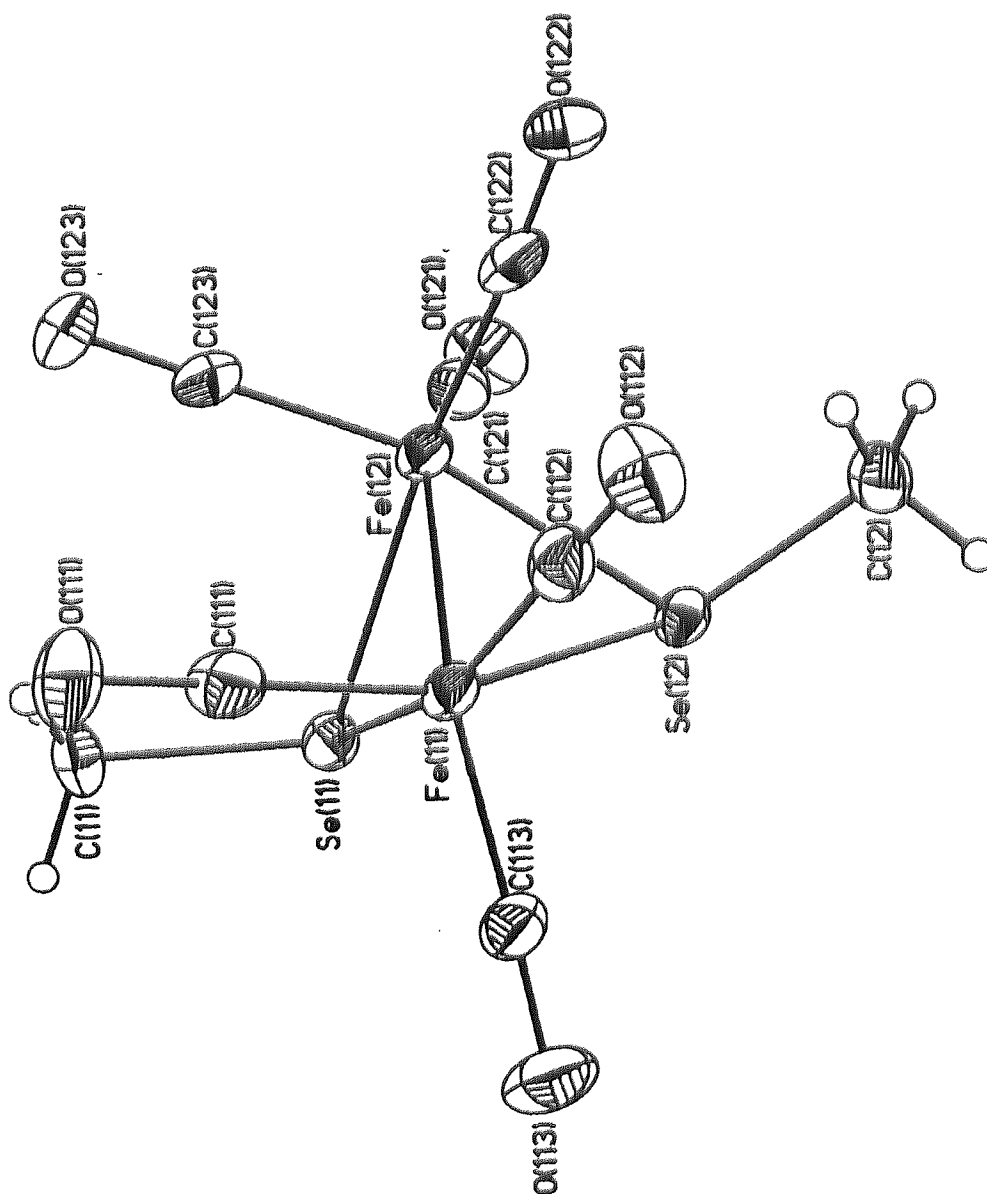
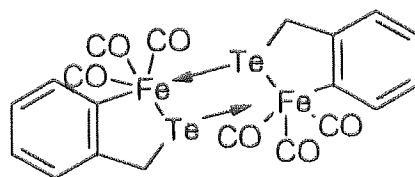


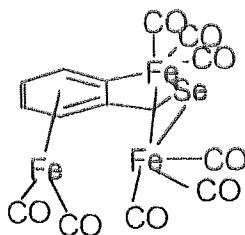
Figure 6.3 The molecular structure of $[\text{Fe}_2(\mu\text{-SeMe})_2(\text{CO})_6]$, (50).

6.5 ^{57}Fe Mössbauer spectroscopy of iron containing compounds

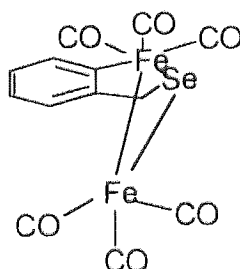
^{57}Fe Mössbauer spectra were determined on an ES-Technology MS105 constant acceleration spectrometer with a 925 MBq ^{57}Co source in a rhodium matrix. Spectra were recorded at 77 K and referenced against an iron foil (25 μm) at 298 K. Samples of compounds (33), (35), (36), (49) and (50) (see below) were prepared for measurement by grinding with boron nitride before transfer to the sample holder.



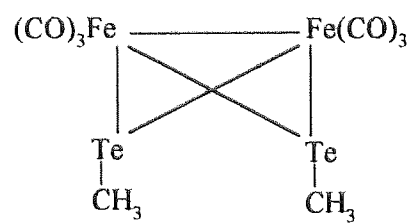
(33)



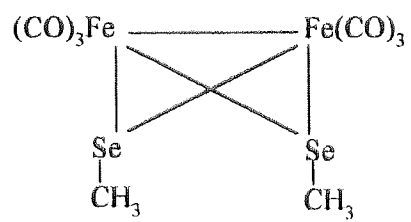
(35)



(36)



(49)



(50)

6.5.1 Results and discussion

The compounds considered in this thesis should give rise to two measurable parameters in their ^{57}Fe Mössbauer spectra: the chemical isomer shift (δ) and the quadrupole splitting (Δ). The chemical isomer shift varies with the s-electron density at the ^{57}Fe nucleus. Given that $\delta r/r$ is negative for ^{57}Fe , a more negative value for δ implies greater s-electron density at the nucleus. Given that the compounds considered here are all diamagnetic, the major contribution to Δ will be from non-cubic components of the ligand field.

The ^{57}Fe Mössbauer data are presented in table 6.11, the compounds being clearly identified. Table 6.12 gives the suggested assignments of the Mössbauer lines.

Table 6.11 Mössbauer spectra results for compounds (33), (35), (36), (49) and (50).

Compound	I.S.	Q.S.	HWHM	%
33	0.01	0.83	0.15	-
35	0.48	1.16(2)	0.23	35(3)
	0.49	0.71	0.19	37(3)
	0.04	0.96	0.22	27(2)
36	0.51(6)	0.76	0.31(8)	32(12)
	0.19(3)	1.10	0.29(4)	67(13)
49	0.06	0.85	0.12	-
50	0.09	1.02	0.16	-
50 (after decomp)	0.47(4)	1.12(22)	0.23(10)	34(3)
	0.47(2)	0.66(13)	0.21(6)	47(3)
	0.06(3)	1.03(4)	0.13(5)	17(1)

Mössbauer analysis was carried out on a decomposed sample of compound (50) [see table 6.12]. On comparing the isomer shift of compound (50) and decomposed (50), one may suggest that there are three inequivalent irons in the decomposed sample. However the isomer shift corresponding to compound (50) in the decomposed sample is 0.06(3).

Units = mms^{-1}

Errors [$\pm 0.01 \text{ mm}^{-1}$] unless shown otherwise in parentheses.

I.S. = isomer shift; Q.S. = quadrupole splitting; HWHM = half width at half maximum.

Comparison of the data for (33), (35) and (36) clearly indicates that the three possible ^{57}Fe environments are characterised by distinctive chemical isomer shifts (see table 6.13).

	δ (mms $^{-1}$)
Fe in ring	0.01 – 0.19
“Fe(CO) $_3$ ” unit	0.49 – 0.51 (Δ , 0.71 – 0.76)
“Fe(CO) $_2$ ” unit	0.48 (Δ , 1.16)

The similar chemical isomer shifts for the extra-ring “Fe(CO) $_3$ ” and “Fe(CO) $_2$ ” units are not unexpected but the lower symmetry of the “Fe(CO) $_2$ ” environment is reflected in the greater quadrupole splitting. The data suggest that ^{57}Fe Mössbauer spectroscopy will prove a convenient means to identify iron environments in related molecules. The shifts are quite similar, but the difference between compound (33) and (36) (0.01 of 0.19 mms $^{-1}$) is significant. Given that Mössbauer parameters are not too sensitive to other than the nearest neighbour effects, the differences observed may indicate stronger back-bonding from the ring iron to the three attached carbonyl-groups in (33) than (36). This may be induced by the weak co-ordinate interaction with tellurium in (33). There is further evidence observed in the FTIR spectra of (33) and (36), where on comparison of the carbonyl regions one observes that compound (33) [2049, 1980 and 1953 cm $^{-1}$] has lower frequency absorptions than (36) [2062, 2021 and 1962 cm $^{-1}$] which therefore suggests stronger π bonding between the iron within the ring and the carbonyl groups in (33). The other data are so similar with respect to experimental errors that speculation is not justified.

The spectra of (49) and (50) are unremarkable and, as expected, show a single iron site (in the pure materials). The difference in the δ between the selenium and tellurium derivatives is within the experimental error, as are the values of Δ .

It was decided to examine the ^1H and ^{13}C NMR spectra of (33), (35) and (36) more closely to ascertain whether these data reflected any measurable differences.

The data given in tables 6.13 and 6.14 are the ^1H and ^{13}C resonances for the CH_2 group for compounds (33) to (36); ^1H and ^{13}C resonances for the CH_3 group in compounds (49) and (50).

Table 6.12 Assignment of the Mössbauer peaks.

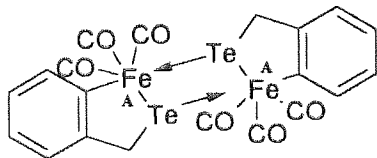
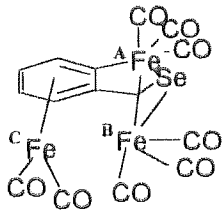
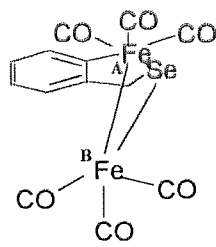
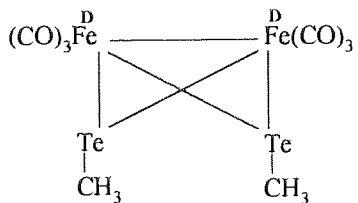
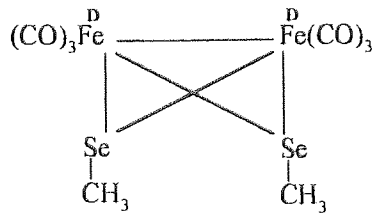
Compound	Isomer Shift
<p>(33)</p> 	<p>A = 0.01</p>
<p>(35)</p> 	<p>A = 0.04 B = 0.49 C = 0.48</p>
<p>(36)</p> 	<p>A = 0.19(3) B = 0.51(6)</p>
<p>(49)</p> 	<p>D = 0.06</p>
<p>(50)</p> 	<p>D = 0.09</p>

Table 6.13 ^1H NMR region of CH_2 group in the heterocyclic ring for products (33), (35) and (36); ^1H NMR region of CH_3 group in products (49) and (50).

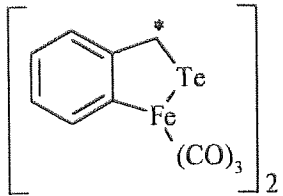
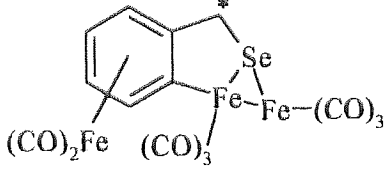
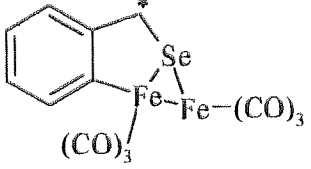
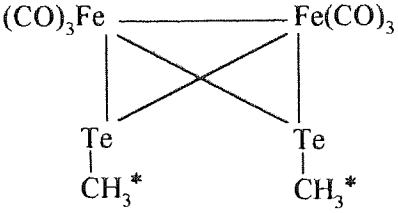
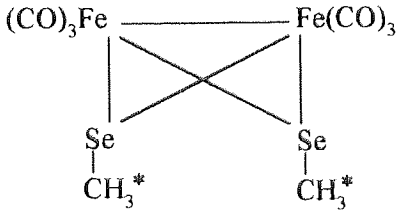
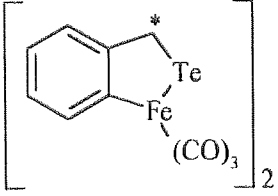
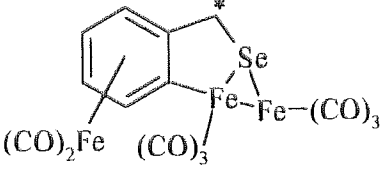
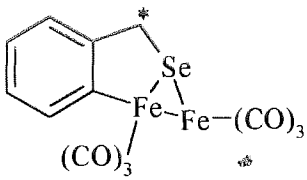
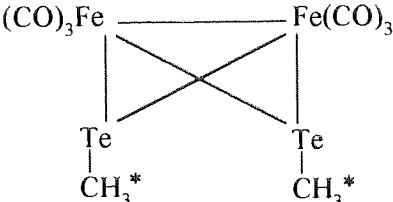
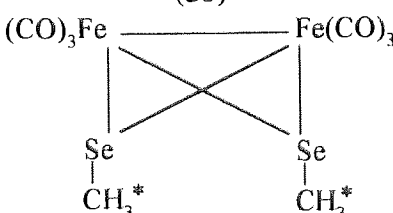
Compound	^1H (CDCl_3) δ , ppm
<p>(33)</p> 	4.15
<p>(35)</p> 	2.15
<p>(36)</p> 	3.78
<p>(49)</p> 	2.06
<p>(50)</p> 	2.08

Table 6.14 ^{13}C NMR region of CH_2 and CO groups in the heterocyclic ring for products (33), (35) and (36); ^{13}C NMR region of CH_3 and CO groups in products (49) and (50).

Compound	^{13}C (CDCl_3) δ , ppm	
	CH_2 or CH_3 , (*)	CO
<p>(33)</p> 	15.6	202.3 205.3 209.4
<p>(35)</p> 	34.7	213.0 212.0 211.2 209.5
<p>(36)</p> 	35.5	209.5
<p>(49)</p> 	-17.2 -13.2*	211.07 211.39*
<p>(50)</p> 	7.95 9.80*	209.5 210.18*

* = Spectrum contained decomposition products

On comparing the methylene protons in compounds (33) and (36), one may suggest that the protons in compound (33) are deshielded, giving rise to a resonance at 4.15ppm. One possible explanation for the deshielding of the protons is that the tellurium atom in compound (33) acts as a Lewis base, which gives rise to a more positive tellurium atom, therefore pulling the electrons away from the methylene group. The methylene protons for compound (36) [3.78ppm] are shielded when compared with compound (33); this may reflect the fact that the selenium atom is not acting as a Lewis base, unlike the tellurium atom.

However on considering the ^{13}C NMR spectra of (33) and (36) the opposite trend is observed. Thus the methylene carbon is shielded in compound (33) giving a resonance of 15.6ppm when compared with the deshielded carbon in compound (36) [34.7ppm]. This may be explained by the differences in electronegativity between the tellurium and selenium atoms where the selenium is more electronegative than tellurium therefore giving a resonance more downfield. One may suggest that this factor outweighs the Lewis base behaviour of tellurium, with respect to the ^{13}C NMR spectrum.

However unlike the Mössbauer and FTIR spectra where the analysed samples are examined as solids, the NMR spectra of the samples are measured for solutions. The dynamic behaviour of (36) has been shown (see chapter three). Therefore given this fact it may be invalid to make simple comparisons between the room temperature NMR data for (33) and (36). This point is illustrated by the fact that the ^1H resonances show an opposite trend to the ^{13}C resonances.

6.5 Conclusion

It is unfortunate that the 2,1,3-benzoselenadiazole, 1,2,5-selenadiazolo[3,4-b]pyridine and 2-phenyl-1,2-benzisoselenazol-3(2H)-one do not react with triiron dodecacarbonyl under the conditions employed.

The reaction of $[\text{Fe}_3(\text{CO})_{12}]$ with 2-methylbenzselenazole gives an insertion product, $[\text{Fe}_2\{\text{C}_6\text{H}_4(\text{NCH}_2\text{CH}_3)\text{Se}\}(\text{CO})_6]$ (**48**). The origin of this product still requires further investigation (see section 6.3.1). Once again the reaction of selenium analogues with $[\text{Fe}_3(\text{CO})_{12}]$ gave products that can be considered as intermediate compounds when compared with the tellurium reaction products.

Reactions of triiron dodecacarbonyl with the intramolecular stabilized organoselenium and organotellurium compounds have failed to produce any products under the conditions employed.

From the reactions of 2-(methyltelluro)benzanilide, 2-(methylseleno)benzanilide with $[\text{Fe}_3(\text{CO})_{12}]$ the products $[\text{Fe}_2(\mu\text{-TeMe})_2(\text{CO})_6]$, (**49**), and $[\text{Fe}_2(\mu\text{-SeMe})_2(\text{CO})_6]$, (**50**), were obtained. The analytical data for (**49**) and (**50**) were in good agreement with the literature values^{74,75}. Less vigorous conditions were employed for the formation of the compounds, compared to the literature methods^{74,75}. It is apparent that the starting materials (2-(methyltelluro)benzanilide and 2-(methylseleno)benzanilide) are a good source of E-Me (where E = tellurium or selenium). A new polymorph of (**50**) was characterised.

⁵⁷Fe Mössbauer spectra “fingerprint” the possible iron environments in this series of compounds. The technique could be valuable analytically in the study of similar materials.

REFERENCES

-
- ¹ H.D. Kaesz, R.B. King, T.A. Manuel, L.D. Nichols and F.G.A. Stone. Chemistry of the metal carbonyls. V. The desulfurization of thiophene. *J. Am. Chem. Soc.*, (1960), **132**, 4749-4750.
- ² A.E. Ogilvy, M. Draganjac, T.B. Rauchfuss and S.R. Wilson. Activation and desulfurization of thiophene and benzothiophene by iron carbonyls. *Organometallics* (1988), **7**, 1171-1177.
- ³ K. Singh, W.R. McWhinnie, H.L. Chen, M. Sun and T.A. Hamor. Reactions of heterocyclic organotellurium compounds with triiron dodecacarbonyl: reactions of thiophenes revisited. *J. Chem. Soc., Dalton Trans.*, (1996), 1545-1549.
- ⁴ F. Fringuelli and A. Taticchi. Tellurophene and some of its derivatives. *J. Chem. Soc., Perkin I*, (1972), 199-203.
- ⁵ F. Fringuelli, G. Marino, G. Savelli and A. Taticchi. The aromatic reactivity of tellurophene. *J. Chem. Soc., Chem. Comm.*, (1971), 1441.
- ⁶ F. Fringuelli, G. Marino and A. Marino, A comparative study of the aromatic character of furan, thiophene, selenophene and tellurophene. *J. Chem. Soc., Perkin Trans. II*, (1974), 332-337.
- ⁷ J.A Kerr. Chemical Rubber Company Handbook of chemistry and physics, D.R Lide, (ed.), CRC Press, Boca Raton, Floride, USA, 77th edition, (1996).
- ⁸ A.J. Arce, R. Machado, C. Rivas and Y. De Sanctis. Extrusion of selenium and tellurium atoms from selenophene and tellurophene by reaction with trinuclear iron, ruthenium, and osmium clusters: crystal structures of $[\text{Os}_6(\mu\text{-H})(\mu_3\text{-Se})(\mu_4\text{-$

$\text{C}_4\text{H}_3)(\text{CO})_{20}]$ and of $[\text{Ru}_4(\mu_3\text{-Se})\mu\text{-C}_4\text{H}_4)(\text{CO})_{11}]$. *J. Organomet. Chem.*, (1991), **419**, 63-75.

⁹ K. Oefele and E. Dotzauer. $\text{Kbergangsmetall-Komplexe des tellurophens}$. *J. Organomet. Chem.*, (1972), **42**, C87-C90.

¹⁰ A.J. Arce, A. Karam, Y. De Sanctis, R. Machado, M.V. Capparelli and J. Manzur. Ring opening and extrusion of tellurium atoms in the reaction of benzo[b]tellurophene with trinuclear iron, ruthenium and osmium clusters: X-ray crystal structures of $[\text{Os}_3(\mu\text{-C}_8\text{H}_6\text{Te})(\text{CO})_{10}]$, $[\text{Os}_4(\mu\text{-C}_8\text{H}_4)(\mu^3\text{-Te})(\text{CO})_{11}]$, $[\text{Ru}_2(\mu\text{-C}_8\text{H}_6\text{Te})(\text{CO})_6]$, $[\text{Ru}_4(\mu^3\text{-Te})(\mu\text{-C}_8\text{H}_6)(\text{CO})_{11}]$ and $[\text{Fe}_2(\mu\text{-C}_8\text{H}_6\text{Te})(\text{CO})_6]$. *Inorganica Chimica Acta*, (1997), **254**, 119-130.

¹¹ K. Badyal, W.R. McWhinnie, T.A. Hamor and H. Chen. Reaction of $\text{Fe}_3(\text{CO})_{12}$ with tellurium – nitrogen heterocycles: A source of novel organoiron compounds. *Organometallics*, (1997), **16**, 3194-3198.

¹² R.C. Pettersen, K.H. Pannell and A.J. Mayr. $\mu\text{-}\{1\text{-}2\text{-}\eta\text{-}[\text{Hydroseleno-1-cyclohexene-1-carbaldehydato(2-)}]\text{-}\mu\text{-Se}\}$ bis(tricarbonyliron)(Fe-Fe). *Acta Cryst.* (1980), **B36**, 2434-2436.

¹³ G.T. Morgan and F.H. Burstall. Cyclotellurobutane. *J. Chem. Soc.*, (1931), 180-184.

¹⁴ K. Akashi, Y. Hayashi, T. Arakawa, T. Kimura and H. Kobayashi. Photothermographic photosensitive materials. Japanese Patent 53/143216, Asahi Chemical Industry, (1978); *Chem. Abstr.*, (1979), **90**, 195607s.

¹⁵ Y. Hayashi, T. Arakawa, T. Shiga, M. Ozaki and H. Kobayashi. Organic tellurium-silver complexes. Japanese Patent 53/65, 827, Asahi Chemical Industry, (1978); *Chem. Abstr.*, (1978), **89**, 146588g.

-
- ¹⁶ W.R. McWhinnie, I.D. Sadekov and V.I. Minkin. Structural and chemical consequences of *intra*-molecular N(O)→Te co-ordination in organotellurium compounds. *Sulfur Reports*, (1995), **18**, 295-335.
- ¹⁷ Z. Majeed, W.R. McWhinnie and T.A. Hamor. Observations on the synthesis and chemistry of a complete series of phenylazophenyl(C,N')tellurium(II) halides (fluoride, chloride, bromide and iodide). *J. Organomet. Chem.*, (1997), **549**, 257-262.
- ¹⁸ R.E. Cobbledick, F.W.B. Einstein, W.R. McWhinnie and F.H. Musa. Some new organotellurium compounds derived from azobenzene: The crystal and molecular structure of (2-phenylazophenyl-C,N')tellurium(II) chloride. *J. Chem. Res. (S)*, (1979) 145; *J. Chem. Res. (M)*, (1979), 1901-1909.
- ¹⁹ Z. Majeed. New aspects in organotellurium halide chemistry. M.Phil. Thesis, Aston University, Aston Triangle, Birmingham, B4 7ET. (1996).
- ²⁰ K. Badyal, W.R. McWhinnie, H.L. Chen and T.A. Hamor. Heterocyclic organotellurium compounds as precursors for new organometallic derivatives of rhodium. *J. Chem. Soc. Dalton Trans.*, (1997), 1579-1585.
- ²¹ T. B. Rauchfuss. Thiophene desulfurization of organometallic compounds. Abstracts of papers of the American Chemistry, (1991), **201**, 37.
- ²² R.J. Angelici. Structural aspects of thiophene in transition-metal complexes. *Coord Chem. Rev.*, (1990), **105**, 61-67.
- ²³ L. Engman and M. P. Cava. Organotellurium chemistry. 4. Synthesis and reactions of tellurophthalide. The first alkyltellurenyl halides. *J. Org. Chem.*, (1981), **46**, 4194-4197.
- ²⁴ J. Bergman and L. Engman. Preparation of seleno- and telluro phthalic anhydride. *Organic preparations and procedures int.*, (1978), **10(6)**, 289-306.

-
- ²⁵ C.J. Belke, S.C.K. Su and J.A. Shafer. Imidazole – Catalyzed displacement of an amine from an amide by neighboring hydroxyl group. A model for the acylation of chymotrypsin. *J. Am. Chem. Soc.*, (1971), **93**, 4552-4560.
- ²⁶ W. H. H. Gunther. Methods in selenium chemistry. II. Bis(methoxymagnesium)diselenium, a novel reagent for the introduction of selenium into organic molecules. *J. Org. Chem.*, (1967), **32**, 3929-3931.
- ²⁷ The Aldrich library of ¹³C and ¹H FTNMR spectra. Edition I, volume II, 1306, c, (1993).
- ²⁸ A. Klose, E. Solari, C. Floriani, N. Re, A. Chiesivila and C. Rizzoli. Iron-carbene functionalities supported by a macrocyclic ligand: iron-carbon double bond stabilized by tetramethyldibenzotetraazaannulene. *Chem. Commun.*, (1997), **23**, 2297-2298.
- ²⁹ TEXSAN, Single Crystal Structure Analysis Software, version 1.6, Molecular Structure Corporation, Houston, TX, (1993).
- ³⁰ G.M. Sheldrick. SHELXL-93, Program for Crystal Structure Refinement, University of Göttingen, (1993).
- ³¹ C.K. Johnson. ORTEP, Report ORNL-5138, Oak Ridge National Laboratory, Oak Ridge, TN, (1976).
- ³² A) P. Mathur, D. Chakrabarty, M.M. Hossain, R.S. Rashid, V. Rugmini and A.L. Rheingold. Synthesis and characterization of the new mixed-metal cluster complexes [Fe₂M(μ₃-E)₂(CO)₁₀](M = W, E = Se, Te; M = Mo, E = Se). Crystal structure of [Fe₂W(μ₃-Te)₂(CO)₁₀]. *Inorg. Chem.*, (1992), **31**, 1106-1108.
- ³² B) G. Gervasio. Crystal and molecular structure of bis(μ₃-tellurido)-decacarbonyltriiron, [Fe₃(CO)₁₀Te₂]. *J. Organomet. Chem.*, (1992), **441**, 271-276.
- ³² C) L.C. Roof, D.M. Smith, G.W. Drake, W.T. Pennington and J.W. Kolis. Synthesis and reactivity of [Fe₃(CO)₉Te]⁻². *Inorg. Chem.*, (1995), **34**, 337-345.

- ³² D) J.R. Eveland and K.H. Whitmire. Synthesis and characterization of the novel iron carbonyl tellurium chloride cluster $[\text{Fe}_2(\text{CO})_6(\mu\text{-Cl})(\mu\text{-TeCl})_2][\eta^2, \mu_2, \mu_2\text{-TeCl}_{10}]$, and its decomposition to the zintl ion complex $[\text{Fe}_2(\text{CO})_6(\eta^2, \mu_2, \mu_2\text{-Te}_4)(\mu\text{-TeCl}_2)]$. *Angew. Chem., Int. Ed. Engl.*, (1996), **35**, 741-743.
- ³³ F.H. Allen, O. Kennard, D.G. Watson, L. Brammer, A.G. Orpen and R. Taylor. Tables of bond lengths determined by X-ray and neutron diffraction. Part 1. Bond lengths in organic compounds. *J. Chem. Soc., Perkin Trans. I*, (1987), 1-19.
- ³⁴ A) K.Y. Abid, N.I. Al-Salim, M. Greaves, W.R. McWhinnie, A.A. West and T.A. Hamor. Synthesis and reactions of 1,6-bis(2-butyltellurophenyl)-2,5-diazahexa-1,5-diene and related compounds. The crystal and molecular structures of 2-(butyldichlorotelluro)benzaldehyde and bis[hydroxyiminomethyl]phenyl] ditelluride. *J. Chem. Soc., Dalton Trans.*, (1989), 1697-1703.
- ³⁴ B) H.B. Singh, N. Sudha, A.A. West and T.A. Hamor. Orthotellurated derivatives of N,N-dimethylbenzylamine: Crystal and molecular structures of [2-(dimethylaminomethyl)phenyl]tellurium(IV) tribromide and [2-(butyldichlorotelluro)benzyl]dimethylammonium chloride. *J. Chem. Soc., Dalton Trans.*, (1990), 907-913.
- ³⁵ R.B. Bates and R.S. Cutler. Phthalic anhydride. *Acta Crystallogr., Sect. B*, (1977), **33**, 893-895.
- ³⁶ M.G. Choi and R.J. Angelici. Synthesis, reactivity, and ^{77}Se NMR studies of the η^2 - and $\eta^1(\text{Se})$ -selenophene complexes $\text{Cp}'(\text{CO})_2\text{Re}(\text{Sel})$. *J. Am. Chem. Soc.*, (1991), **113**, 5651-5657.
- ³⁷ N.S. Nametkin, V.D. Tyurin, A.I. Nekhaev, Yu.P. Sobolev, M.G. Kondrateva, A.S. Batsanov and Yu.T. Struchkov. Iron carbonyl complexes containing an azomethyne

-
- moiety. I. Synthesis and X-ray structure of a novel σ,π -arene-bridged complex, μ -(σ - $\text{C}_6\text{H}_4\text{CH}_2\text{NC}_6\text{H}_5$) $\text{Fe}_3(\text{CO})_8$. *J. Organomet. Chem.*, (1983), **243**, 323-330.
- ³⁸ J. Chen, J. Yin, Z. Fan and W. Xu. Studies on olefin-co-ordinating transition metal carbene complexes. Part 12. Novel synthesis and structural characterization of (η^6 -arene)dicarbonyliron complexes, and their oxidation products. *J. Chem. Soc., Dalton Trans.*, (1988), 2803-2808.
- ³⁹ N.B. Pahor and M. Calligaris. Crystal and molecular structure of thiophthalic anhydride. *Acta Crystallogr. Sect. B*: (1975), **31**, 2685-2686.
- ⁴⁰ R.B. Bates and R.S. Cutler. Phthalic anhydride. *Acta Crystallogr. Sect. B*: (1977), **33**, 893.
- ⁴¹ N.N. Magdesieva and V.A. Vdovin. Synthesis of 1,3-Dihydrobenzo[c]selenophene. *Khim Geterotsiki Soedin*, (1972), **8**, 22-23.
- ⁴² E.H. Mørkved, G. Faccin, D. Manfrotto, H. Kjøsen, J.Y. Becker, L. Shapiro, A. Ellern, J. Bernstein and V. Khodorkovsky. Synthesis and properties of novel compounds for organic metals: dihydrotellurophene derivatives. *J. Mater. Chem.*, (1997), **7(9)**, 1697-1700.
- ⁴³ A) J.D. McCullough, T.W. Campbell and E.S. Gould. A new synthesis of dibenzoselenophene. *J. Chem. Soc.*, (1950), 5753-5754.
- ⁴³ B) S. Murata and T. Suzuki. Syntheses of dibenzo[c,e][1,2]diselenin and related novel chalcogenide heterocyclic compounds. *J. Heterocyclic Chem.*, (1991), **28**, 433-438.
- ⁴⁴ H.D.K. Drew. LXVI. Cyclic organo-metallic compounds. Part V. Phenoxselenine and phenoxthionine from phenoxtellurine. Selenylium and thionylium compounds. *J. Chem. Soc.*, (1926), 511-524.

- ⁴⁵ H.B. Singh, P.K. Khanna and S.K. Kumar. Charge transfer complexes: synthesis of 3,5-naphtho-1-telluracyclohexane, a new electron donor. *J. Organomet. Chem.* (1988), **338**, 1-7.
- ⁴⁶ T. A. Hamor, H.L. Chen, W. R. McWhinnie, S. L. W. McWhinnie and Z. Majeed. The crystal and molecular structures of 2-(2-pyridyl)phenyltellurium(II) chloride and of two modifications of 2-(2-pyridyl)phenyltellurium(II) iodide; chemical investigations of organotellurium iodides. *J. Organomet. Chem.*, (1996), **523**, 53-61.
- ⁴⁷ T.A. Hamor, A.G. Maslakov and W.R. McWhinnie. 1-iodo-2-p-tolyl-1-tellura-2-azaindene. *Acta Crystallogr. Sect. C.*, (1995), **51**, 2062-2064.
- ⁴⁸ R.H. Jones and T.A. Hamor. The crystal structures of 1-allyl-1-bromo-3,4-benzo-1-telluracyclopentane $[C_8H_8Te(C_3H_5)Br]$, 1-phenacyl-1-bromo-3,4-benzo-1-telluracyclopentane $[C_8H_8Te(C_6H_7O)Br]$ and 1-deuteromethyl-1-iodo-3,4-benzo-1-telluracyclopentane $[C_8H_8Te(CD_3)I]$; the trans effect in organotellurium bromides and iodides. *J. Organomet. Chem.*, (1982), **234**, 299-308.
- ⁴⁹ N.W. Alcock. Secondary bonding to nonmetallic elements. *Adv. Inorg. Chem. Radiochem.*, (1972), **15**, 1.
- ⁵⁰ A.G. Maslakov, E. Gresham, T.A. Hamor, W.R. McWhinnie, M.C. Perry, N. Shaikh. Bis-(8-oxo quinoline)diorgano tellurium(IV) compounds; structural and spectroscopic studies. *J. Organomet. Chem.*, (1994), **480**, 261-266.
- ⁵¹ A. Bondi. Van der Waals volumes and radii. *J. Phys. Chem.*, (1964), **68**, 441-451.
- ⁵² H.B. Singh, W.R. McWhinnie, T.A. Hamor, R.H. Jones. Synthesis and chemistry of 1,3-dihydrotellurolo[3,4-b]quinoxaline and derivatives: Crystal and molecular structure of 1,3-dihydro-2,2-diiodo-2 λ^4 -tellurolo[3,4-b]quinoxaline-2,3-bis(iodo methyl)quinoxaline (1:1). *J. Chem. Soc. Dalton Trans.*, (1984), 23-28.

-
- ⁵³ Cambridge Structural Database, Cambridge Crystallographic Data Centre, Cambridge, April, (1998).
- ⁵⁴ C. Knobler, R.F. Ziolo. Organotellurium diiodides. The molecular structure of the modification of 1,1-diiodo-3,4-benzo-1-telluracyclopentane, $C_8H_8TeI_2$. J. Organomet. Chem., (1979), **178**, 423-431.
- ⁵⁵ J.D. McCullough, C. Knobler, R.F. Ziolo. Crystal and molecular structure of the β modification of 1,1-diiodo-3,4-benzo-1-telluracyclopentane, β - $C_8H_8TeI_2$. Comparative study of secondary bonding systems and colors in organotellurium iodides. Inorg. Chem., (1985), **24**, 1814-1818.
- ⁵⁶ P.V. Rloing, D.D. Kirt, J.L. Dill, S. Hall and C. Hollstrom. Direct *ortho*-mercuration reactions of azobenzene and *ortho*-substituted azobenzene. J. Organometal. Chem., (1976), **116**, 39-53.
- ⁵⁷ L. Engman and A. Hallberg. Expedient synthesis of ebselen and related compounds. J. Org. Chem., (1989), **54**, 2964-2966.
- ⁵⁸ M.A.K. Ahmed, A.E. McCarthy, W.R. McWhinnie and F.J. Berry. Organyltellurium-(IV) and -(II) dithiocarbamates: Crystal and molecular structure of dimethyldithiocarbamato(2-phenylazophenyl-C,N')tellurium(II). J. Chem. Soc. Dalton Trans., (1986), 771-775.
- ⁵⁹ C. Lau, J. Passmore, E. K. Richardson, T. K. Whidden and P. S. White. The preparation of bis(perfluoroethyl) tellurium difluoride and dichloride, *trans* perfluoroethyl tellurium monochloride, *trans* bis(perfluoroethyl) tellurium tetrafluoride; and the preparation and X-ray crystal structure of perfluoroethyl tellurium trifluoride. Can. J. Chem., (1985), **63**, 2273-2280.

-
- ⁶⁰ N.P. Luthra, R.B. Dunlap and J.D. Odom. The use of dimethylselenide as a chemical-shift reference in Se-77 NMR spectroscopy. *J. Magn. Reson.*, (1982), **46**, 152.
- ⁶¹ N.S. Dance, W.R. McWhinnie, J. Mallaki and Z. Monsef-Mirzai. Solution studies of triorganotelluronium salts. *J. Organomet. Chem.*, (1980), **198**, 131-143.
- ⁶² J. W. Lauher. CHARON, *A Graphics Program for Postscript Printers*, The Research Foundation of the State of New York, (1989).
- ⁶³ M.R. Greaves, T.A. Hamor, B.J. Howlin, T.S. Lobana, S.A. Mbogo, W.R. McWhinnie and D.C. Povey. The crystal structures of 2-(2'-pyridyl)phenyltellurium(II) bromide and of the inclusion compound bis[2-(2'-pyridyl)phenyltellurium(II) chloride]-p-ethoxyphenyl-mercury(II) chloride. *J. Organomet. Chem.*, (1991), **420**, 327-335.
- ⁶⁴ H.B. Singh, N. Sudha, A.A. West and T.A. Hamor. Orthotellurated derivatives of N,N-dimethylbenzylamine: Crystal and molecular structures of [2-(dimethylaminomethyl)phenyl]tellurium(IV) tribromide and [2-(butylchlorotelluro)benzyl]dimethylammonium chloride. *J. Chem. Soc. Dalton Trans.*, (1990), 907-913.
- ⁶⁵ O. Vikone. The structures of two crystalline forms of bromo-(ethylenethiourea)phenyltellurium(II). *Acta. Chem. Scand.*, (1975), **A29**, 738-744.
- ⁶⁶ G. M. Sheldrick. Phase annealing in SHELX-90: Direct methods for larger structures. *Acta Crystallographer*, (1990), **A46**, 467-473.
- ⁶⁷ P. G. Jones and M. C. Ramires de Arellane. A T-shaped selenenyl halide: Synthesis and characterisation of a proposed reaction intermediate. *Chem. Ber.*, (1995), **128**, 741-742.

-
- ⁶⁸ W. du Mont, S. Kubiniok, K. Peters and H. Von Schnering. Synthesis and structure of a stable iodoselenide. *Angew. Chem. Int. Ed. Engl.*, (1987), **26**, 780-781.
- ⁶⁹ A.F. Wells. *Structural inorganic chemistry*, 5th Ed., Clarendon Press, Oxford (1984), 289.
- ⁷⁰ A) C.W. Bird, G.W.H Cheeseman and A.A. Sarsfield. 2,1,3-Benzoselenadiazoles as intermediates in σ -phenylenediamine synthesis. *J. Chem. Soc. Pt 4*, (1963), 4767-4770.
- ⁷⁰ B) C.W. Bird and G.W.H Cheeseman. The infrared spectra and structure of 2,3,1-benzoselenadiazoles. *Tetrahedron*, (1964), **20**, 1701-1705.
- ⁷¹ N.M.D. Brown and P. Bladon. Synthesis and spectroscopy of 1,2,5-selenadiazolo-[3,4-b]-pyridine and 1,2,5-selenadiazolo-[3,4-c]-pyridine. *Tetrahedron* (1968), **24**, 6577-6585.
- ⁷² K. Badyal. The use of organotellurium heterocycles as precursors for novel organometallic compounds. Ph.D Thesis, Aston University, (1996).
- ⁷³ A. Klose, E. Solari, C. Floriani, N. Re, A. Chiesivila and C. Rizzoli. Iron-carbene functionalities supported by macrocyclic ligand: iron-carbon double bond stabilized by tetramethyldibenzotetraazaannulene. *Chem. Commun.*, (1997), 2297-2298.
- ⁷⁴ R.E. Bachman and K.H. Whitmire. Reduction of tellurium by $\text{Na}_2[\text{Fe}(\text{CO})_4]$: Synthesis and reactivity of $[\text{PPN}]_2[\text{Fe}_2(\text{CO})_6(\text{Te}_2)_2]$. *Organomet.* (1993), **12**, 1988-1922.
- ⁷⁵ P. Mathur, R. Trivedi, M. Hossain Md, S.S. Tavale and V.G. Puranik. Synthesis and crystal structure of $[(\text{CO})_6\text{Fe}_2(\mu\text{-SeCH}_3)_2]$. *J. Organomet. Chem.* (1995), **491**, 291-294.
- ⁷⁶ G.M. Sheldrick. *SHELXTL, Crystallographic System* (Siemens Analytical Instrument Division, Madison, Wis). (1986).

⁷⁷ D.T. Cromer and J.T. Waber. International Tables for X-Ray Crystallography, Vol IV, The Kynoch Press, Birmingham, England. (1974)

⁷⁸ G.M. Sheldrick and T.R. Schneider. Methods in Enz., in press.

APPENDIX

**PAPER 1 : THE REACTIONS OF HETEROCYCLIC
ORGANOTELLURIUM AND SELENIUM COMPOUNDS WITH
TRIIRON DODECACARBONYL**

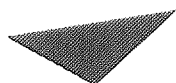
The reactions of heterocyclic organotellurium and selenium compounds with triiron dodecacarbonyl

Zulfiqar Majeed,^a William R. McWhinnie,^a Keith Paxton^a and Thomas A. Hamor^b

^a *Chemical Engineering and Applied Chemistry, Aston University, Aston Triangle, Birmingham, UK B4 7ET*

^b *School of Chemistry, The University of Birmingham, Edgbaston, Birmingham, UK B15 2TT*

Received 28th July 1998, Accepted 2nd October 1998



Aston University

Content has been removed due to copyright restrictions

**PAPER 2 : THE STRUCTURAL CHARACTERISATION OF
TELLURAPHTHALIC ANHYDRIDE, SELENAPHTHALIC
ANHYDRIDE AND OF 2-SELENAPHTHALIDE**



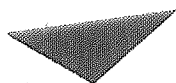
The structural characterisation of telluraphthalic anhydride, selenaphthalic anhydride and of 2-selenaphthalide

Zulfiqar Majeed ^a, William R. McWhinnie ^{a,*}, Keith Paxton ^b, Thomas A. Hamor ^b

^a *Chemical Engineering and Applied Chemistry, Aston University, Aston Triangle, Birmingham B4 7ET, UK*

^b *School of Chemistry, The University of Birmingham, Edgbaston, Birmingham B15 2TT, UK*

Received 6 August 1998



Aston University

Content has been removed due to copyright restrictions

**PAPER 3 : OBSERVATIONS ON THE SYNTHESIS AND
CHEMISTRY OF A COMPLETE SERIES OF
PHENYLAZOPHENYL(C,N')TELLURIUM(II) HALIDES
(FLUORIDE, CHLORIDE, BROMIDE AND IODIDE)**

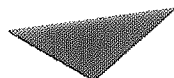


Observations on the synthesis and chemistry of a complete series of
phenylazophenyl(*C,N'*) tellurium(II) halides (fluoride, chloride, bromide
and iodide)

Zulfiqar Majeed ^a, William R. McWhinnie ^{a,*}, Thomas A. Hamor ^b

^a Department of Chemical Engineering and Applied Chemistry, Aston University, Aston Triangle, Birmingham B4 7ET, UK
^b School of Chemistry, The University of Birmingham, Edgbaston, Birmingham B15 2TT, UK

Received 28 June 1997



Aston University

Content has been removed due to copyright restrictions